

**International
Progress Report**

IPR-05-20

Äspö Hard Rock Laboratory

Temperature Buffer Test

**Sensors data report
(Period 030326-050701)
Report No:6**

Reza Goudarzi
Mattias Åkesson
Harald Hökmark

Clay Technology AB

July 2005

Svensk Kärnbränslehantering AB

Swedish Nuclear Fuel
and Waste Management Co
Box 5864
SE-102 40 Stockholm Sweden
Tel 08-459 84 00
+46 8 459 84 00
Fax 08-661 57 19
+46 8 661 57 19



**Äspö Hard Rock
Laboratory**

Report no.
IPR-05-20

Author
Reza Goudarzi
Mattias Åkesson
Harald Hökmark

Checked by
Bertrand Vignal

Approved
Anders Sjöland

No.
F12K

Date
July 2005

Date
2005-09-29

Date
2005-10-19

Äspö Hard Rock Laboratory

Temperature Buffer Test

Sensors data report (Period 030326-050701) Report No:6

Reza Goudarzi
Mattias Åkesson
Harald Hökmark

Clay Technology AB

July 2005

Keywords: Field test, Data, Repository, Bentonite, Rock, Canister, Measurements, Water pressure, Total pressure, Relative humidity, Temperature, Displacements

This report concerns a study which was conducted for SKB. The conclusions and viewpoints presented in the report are those of the author(s) and do not necessarily coincide with those of the client.

Résumé

TBT (Test de Barrière ouvragée en Température) est un projet mené par SKB et l'ANDRA, soutenue par ENRESA et DBE qui vise à comprendre et modéliser le comportement thermo-hydro-mécanique de barrières ouvragées à base d'argile gonflante soumises à des températures élevées ($> 100^{\circ}\text{C}$).

L'essai est conduit dans le HRL d'Äspö dans une alvéole de 8 m de profondeur et 1,75 m de diamètre. Deux sondes chauffantes (chacune de 3 m de long et 0,6 m de diamètre) sont entourés d'argile gonflante, de bentonite, laquelle est confinée par un bouchon ancré sur 9 câbles. L'essai fonctionne depuis le printemps 2003. Les sondes sont chauffées chacune à la puissance nominale de 1500 W. Un système d'alimentation artificiel par filtre de sable fournit de l'eau sous 600 kPa de pression.

Ce rapport présente les données de TBT enregistrées depuis son début le 26 mars 2003 jusqu'au premier juillet 2005.

Dans la bentonite la pression totale est mesurée en 29 points, la pression de pore en 8 points et l'humidité relative en 35 points. La température est mesurée en 92 points et l'est aussi à l'emplacement de chaque capteur dont la mesure nécessite d'être compensée en température.

Des mesures additionnelles sont faites : température en 40 points dans la roche alentour, en 11 points à la surface et 6 à l'intérieur des sondes. La force de confinement est mesurée sur trois des neuf câbles. Le déplacement vertical du bouchon est mesuré en trois points. Le débit et la pression d'eau fournie au système sont également mesurés.

Globalement, le système de mesure et de transmission des données fonctionne bien et l'essentiel des capteurs fournissent des valeurs fiables. La seule exception concerne la mesure d'humidité relative au droit de la sonde inférieure où plusieurs capteurs ne fonctionnent plus.

La température maximale mesurée sur la sonde inférieure est de 138°C et de 148°C sur la supérieure. Une forte hydratation ($\text{RH} > 90\%$) et des pressions de gonflement élevées (de 3 à 9 MPa) sont observées sur quelques 25 cm d'épaisseur en périphérie de la barrière ouvragée, sauf pour les bloc d'argile placés entre la sonde supérieure et le bouchon.

En plus de l'eau de remplissage initial du filtre de sable, plus de 100 % de l'eau théoriquement nécessaire à la saturation de la bentonite a été injectée. La pression nécessaire pour maintenir le débit d'injection indique une augmentation de la résistance hydraulique soit à cause d'un colmatage des embouts des tubes d'injection, soit par intrusion de particules d'argile dans le sable.

La baisse de la pression totale et la hausse de la succion observées autour de la sonde d'en haut est interprétée comme due à un manque d'approvisionnement en eau de la partie supérieure du filtre de sable. Début avril 2004 le filtre a été rempli et mis en pression aussi par les injecteurs supérieurs provoquant dans la bentonite un accroissement soudain de la pression totale et une reprise de la décroissance de la succion.

La densité des dispositifs de mesure de température par thermocouples à mi-hauteur de chaque sonde chauffante se révèle utile pour observer de façon qualitative les cycles saturation - désaturation. Dans la section du bas des indications claires de désaturation sont apparues très tôt dans l'expérience sur une zone annulaire de 0.15 m autour de la sonde chauffante. Cette partie se resature lentement à l'heure actuelle.

Abstract

TBT (Temperature Buffer Test) is a joint project between SKB/ANDRA and supported by ENRESA (modelling) and DBE (optical sensors), which aims at understanding and modelling the thermo-hydro-mechanical behaviour of buffers made of swelling clay submitted to high temperatures (over 100°C) during the water saturation process.

The test is carried out in Äspö HRL in a 8 meters deep and 1.75 m diameter deposition hole, with two canisters (3 m long, 0.6 m diameter), surrounded by a bentonite buffer and a confining plug on top anchored with 9 rods. It was installed during spring 2003. The canisters are heated with 1500 W power and an artificial wetting is in progress, at present with a water pressure of 600 kPa.

This report presents data from the measurements in the Temperature Buffer Test from 030326 to 050701 (26 March 2003 to 01 July 2005).

The following measurements are made in the bentonite: Temperature is measured in 92 points, total pressure in 29 points, pore water pressure in 8 points and relative humidity in 35 points. Temperature is also measured by all gauges as an auxiliary measurement used for compensation.

The following additional measurements are done: Temperature is measured in 40 points in the rock, in 11 points on the surface of each canister and in 6 points inside each canister. The force on the confining plug is measured in 3 of the 9 rods and its vertical displacement is measured in three points. The water inflow and water pressure in the outer sand filter is also measured.

A general conclusion is that the measuring systems and transducers work well and almost all sensors deliver reliable values. The only exception is the Relative Humidity sensors in the high temperature area around the lower canister, where several sensors have failed.

The highest temperature measured on the canister surfaces is 138 °C on the lower canister and 148 °C on the upper. Strong wetting with measured high RH (>90%) and high swelling pressure (3-9 MPa) has reached about 25 cm into the buffer everywhere with exception of the top blocks between the plug and heater 2.

Over 100% of the water theoretically needed to saturate the bentonite has been injected, in addition to the water needed to fill up the outer sand slot. The sand slot injection pressure required to maintain the inflow indicates that some change in the flow resistance of the filter/sand system has taken place. It is not clear if this is a result of clogging of the filter tips or a successive intrusion of bentonite particles in the sand slot.

The decrease in total pressure and increase in suction that was recorded around the upper canister was interpreted to be caused by lack of water supply in the upper part of the sand filter. In the beginning of April 2004 the sand filter was water filled and pressurised also from above. The result of this change was that the total pressure increased and the suction decreased again.

The dense arrays of thermocouples at the mid-height of the two heaters appear to be useful for examining the dehydration/hydration process qualitatively. In the lower section there are clear signs of early dehydration in a 0.15 m annular zone around the heater. Resaturation of this part is now slowly in progress.

Sammanfattning

TBT (Temperature Buffer Test) är ett gemensamt SKB/ANDRA projekt med deltagande av ENRESA (modellering) och DBE (optiska mätinstrument), syftet är att öka förståelsen för de termiska, hydrauliska och mekaniska processerna i en buffert gjord av svällande lera som utsätts för höga temperaturer (över 100 °C) under vattenmättnadsfasen och kunna modellera dessa processer.

Försöket görs på 420-metersnivån i Äspö HRL i ett 8 m djupt deponeringshål med diametern 1,75 m, där två kapslar, omgivande bentonitbuffert och en ovanliggande plugg, som förankrats med 9 stag, installerades våren 2003. Kapslarna värms med en effekt på 1500 W och konstgjord bevätning i sandfiltret pågår, för närvarande med vattentrycket 600 kPa.

I denna rapport presenteras data från mätningar i TBT under perioden 030326-050701.

Följande mätningar görs i bentoniten: Temperaturen mäts i 92 punkter, totaltryck i 29 punkter, porvattentryck i 8 punkter och relativa fuktigheten i 35 punkter. Temperaturen mäts även i alla relativa fuktighetsmätare, för att kompensera för temperaturens inverkan på mätresultaten.

Följande övriga mätningar görs: Temperaturen mäts i 40 punkter i berget, i 11 punkter på ytan av varje kapsel och i 6 punkter inne varje kapsel. Kraften på den ovanliggande pluggen mäts i 3 av de 9 stagen och vertikala förskjutningen av pluggen mäts i tre punkter. Vatteninflödet och vattentrycket i den yttre sandfyllda spalten mäts också.

En generell slutsats är att mätsystemen och givarna fungera bra och i stort sett alla givare leverar pålitliga mätvärden. Enda undantaget är mätningarna av relativa fuktigheten i högttemperaturområdet runt den undre kapseln, där ett flertal givare inte fungerar.

Högsta temperaturen som mäts på kapselytorna är 138 °C på nedre kapseln respektive 148 °C på övre. Stark bevätning med mätta höga RH (>90%) och höga svälltryck (3-8 MPa) har nått cirka 25 cm in i buffereten överallt utom i de översta blocken mellan pluggen och kapsel 2.

Över 100 % av den teoretiska vattenmängd som behövs för att vattenmätta bentoniten har nu tillförts, förutom den mängd vatten som har behövts för att fylla upp den yttre sandspalten. Det injekteringstryck i sandspalten som fordras för att upprätthålla inflödet tyder på att en förändring av flödesmotståndet i systemet filter/sandspalt har ägt rum. Det är oklart om detta beror på långsam igensättning av filterspetsarna eller en successiv inträngning av bentonitpartiklar i spalten.

Den sänkning av totaltrycket och höjning av buffertens inre undertryck som noterats runt den översta kapseln har tolkats bero på brist på vattentillgång i övre delen av sandfiltret. I början på april 2004 vattenfylldes och trycksattes sandfiltret även ovanifrån. Resultatet av denna förändring var att totaltrycket åter höjdes och buffertens inre undertryck minskade.

De täta linjerna av termoelement vid de två värmarnas höjdcentrum visar sig vara användbara för att undersöka torkning/mättnadsprocessen kvalitativt. I den undersektionen finns det tydliga tecken på uttorkning inom ett avstånd av 0,15 m från värmerytan. En långsam återmättnad av denna zon pågår nu.

Contents

| | | |
|----------|---|-----------|
| 1 | Introduction | 11 |
| 2 | Comments | 13 |
| 2.1 | General | 13 |
| 2.2 | Total pressure, Geokon (App. A, pages 51-59) | 14 |
| 2.3 | Suction, Wescore Psychrometers (App. A, pages 60-64) | 14 |
| 2.4 | Relative humidity, Vaisala and Rotronic (App. A, pages 65-70) | 14 |
| 2.5 | Pore water pressure, Geokon (App. A, pages 71-72) | 15 |
| 2.6 | Water flow and water pressure in the sand (App. A, pages 73-74) | 15 |
| 2.7 | Forces on the plug (App. A, page 75) | 15 |
| 2.8 | Displacement of the plug (App. A, page 76) | 16 |
| 2.9 | Canister power (App. A, page 77-78) | 16 |
| 2.10 | Temperature in the buffer (App. A, pages 79-84) | 16 |
| 2.11 | Temperature in the rock (App. A, pages 85-88) | 16 |
| 2.12 | Temperature on the canister surface (App. A, pages 89-90) | 17 |
| 2.13 | Temperature inside the canister (App. A, pages 91-92) | 17 |
| 3 | Coordinate system | 19 |
| 4 | Location of instruments | 21 |
| 4.1 | Brief description of the instruments | 21 |
| | Measurements of temperature | 21 |
| | Measurement of total pressure in the buffer | 21 |
| | Measurement of pore water pressure in the buffer | 21 |
| | Measurement of the water saturation process | 21 |
| | Measurements of forces on the plug | 22 |
| | Measurements of plug displacement | 22 |
| | Measurement of water flow into the sand | 22 |
| 4.2 | Strategy for describing the position of each device | 22 |
| 4.3 | Position of each instrument in the bentonite | 23 |
| 4.4 | Instruments in the rock | 28 |
| | Temperature measurements | 28 |
| 4.5 | Instruments in the canister | 30 |
| 4.6 | Instruments on the plug | 32 |
| 5 | Discussion of results | 33 |
| 5.1 | General | 33 |
| 5.2 | Total inflow of water | 33 |
| | 5.2.1. Injection system behaviour | 35 |
| 5.3 | Temperatures | 37 |
| 5.4 | Relative humidity/suction | 43 |
| 5.5 | Total pressure | 44 |
| | References | 47 |
| | Appendix A | 49 |

1 Introduction

The installation of the Temperature Buffer Test was made during spring 2003 in Äspö Hard Rock Laboratory, Sweden.

The Temperature Buffer Test, TBT, is a full-scale experiment that ANDRA and SKB carry out at the SKB Äspö Hard Rock Laboratory. In addition ENRESA supports TBT with THM modelling and DBE has installed a number of optic pressure sensors.

The test aims at understanding and modelling the thermo-hydro-mechanical behaviour of buffers made of swelling clay submitted to high temperatures (over 100°C) during the water saturation process. No other full scales tests have been carried out with buffer temperatures exceeding 100°C so far.

The test consists of a full-scale KBS3 deposition hole, 2 steel canisters equipped with electrical heaters simulating the power of radioactive decay and a mechanical plug at the top. Figure 1-1 shows the layout and denomination of blocks and canisters. The canisters are embedded in dense clay buffer consisting of blocks (cylindrical and ring shaped) of compacted bentonite powder.

An artificial water pressure is applied in the outer slot between the buffer and the rock, which is filled with compacted sand and functions as a filter.

The upper canister is surrounded by sand in order to reduce the temperature in the bentonite.

The buffer material is instrumented with pressure cells (total and water pressure), thermocouples and moisture gauges. Thermocouples are also installed in the rock.

A retaining plug is built in order to confine the buffer swelling.

Measured results and general comments concerning the collected data are given in chapter 2. A test overview with the positions of the measuring points and a brief description of the instruments are presented in chapters 3 and 4. Finally analyses and discussions of the results are given in chapter 5.

In general the data in this report are presented in diagrams covering the time period 030326 to 050701¹. The time axis in the diagrams represents days from 030326. The diagrams are attached in Appendix A.

Results regarding the fibre optic sensing system are not available yet, as there are problems with calibration of these sensors.

¹ YYMMDD (Swedish way of expressing dates implying that the first two numbers are the year, the next two numbers are the month and the final two numbers are the date)

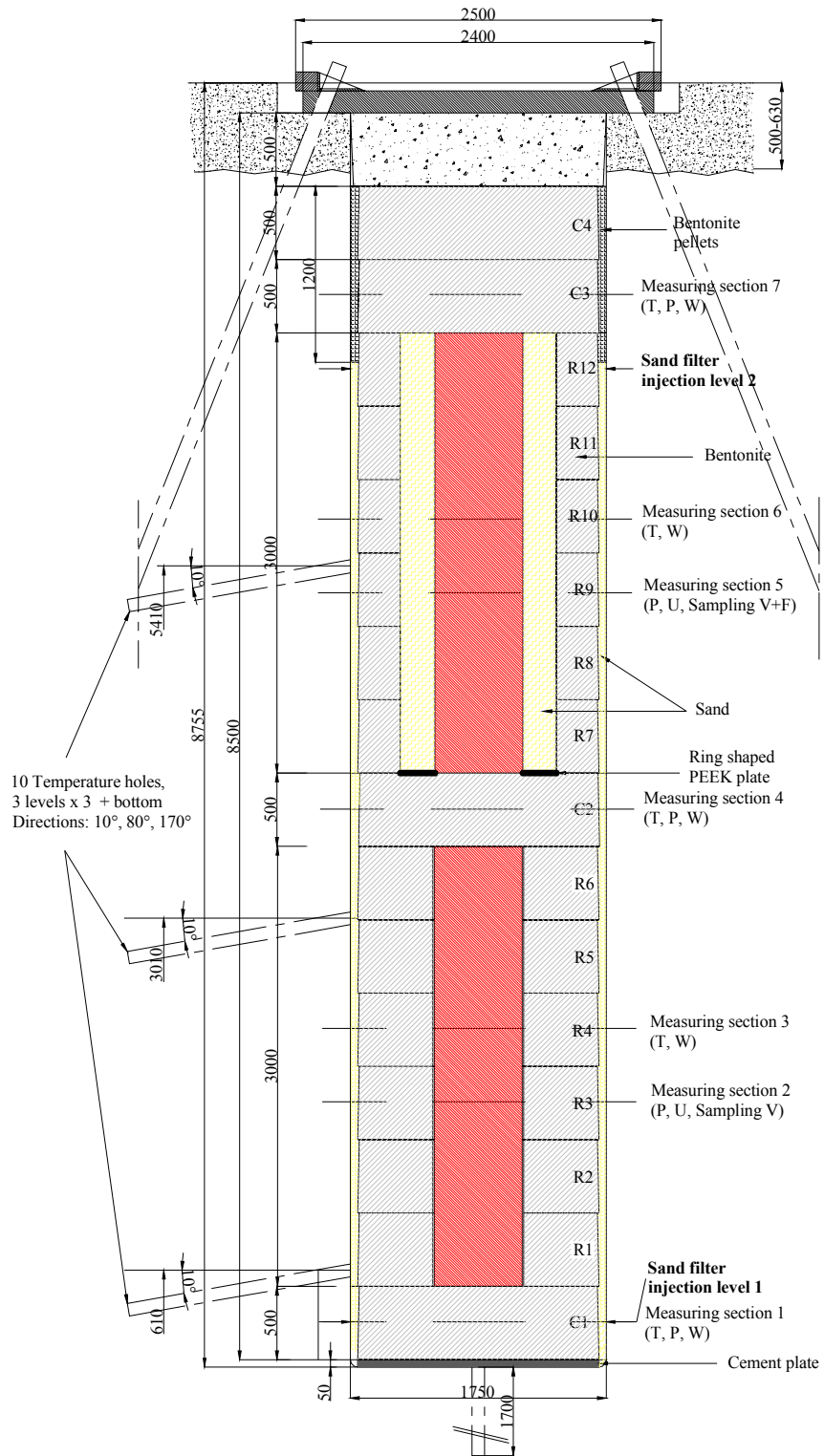


Figure 1-1. Schematic view showing the layout of the experiment and the numbering of bentonite blocks. The lower heater is denominated No. 1 and the upper heater is No. 2.

2 Comments

2.1 General

In this chapter short comments on general trends in the measurements are given. Sensors that are not delivering reliable data or no data at all are noted and comments on the data in general are given but no evaluation or comparison with predictions will be given here.

The heating of both canisters started with an initially applied constant power of 900 W on 030326. This date is also marked as start date. The power was raised to 1200 W on 030403. The power was further raised to 1500 W on 030410. Several power failures have occurred. Important events and dates are shown in Table 2-1.

Table 2-1: Key dates for TBT

| Activity | Date (time) | Day No. |
|---|--|---------|
| 900 W power applied | 030326 | 0 |
| Start water filling of filter | 030327 | 1 |
| 1200 W power applied | 030403 | 8 |
| 1500 W power applied | 030410 | 15 |
| Finished water filling | ~030604 | ~70 |
| Power failure heater 1 | 030423 (~20.00)-030424 (~10.00) | 27-28 |
| Power failure heater 1 | 030527 (~01.00)-030527 (~12.00) | 62 |
| Power failure heater 1 | 030603 (~12.00)-030603 (~14.00) | 69 |
| Power failure heater 1 | 030606 (~19.00)-030609 (~10.00) | 72-75 |
| Power failure heater 1 | 030612 (~12.00)-030612 (~14.00) | 78 |
| Power failure heaters 1 and 2 | 030923 (~12.00 ¹⁾ -030923 (~18.00 ¹⁾) | 181 |
| Power failure heaters 1 and 2 | 031028 (~18.00 ¹⁾ -031029 (~11.00 ¹⁾) | 216 |
| Power failure heater 1 | 040120 (~16.00)-040120 (~19.00) | 300 |
| Power failure heater 2 | 040120 (~18.00)-040120 (~20.00) | 300 |
| Filling and pressurisation of the sand filter also through the upper tubes | 040406 | 377 |
| Flushing and pressurisation of filters through both upper and lower tubes (160 kPa) | 040615-040616 | 448-449 |
| Pressurisation of filters through both upper and lower tubes | 041011-041014 | 565-568 |
| Filling and pressurisation of the sand filter through AS205 and AS207 | 041014 | 568 |
| Filling and pressurisation of the sand filter through AS201, AS202, AS204, AS205, AS206 and AS208 | 041110 | 595 |
| Power failure heater 2 | 050622-050701 | 819- |
| 50 w more power | | 828 |

1) The duration of the power loss is not known since no data was recorded between the times noted.

The water filling was done through four tubes leading to the bottom of the sand filter. The filling was slow due to flow resistance in the sand and the rate was increased by pressurizing the water (see chapter 2.6). The filling was completed after 60-80 days. The water pressure in the bottom of the sand filter has been kept with periodical interruptions (see chapter 2.6) but the valves to the 4 upper tubes leading out water from the top of the sand filter have been open at all times until 040615.

On day 377 (040406) water was supplied to the sand filter also through the tubes leading to the top of the sand filter and a small pressure applied. On days 448-449 the filters were flushed and a water pressure of 160 kPa was applied on the sand filter through both the top tubes and the bottom tubes.

This report is the sixth one and covers the results up to 050701.

2.2 Total pressure, Geokon (App. A, pages 51-59)

The measured pressure ranges from 2.1 to 8.9MPa. The start of the pressure increase takes place shortly after the water filling has reached the level of the different transducer.

Notable is that all transducers in ring 9 around heater 2 except the one at the rock are recording decreasing total pressure in a period between day ~230 and day ~370. The reason for this and other observations are discussed in chapter 5.

Five transducers are out of order.

2.3 Suction, Wescor Psychrometers (App. A, pages 60-64)

Wescor psychrometers are only working at suction below ~7000 kPa, which correspond to high relative humidity (higher than 95%).

Eleven transducers have started yielding interpretable values, which means that they are close to water saturation. Two of them have ceased functioning. Notable is that two transducers around heater 2 are yielding increasing suction (drying) during a period of about 80 days, which is consistent with the measured decrease in total pressure. On the other hand the suction of those transducers is again dropping in suction during the last 2 months, which is also in consistence with the total pressure observations.

Two transducers (WB213 and WB220) are out of order.

2.4 Relative humidity, Vaisala and Rotronic (App. A, pages 65-70)

Relative humidity and temperature measured with Vaisala and Rotronic transducers are shown on pages 65-70. For most transducers RH starts to increase just after the filling of water has reached the sensor level. Only one sensor in the buffer shows an obvious reduction in RH, namely WB206, which is located in the high temperature zone close to

the lower heater. Sensors WB221 and WB222 are located in the sand in contact with the bentonite rings 9 and 10. The high initial RH measured by WB221 may be caused by the free water in the sand that had the water content of about 1% from start.

8 of 23 sensors are presently out of order for other reasons than high degree of saturation. Six of them is placed in ring 4.

2.5 Pore water pressure, Geokon (App. A, pages 71-72)

Transducers UB208 and UB204 show increasing of pore water pressure to about 0.40 MPa and 0.10 MPa during this measuring period.

The other water pressure sensors yield pressure close to zero.

2.6 Water flow and water pressure in the sand (App. A, pages 73-74)

Water filling and measurement of water inflow into the sand started on 030327. The total inflow to the sand has since that date been 2840 litre. The total volume of voids in the sand filter was initially about 790 litres. The inflow rate has been in average about 2.18 l/day since day 110. The inflow rate has been in average about 4.3 l/day in the last six month.

There was also an outflow that started after completed filling since the valves from the top of the sand filter was kept open. The outflow stopped rather early and the total outflow of water has been 44 litres.

The water injection pressure upstream the filter tips is shown on page 74. The water pressure was increased to 800 – 900 kPa during the first 50 days and then kept “constant” until day ~370. However, problems with the water pump have lead to many interruptions in the applied pressure. At day 377 the water pressure was reduced in connection with the start of water supply also from the tubes leading to the top of the filter.

It should be noted that the actual water pressure in the sand filter is only measured at those injection points that are closed to the atmosphere and not pressurized, at present points AS203 and AS207.

2.7 Forces on the plug (App. A, page 75)

The forces on the plug have been measured since 030404. The total force is about 8850 kN at 050704. The influence of the additional water supply from the upper tubes after ~370 days is clearly seen.

During the first about 15 days the plug was only fixed with 3 rods. When the total force exceeded 1100 kN the rest of the 9 rods were fixed in a prescribed manner. This procedure took place 10-11 April 2003 that is 15-16 days after test start. From that time only every third anchor is measured and the results should thus be multiplied with 3. The diagram shows both the actual measurements and after multiplication with 3.

2.8 Displacement of the plug (App. A, page 76)

The three displacement gauges were placed and started to measure displacements from 030409 (day 14) (except for zero reading that was done day 0). One of them (DP201) did not work well and was replaced on 030923 with a new transducer.

Transducer DP203 does not work well during this measuring period.

The measured displacements are in good agreement with the measured forces.

2.9 Canister power (App A, page 77-78)

The heating of both canisters started with an initially applied constant power of 900 W on 030326 and was raised to 1500 W according to Table 2-1. Only one out of three heaters in each canister is presently used (RAH1 and RAH2).

The failure in one of heater (RCH2) in canister 2 caused increasing of power with 50 W on 2005-06-22 to 2005-07-01.

2.10 Temperature in the buffer (App. A, pages 79-84)

Temperature is measured in a large number of points. The plotting of results is done so that the effect of wetting and cracking can be traced, since sensors placed close to each other are collected in the same diagrams.

The highest measured temperature in the bentonite is 135 °C by sensor TB215 located in the midplane of canister 1 at the distance 15 mm from the canister surface. The corresponding temperature on the canister surface is 138 °C, which shows that the temperature drop at the slot between the canister and the bentonite ring is very small.

Temperature is also measured (TB254, TB255 and TB256) in the sand around canister 2 (page 86), where the temperature drop is rather large (~2.7 °C/cm).

The increase in temperature with about one degree °C seen in the upper part of the buffer in the beginning of June (day ~435) is judged to be caused by the increase in tunnel air temperature that takes place in the summer (page 88).

On day ~335 three additional transducers (TB290, TB291 and TB292) placed in Ring 12 were connected to the data scanner and are reported on page 85. One of them was out of order from start.

Six transducers (TB242, TB255, TB276, TBT290, TB291 and TB292) are out of order.

2.11 Temperature in the rock (App. A, pages 85-88)

The maximum temperature measured in the rock (72 degrees) is measured in the central section on the surface of the deposition hole. The deviation from axial symmetry of the temperature measured in the rock is caused by the influence from the heating of the neighbouring Canister Retrieval Test. The notches in the curves seen in the end of the reporting period were caused by data scanner problems that are now solved.

2.12 Temperature on the canister surface (App. A, pages 89-90)

The maximum temperature measured on the surface of canister 1 is about 138 °C and on the surface of canister 2 about 148 °C on 050701. There are strong temperature differences in the canisters, both radial and axial. The highest measured difference on the surface is 24 °C on canister 1 and 36 °C on canister 2.

The steady increase in temperature of heater 1 has turned into a slow decrease. The temperature of heater 2 has decreased since day 50.

2.13 Temperature inside the canister (App. A, pages 91-92)

The maximum temperature measured inside canister 1 is about 161 °C and about 206 °C in canister 2 on 050701. However, the very high value 206 °C may be questioned since it deviates from all other values measured in canister 2. The other sensor at the same level (upper part of the canister) measures only about 173 °C, which is consistent with the other measurements in canister 2.

3 Coordinate system

Measurements are done in 7 measuring sections placed on different levels (see Figure 1-1). On each level, sensors are placed in eight main directions A, AB, B, BC, C, CD, D and DA according to Figure 3-1. Direction A and C are placed in the tunnels axial direction with A headed against the end of the tunnel i.e. almost to the South (see Figure 1-1, 3-1 and 4-1). The angle α is counted anti-clockwise from direction A. The z-coordinate is counted from the bottom of the deposition hole (the cement base).

The bentonite blocks are called cylinders and rings. The cylinders are numbered C1-C4 and the rings R1-R12 respectively (see Figure 1-1).

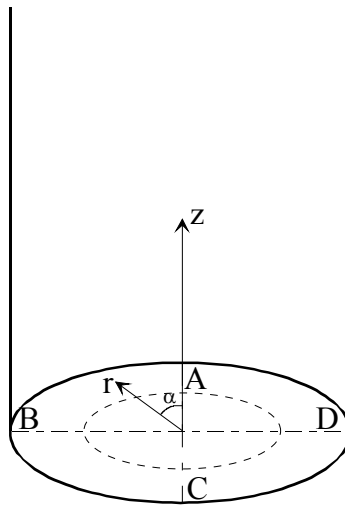


Figure 3-1. Figure describing the coordinate system used when determining the instrument positions.

4 Location of instruments

4.1 Brief description of the instruments

The different instruments that are used in the experiment are briefly described in this chapter. For additional information, see /4-1/.

Measurements of temperature

Buffer

Thermocouples from Pentronic have been installed for measuring temperature in the buffer. Measurements are done in 92 points in the test hole. In addition, temperature gauges are built in into the capacitive relative humidity sensors (23 sensors) as well as in the pressure gauges of vibrating wire type (37 gauges). Temperature is also measured in the psychrometers.

Canister

Temperature is measured in 11 points on the surface of the each canister. Temperature is also measured in each canister insert in 6 points.

Rock

Temperature in the rock and on the rock surface of the hole is measured in 40 points with thermocouples from Pentronic.

Measurement of total pressure in the buffer

Total pressure is the sum of the swelling pressure and the pore water pressure. It is measured with Geokon total pressure cells with vibrating wire transducers. 29 cells of this type have been installed.

Measurement of pore water pressure in the buffer

Pore water pressure is measured with Geokon pore pressure cells with vibrating wire transducer. 8 cells of this type have been installed.

Measurement of the water saturation process

The water saturation process is recorded by measuring the relative humidity in the pore system, which can be converted into water ratio or total suction (negative water pressure). The following techniques and devices are used:

- Vaisala relative humidity sensor of capacitive type. 29 cells of this type have been installed. The measuring range is 0-100 % RH.
- Wescor psychrometers measure the dry and the wet temperature in the pore system. The measuring range is 95.5-99.6 % RH corresponding to the pore water pressure -0.5 to -6MPa. 12 cells of this type have been installed.

Measurements of forces on the plug

The force on the plug caused by the swelling pressure of the bentonite is measured in 3 of the 9 anchors. The force transducers are of the type GLÖTZL.

Measurements of plug displacement

Due to straining of the anchors the swelling pressure of the bentonite will cause not only a force on the plug but also displacement of the plug. The displacement is measured in three points with transducers of the type LVDT with the range 0 – 50 mm.

Measurement of water flow into the sand

An artificial water pressure is applied in the outer slot, which is filled with sand. Titanium tubes equipped with filter tips are placed in the sand on two levels, 250 mm and 6750 mm from bottom (four at each level).

4.2 Strategy for describing the position of each device

Every instrument is named with a unique name consisting of 1 letter describing the type of measurement, (T-Temperature, P-Total Pressure, U-Pore Pressure, W-Relative Humidity, C-Chemical sampling, D-Displacement and A-Artificial water), 1 letter describing where the measurement takes place (B-Buffer, H-Heater, S-Sand, R-Rock and P-plug), 1 figure denoting the deposition hole (1 is used for the CRT test and 2 is used for this experiment), and 2 figures specifying the position in the buffer according to a separate list (see Table 4-1 to 4-7). Every instrument position is described with three coordinates according to Figure 3-1. The r-coordinate is the horizontal distance from the centre of the hole and the z-coordinate is the height from the bottom of the hole (the block height is set to 500mm). The coordinate is the angle from the vertical direction A (almost South).

The position of each instrument is described in the legend in the diagrams according to the following strategy:

Buffer: Three positions according to Figure 3-1: ($z \setminus \alpha \setminus r$) meaning (z -coordinate in m. from the bottom \ the angle α \ the radius in m.)

The cells measuring total pressure have been installed in three different directions in order to measure the radial stress (R), the axial stress (A) and the tangential stress (T). The direction of the pressure measurement is added in Table 4-2 and in the legend for each cell.

Rock: Three positions with the following meaning: (distance in meters from the bottom \ α according to Fig 3-1 \ distance in meters from the rock surface)

The bentonite blocks are called cylinders and rings. The cylinders are numbered C1-C4 and the rings R1-R12 respectively (Figure 1-1).

Canister: The denomination of the instruments in the canister differs a little from the other instruments. At first there are two letters and one figure describing the type of measurement and the place (TH for temperature and heater) and which heater (1 for lower heater and 2 for upper). Then there are again two letters describing if it is an external or internal sensor (SE or SI) and one figure describing the position on the canister (0-4 according to Figure 4-2). Finally the angle clockwise from direction A is written.

4.3 Position of each instrument in the bentonite

Measurements are done in 7 measuring sections placed on different levels (see Figure 1-1). On each level, sensors are placed in eight main directions A, AB, B, BC, C, CD, D and DA according to Figure 4-1. The bentonite blocks are called cylinders and rings. The cylinders are numbered C1-C4 and the rings R1-R12 respectively (see Figure 1-1).

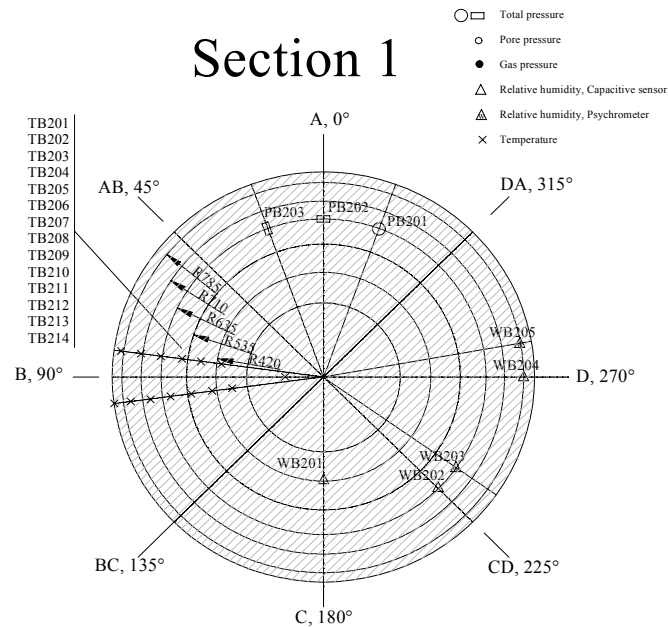


Figure 4-1. Schematic view, showing the main directions of the instrument positioning. The drawing shows the instrumentation in measuring section 1.

An overview of the positions of the instruments is shown in Fig 1-1 and 4-1. Exact positions are described in Tables 4-1 to 4-6. These tables have been updated since the last report and the measured exact position of the transducers have been inserted.

The instruments are located in three main levels in each instrumented block, the surface of the block (only total pressure cells measuring the horizontal pressure) and 50 mm and 250 mm from the upper block surface. The thermocouples and the total pressure cells are placed in the 50 mm level by practical reasons and the other sensors in the 250 mm level.

Table 4-1 Numbering and position of instruments for measuring temperature (T)

| Type and number | Measuring section | Block | Instrument position in block | | | | Instrument Fabricate |
|-----------------|-------------------|--------|------------------------------|--------------------|--------|--------|----------------------|
| | | | Direction | α degree | r m | Z m | |
| TB201 | 1 | Cyl. 1 | B | 90 | 0,150 | 0,452 | Pentronic |
| TB202 | 1 | Cyl. 1 | B | 95 | 0,360 | 0,452 | Pentronic |
| TB203 | 1 | Cyl. 1 | B | 85 | 0,400 | 0,452 | Pentronic |
| TB204 | 1 | Cyl. 1 | B | 95 | 0,440 | 0,452 | Pentronic |
| TB205 | 1 | Cyl. 1 | B | 85 | 0,480 | 0,452 | Pentronic |
| TB206 | 1 | Cyl. 1 | B | 95 | 0,520 | 0,452 | Pentronic |
| TB207 | 1 | Cyl. 1 | B | 85 | 0,560 | 0,452 | Pentronic |
| TB208 | 1 | Cyl. 1 | B | 95 | 0,600 | 0,452 | Pentronic |
| TB209 | 1 | Cyl. 1 | B | 85 | 0,640 | 0,452 | Pentronic |
| TB210 | 1 | Cyl. 1 | B | 95 | 0,680 | 0,452 | Pentronic |
| TB211 | 1 | Cyl. 1 | B | 85 | 0,720 | 0,452 | Pentronic |
| TB212 | 1 | Cyl. 1 | B | 95 | 0,760 | 0,452 | Pentronic |
| TB213 | 1 | Cyl. 1 | B | 85 | 0,800 | 0,452 | Pentronic |
| TB214 | 1 | Cyl. 1 | B | 95 | 0,840 | 0,452 | Pentronic |
| TB215 | 3 | Ring 4 | B | 97,5 | 0,320 | 2,469 | Pentronic |
| TB216 | 3 | Ring 4 | B | 82,5 | 0,360 | 2,469 | Pentronic |
| TB217 | 3 | Ring 4 | B | 97,5 | 0,390 | 2,469 | Pentronic |
| TB218 | 3 | Ring 4 | B | 92,5 | 0,420 | 2,469 | Pentronic |
| TB219 | 3 | Ring 4 | B | 87,5 | 0,435 | 2,469 | Pentronic |
| TB220 | 3 | Ring 4 | B | 82,5 | 0,450 | 2,469 | Pentronic |
| TB221 | 3 | Ring 4 | B | 97,5 | 0,465 | 2,469 | Pentronic |
| TB222 | 3 | Ring 4 | B | 92,5 | 0,480 | 2,469 | Pentronic |
| TB223 | 3 | Ring 4 | B | 87,5 | 0,495 | 2,469 | Pentronic |
| TB224 | 3 | Ring 4 | B | 82,5 | 0,510 | 2,469 | Pentronic |
| TB225 | 3 | Ring 4 | B | 97,5 | 0,525 | 2,469 | Pentronic |
| TB226 | 3 | Ring 4 | B | 92,5 | 0,540 | 2,469 | Pentronic |
| TB227 | 3 | Ring 4 | B | 87,5 | 0,555 | 2,469 | Pentronic |
| TB228 | 3 | Ring 4 | B | 82,5 | 0,570 | 2,469 | Pentronic |
| TB229 | 3 | Ring 4 | B | 97,5 | 0,585 | 2,469 | Pentronic |
| TB230 | 3 | Ring 4 | B | 92,5 | 0,600 | 2,469 | Pentronic |
| TB231 | 3 | Ring 4 | B | 87,5 | 0,615 | 2,469 | Pentronic |
| TB232 | 3 | Ring 4 | B | 82,5 | 0,630 | 2,469 | Pentronic |
| TB233 | 3 | Ring 4 | B | 97,5 | 0,645 | 2,469 | Pentronic |
| TB234 | 3 | Ring 4 | B | 92,5 | 0,660 | 2,469 | Pentronic |
| TB235 | 3 | Ring 4 | B | 87,5 | 0,690 | 2,469 | Pentronic |
| TB236 | 3 | Ring 4 | B | 92,5 | 0,720 | 2,469 | Pentronic |
| TB237 | 3 | Ring 4 | B | 87,5 | 0,750 | 2,469 | Pentronic |
| TB238 | 3 | Ring 4 | B | 92,5 | 0,780 | 2,469 | Pentronic |
| TB239 | 3 | Ring 4 | B | 87,5 | 0,810 | 2,469 | Pentronic |
| TB240 | 4 | Cyl. 2 | B | 90 | 0,150 | 3,983 | Pentronic |
| TB241 | 4 | Cyl. 2 | B | 95 | 0,360 | 3,983 | Pentronic |
| TB242 | 4 | Cyl. 2 | B | 85 | 0,400 | 3,983 | Pentronic |
| TB243 | 4 | Cyl. 2 | B | 95 | 0,440 | 3,983 | Pentronic |
| TB244 | 4 | Cyl. 2 | B | 85 | 0,480 | 3,983 | Pentronic |
| TB245 | 4 | Cyl. 2 | B | 95 | 0,520 | 3,983 | Pentronic |

| Type and number | Measuring section | Block | Instrument position in block | | | | Instrument Fabricate |
|-----------------|-------------------|---------|------------------------------|--------------------|--------|--------|----------------------|
| | | | Direction | α degree | r m | Z m | |
| TB246 | 4 | Cyl. 2 | B | 85 | 0,560 | 3,983 | Pentronic |
| TB247 | 4 | Cyl. 2 | B | 95 | 0,600 | 3,983 | Pentronic |
| TB248 | 4 | Cyl. 2 | B | 85 | 0,640 | 3,983 | Pentronic |
| TB249 | 4 | Cyl. 2 | B | 95 | 0,680 | 3,983 | Pentronic |
| TB250 | 4 | Cyl. 2 | B | 85 | 0,720 | 3,983 | Pentronic |
| TB251 | 4 | Cyl. 2 | B | 95 | 0,760 | 3,983 | Pentronic |
| TB252 | 4 | Cyl. 2 | B | 85 | 0,800 | 3,983 | Pentronic |
| TB253 | 4 | Cyl. 2 | B | 95 | 0,825 | 3,983 | Pentronic |
| TB254 | 6 | Ring 10 | B | 90 | 0,343 | 6,056 | Pentronic |
| TB255 | 6 | Ring 10 | B | 90 | 0,400 | 6,056 | Pentronic |
| TB256 | 6 | Ring 10 | B | 90 | 0,463 | 6,056 | Pentronic |
| TB257 | 6 | Ring 10 | B | 97,5 | 0,540 | 6,006 | Pentronic |
| TB258 | 6 | Ring 10 | B | 92,5 | 0,555 | 6,006 | Pentronic |
| TB259 | 6 | Ring 10 | B | 87,5 | 0,570 | 6,006 | Pentronic |
| TB260 | 6 | Ring 10 | B | 82,5 | 0,585 | 6,006 | Pentronic |
| TB261 | 6 | Ring 10 | B | 97,5 | 0,600 | 6,006 | Pentronic |
| TB262 | 6 | Ring 10 | B | 92,5 | 0,615 | 6,006 | Pentronic |
| TB263 | 6 | Ring 10 | B | 87,5 | 0,630 | 6,006 | Pentronic |
| TB264 | 6 | Ring 10 | B | 82,5 | 0,645 | 6,006 | Pentronic |
| TB265 | 6 | Ring 10 | B | 97,5 | 0,660 | 6,006 | Pentronic |
| TB266 | 6 | Ring 10 | B | 92,5 | 0,675 | 6,006 | Pentronic |
| TB267 | 6 | Ring 10 | B | 87,5 | 0,690 | 6,006 | Pentronic |
| TB268 | 6 | Ring 10 | B | 82,5 | 0,705 | 6,006 | Pentronic |
| TB269 | 6 | Ring 10 | B | 97,5 | 0,720 | 6,006 | Pentronic |
| TB270 | 6 | Ring 10 | B | 92,5 | 0,735 | 6,006 | Pentronic |
| TB271 | 6 | Ring 10 | B | 87,5 | 0,750 | 6,006 | Pentronic |
| TB272 | 6 | Ring 10 | B | 82,5 | 0,765 | 6,006 | Pentronic |
| TB273 | 6 | Ring 10 | B | 97,5 | 0,780 | 6,006 | Pentronic |
| TB274 | 6 | Ring 10 | B | 92,5 | 0,795 | 6,006 | Pentronic |
| TB275 | 6 | Ring 10 | B | 87,5 | 0,810 | 6,006 | Pentronic |
| TB276 | 7 | Cyl. 3 | B | 90 | 0,150 | 7,524 | Pentronic |
| TB277 | 7 | Cyl. 3 | B | 95 | 0,360 | 7,524 | Pentronic |
| TB278 | 7 | Cyl. 3 | B | 85 | 0,400 | 7,524 | Pentronic |
| TB279 | 7 | Cyl. 3 | B | 95 | 0,440 | 7,524 | Pentronic |
| TB280 | 7 | Cyl. 3 | B | 85 | 0,480 | 7,524 | Pentronic |
| TB281 | 7 | Cyl. 3 | B | 95 | 0,520 | 7,524 | Pentronic |
| TB282 | 7 | Cyl. 3 | B | 85 | 0,560 | 7,524 | Pentronic |
| TB283 | 7 | Cyl. 3 | B | 95 | 0,600 | 7,524 | Pentronic |
| TB284 | 7 | Cyl. 3 | B | 85 | 0,640 | 7,524 | Pentronic |
| TB285 | 7 | Cyl. 3 | B | 95 | 0,680 | 7,524 | Pentronic |
| TB286 | 7 | Cyl. 3 | B | 85 | 0,720 | 7,524 | Pentronic |
| TB287 | 7 | Cyl. 3 | B | 95 | 0,760 | 7,524 | Pentronic |
| TB288 | 7 | Cyl. 3 | B | 85 | 0,800 | 7,524 | Pentronic |
| TB289 | 7 | Cyl. 3 | B | 95 | 0,825 | 7,524 | Pentronic |
| TB290 | | Ring 12 | B | 90 | 0,360 | 6,881 | Pentronic |
| TB291 | | Ring 12 | B | 90 | 0,420 | 6,881 | Pentronic |
| TB292 | | Ring 12 | B | 90 | 0,480 | 6,881 | Pentronic |

Table 4-2 Numbering and position of instruments measuring total pressure (P)

| Type and number | Measuring section | Block | Instrument position in block | | | | Instrument Fabricate | Direction of pressure measurement |
|-----------------|-------------------|--------|------------------------------|--------------------|--------|--------|----------------------|-----------------------------------|
| | | | Direction | α degree | r m | Z m | | |
| PB201 | 1 | Cyl. 1 | A | 340 | 0,635 | 0,502 | Geokon | Axial |
| PB202 | 1 | Cyl. 1 | A | 0 | 0,635 | 0,452 | Geokon | Radial |
| PB203 | 1 | Cyl. 1 | A | 20 | 0,635 | 0,452 | Geokon | Tangential |
| PB204 | 2 | R3 | D | 250 | 0,420 | 1,968 | Geokon | Radial |
| PB205 | 2 | R3 | D | 290 | 0,420 | 2,018 | Geokon | Axial |
| PB206 | 2 | R3 | A | 8 | 0,535 | 1,968 | Geokon | Radial |
| PB207 | 2 | R3 | A | 20 | 0,535 | 1,968 | Geokon | Tangential |
| PB208 | 2 | R3 | AB | 45 | 0,585 | 2,018 | Geokon | Axial |
| PB209 | 2 | R3 | B | 100 | 0,635 | 1,968 | Geokon | Tangential |
| PB210 | 2 | R3 | C | 170 | 0,710 | 1,968 | Geokon | Tangential |
| PB211 | 2 | R3 | C | 180 | 0,710 | 1,968 | Geokon | Radial |
| PB212 | 2 | R3 | D | 260 | 0,748 | 2,018 | Geokon | Axial |
| PB213 | 2 | R3 | D | 270 | 0,875 | 1,950 | Geokon | Radial on rock |
| PB214 | 4 | Cyl. 2 | A | 340 | 0,635 | 4,033 | Geokon | Axial |
| PB215 | 4 | Cyl. 2 | A | 0 | 0,635 | 3,983 | Geokon | Radial |
| PB216 | 4 | Cyl. 2 | A | 20 | 0,635 | 3,983 | Geokon | Tangential |
| PB217 | 5 | Ring 9 | D | 270 | 0,535 | 5,319 | Geokon | Radial, against sand |
| PB218 | 5 | Ring 9 | A | 340 | 0,635 | 5,554 | Geokon | Axial |
| PB219 | 5 | Ring 9 | A | 0 | 0,635 | 5,504 | Geokon | Radial |
| PB220 | 5 | Ring 9 | A | 20 | 0,635 | 5,504 | Geokon | Tangential |
| PB221 | 5 | Ring 9 | B | 70 | 0,710 | 5,554 | Geokon | Axial |
| PB222 | 5 | Ring 9 | B | 110 | 0,710 | 5,504 | Geokon | Radial |
| PB223 | 5 | Ring 9 | C | 160 | 0,745 | 5,554 | Geokon | Axial |
| PB224 | 5 | Ring 9 | C | 180 | 0,770 | 5,504 | Geokon | Radial |
| PB225 | 5 | Ring 9 | C | 200 | 0,740 | 5,504 | Geokon | Tangential |
| PB226 | 5 | Ring 9 | D | 270 | 0,875 | 5,450 | Geokon | Radial on rock |
| PB227 | 7 | Cyl. 3 | A | 340 | 0,635 | 7,574 | Geokon | Axial |
| PB228 | 7 | Cyl. 3 | A | 0 | 0,635 | 7,524 | Geokon | Radial |
| PB229 | 7 | Cyl. 3 | A | 20 | 0,635 | 7,524 | Geokon | Tangential |
| PB230 | 2 | R3 | C | 180 | 0,315 | 1,968 | DBE | Radial |
| PB231 | 5 | R9 | C | 180 | 0,535 | 5,504 | DBE | Radial |

Table 4-3 Numbering and position of instruments measuring pore pressure (U)

| Type and number | Measuring section | Block | Instrument position in block | | | | Instrument Fabricate | Remark |
|-----------------|-------------------|--------|------------------------------|--------------------|--------|--------|----------------------|---------|
| | | | Direction | α degree | r m | Z m | | |
| UB201 | 2 | Ring 3 | D | 270 | 0,420 | 1,768 | Geokon | |
| UB202 | 2 | Ring 3 | A | 350 | 0,535 | 1,768 | Geokon | |
| UB203 | 2 | Ring 3 | B | 90 | 0,635 | 1,768 | Geokon | |
| UB204 | 2 | Ring 3 | D | 280 | 0,785 | 1,768 | Geokon | |
| US205 | 5 | Ring 9 | D | 270 | 0,510 | 5,304 | Geokon | In sand |
| UB206 | 5 | Ring 9 | DA | 315 | 0,635 | 5,304 | Geokon | |
| UB207 | 5 | Ring 9 | B | 90 | 0,710 | 5,304 | Geokon | |
| UB208 | 5 | Ring 9 | CD | 225 | 0,785 | 5,304 | Geokon | |
| UB209 | 2 | Ring 3 | C | 200 | 0,315 | 1,968 | DBE | |
| UB210 | 5 | Ring 9 | C | 150 | 0,510 | 5,304 | DBE | |

Table 4-4 Numbering and position of instruments measuring water content (W)

| Type and number | Measuring section | Block | Instrument position in block | | | Instrument Fabricate | Remark | |
|-----------------|-------------------|---------|------------------------------|-----------------|-------|----------------------|----------|---------|
| | | | Direction | α degree | r m | | | Z m |
| WB201 | 1 | Cyl.1 | C | 180 | 0,420 | 0,252 | Rotronic | |
| WB202 | 1 | Cyl.1 | CD | 225 | 0,635 | 0,252 | Vaisala | |
| WB203 | 1 | Cyl.1 | CD | 235 | 0,635 | 0,252 | Wescor | |
| WB204 | 1 | Cyl.1 | D | 270 | 0,785 | 0,252 | Rotronic | |
| WB205 | 1 | Cyl.1 | D | 280 | 0,785 | 0,252 | Wescor | |
| WB206 | 3 | Ring 4 | BC | 135 | 0,360 | 2,269 | Vaisala | |
| WB207 | 3 | Ring 4 | C | 180 | 0,420 | 2,269 | Rotronic | |
| WB208 | 3 | Ring 4 | CD | 225 | 0,485 | 2,269 | Vaisala | |
| WB209 | 3 | Ring 4 | D | 270 | 0,560 | 2,269 | Rotronic | |
| WB210 | 3 | Ring 4 | DA | 315 | 0,635 | 2,269 | Vaisala | |
| WB211 | 3 | Ring 4 | DA | 325 | 0,635 | 2,269 | Wescor | |
| WB212 | 3 | Ring 4 | A | 0 | 0,710 | 2,269 | Rotronic | |
| WB213 | 3 | Ring 4 | A | 10 | 0,710 | 2,269 | Wescor | |
| WB214 | 3 | Ring 4 | AB | 45 | 0,785 | 2,269 | Vaisala | |
| WB215 | 3 | Ring 4 | AB | 55 | 0,785 | 2,269 | Wescor | |
| WB216 | 4 | Cyl.2 | C | 180 | 0,420 | 3,783 | Rotronic | |
| WB217 | 4 | Cyl.2 | CD | 225 | 0,635 | 3,783 | Vaisala | |
| WB218 | 4 | Cyl.2 | CD | 235 | 0,635 | 3,783 | Wescor | |
| WB219 | 4 | Cyl.2 | D | 270 | 0,785 | 3,783 | Rotronic | |
| WB220 | 4 | Cyl.2 | D | 280 | 0,785 | 3,783 | Wescor | |
| WS221 | 5 | Ring 9 | BC | 135 | 0,525 | 5,304 | Vaisala | In sand |
| WS222 | 6 | Ring 10 | BC | 135 | 0,525 | 5,806 | Vaisala | In sand |
| WB223 | 6 | Ring 10 | C | 180 | 0,585 | 5,806 | Rotronic | |
| WB224 | 6 | Ring 10 | CD | 225 | 0,635 | 5,806 | Vaisala | |
| WB225 | 6 | Ring 10 | D | 270 | 0,685 | 5,806 | Rotronic | |
| WB226 | 6 | Ring 10 | D | 280 | 0,685 | 5,806 | Wescor | |
| WB227 | 6 | Ring 10 | DA | 315 | 0,735 | 5,806 | Vaisala | |
| WB228 | 6 | Ring 10 | DA | 325 | 0,735 | 5,806 | Wescor | |
| WB229 | 6 | Ring 10 | A | 0 | 0,785 | 5,806 | Rotronic | |
| WB230 | 6 | Ring 10 | A | 10 | 0,785 | 5,806 | Wescor | |
| WB231 | 7 | Cyl.3 | C | 180 | 0,420 | 7,374 | Rotronic | |
| WB232 | 7 | Cyl.3 | CD | 225 | 0,635 | 7,374 | Vaisala | |
| WB233 | 7 | Cyl.3 | CD | 235 | 0,635 | 7,374 | Wescor | |
| WB234 | 7 | Cyl.3 | D | 270 | 0,785 | 7,374 | Rotronic | |
| WB235 | 7 | Cyl.3 | D | 280 | 0,785 | 7,374 | Wescor | |

4.4 Instruments in the rock

Temperature measurements

40 thermocouples are located in ten boreholes in the rock (see Figure 1-1). The depth of each borehole is 1.5 m. In each borehole 4 thermocouples are placed at different distances from the rock surface. Observe that the coordinate system does not count the radius but the radial distance from the rock surface of the deposition hole. The position of each instrument is described in Table 4-5.

Table 4-5 Numbering and positions of thermocouples in the rock

| Mark | Level | Direction | Distance from rock surface | Instrument Fabricate |
|-------------|--------------|------------------|-----------------------------------|-----------------------------|
| | m | degree | m | |
| TR201 | 0 | Center | 0,000 | Pentronic |
| TR202 | 0 | Center | 0,375 | Pentronic |
| TR203 | 0 | Center | 0,750 | Pentronic |
| TR204 | 0 | Center | 1,500 | Pentronic |
| TR205 | 0,61 | 10° | 0,000 | Pentronic |
| TR206 | 0,61 | 10° | 0,375 | Pentronic |
| TR207 | 0,61 | 10° | 0,750 | Pentronic |
| TR208 | 0,61 | 10° | 1,500 | Pentronic |
| TR209 | 0,61 | 80° | 0,000 | Pentronic |
| TR210 | 0,61 | 80° | 0,375 | Pentronic |
| TR211 | 0,61 | 80° | 0,750 | Pentronic |
| TR212 | 0,61 | 80° | 1,500 | Pentronic |
| TR213 | 0,61 | 170° | 0,000 | Pentronic |
| TR214 | 0,61 | 170° | 0,375 | Pentronic |
| TR215 | 0,61 | 170° | 0,750 | Pentronic |
| TR216 | 0,61 | 170° | 1,500 | Pentronic |
| TR217 | 3,01 | 10° | 0,000 | Pentronic |
| TR218 | 3,01 | 10° | 0,375 | Pentronic |
| TR219 | 3,01 | 10° | 0,750 | Pentronic |
| TR220 | 3,01 | 10° | 1,500 | Pentronic |
| TR221 | 3,01 | 80° | 0,000 | Pentronic |
| TR222 | 3,01 | 80° | 0,375 | Pentronic |
| TR223 | 3,01 | 80° | 0,750 | Pentronic |
| TR224 | 3,01 | 80° | 1,500 | Pentronic |
| TR225 | 3,01 | 170° | 0,000 | Pentronic |
| TR226 | 3,01 | 170° | 0,375 | Pentronic |
| TR227 | 3,01 | 170° | 0,750 | Pentronic |
| TR228 | 3,01 | 170° | 1,500 | Pentronic |
| TR229 | 5,41 | 10° | 0,000 | Pentronic |
| TR230 | 5,41 | 10° | 0,375 | Pentronic |
| TR231 | 5,41 | 10° | 0,750 | Pentronic |
| TR232 | 5,41 | 10° | 1,500 | Pentronic |
| TR233 | 5,41 | 80° | 0,000 | Pentronic |
| TR234 | 5,41 | 80° | 0,375 | Pentronic |
| TR235 | 5,41 | 80° | 0,750 | Pentronic |
| TR236 | 5,41 | 80° | 1,500 | Pentronic |
| TR237 | 5,41 | 170° | 0,000 | Pentronic |
| TR238 | 5,41 | 170° | 0,375 | Pentronic |
| TR239 | 5,41 | 170° | 0,750 | Pentronic |
| TR240 | 5,41 | 170° | 1,500 | Pentronic |

4.5 Instruments in the canister

Temperature is measured both on the canister surface and inside the canister /4-2/. Eleven thermocouples are installed on each canisters surface. Three groups of three thermocouples are installed 100 mm from each heater end, and in the middle of the heater, with a distribution of 120°. Two additional thermocouples are installed in the centre of the bottom lid and the top cover. Temperature inside the canister insert is measured at 6 points with thermocouples.

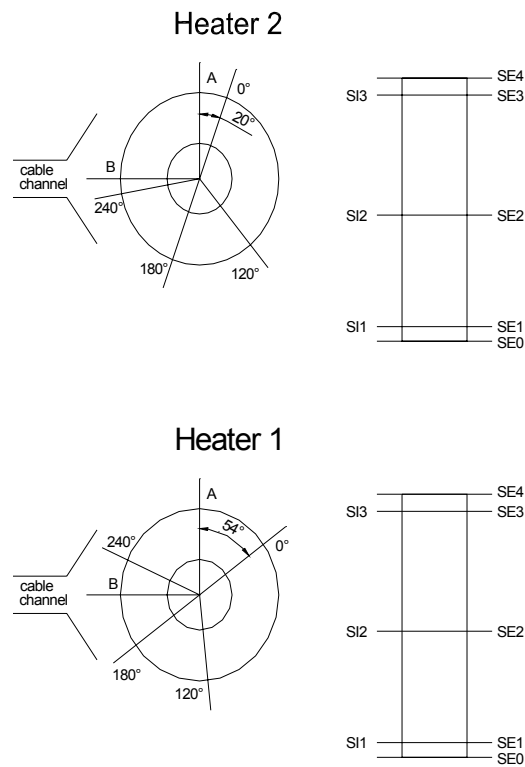
Figure 4-2 shows how these thermocouples are placed (see also chapter 4.2). Table 4-6 and 4-7 show the positions.

Table 4-6 Numbering and position of instruments for measuring the temperature on the heaters surface (T)

| Type and number | Heater | Instruments coordinates | | | Instrument Fabricate | Remark |
|-----------------|--------|-------------------------|--------------------|--------|----------------------|--------|
| | | Position | α degree | r m | | |
| TH1 SE0 | 1 | Bottom | 0 | 0,000 | 0,500 | |
| TH1 SE1 0° | 1 | Lower sec. | 0 | 0,305 | 0,600 | |
| TH1 SE1 240° | 1 | Lower sec. | 240 | 0,305 | 0,600 | |
| TH1 SE1 120° | 1 | Lower sec. | 120 | 0,305 | 0,600 | |
| TH1 SE2 0° | 1 | Middle sec. | 0 | 0,305 | 2,000 | |
| TH1 SE2 240° | 1 | Middle sec. | 240 | 0,305 | 2,000 | |
| TH1 SE2 120° | 1 | Middle sec. | 120 | 0,305 | 2,000 | |
| TH1 SE3 0° | 1 | Upper sec. | 0 | 0,305 | 3,400 | |
| TH1 SE3 240° | 1 | Upper sec. | 240 | 0,305 | 3,400 | |
| TH1 SE3 120° | 1 | Upper sec. | 120 | 0,305 | 3,400 | |
| TH1 SE4 | 1 | Top | 0 | 0,000 | 3,500 | |
| TH2 SE0 | 2 | Bottom | 0 | 0,000 | 4,000 | |
| TH2 SE1 0° | 2 | Lower sec. | 0 | 0,305 | 4,100 | |
| TH2 SE1 240° | 2 | Lower sec. | 240 | 0,305 | 4,100 | |
| TH2 SE1 120° | 2 | Lower sec. | 120 | 0,305 | 4,100 | |
| TH2 SE2 0° | 2 | Middle sec. | 0 | 0,305 | 5,500 | |
| TH2 SE2 240° | 2 | Middle sec. | 240 | 0,305 | 5,500 | |
| TH2 SE2 120° | 2 | Middle sec. | 120 | 0,305 | 5,500 | |
| TH2 SE3 0° | 2 | Upper sec. | 0 | 0,305 | 6,900 | |
| TH2 SE3 240° | 2 | Upper sec. | 240 | 0,305 | 6,900 | |
| TH2 SE3 120° | 2 | Upper sec. | 120 | 0,305 | 6,900 | |
| TH2 SE4 | 2 | Top | 0 | 0,000 | 7,000 | |

Table 4-7 Numbering and position of instruments for measuring the temperature inside the heaters (T)

| Type and number | Heater | Instruments coordinates | | | Instrument Fabricate | Remark |
|-----------------|--------|-------------------------|--------------------|--------|----------------------|--------|
| | | Position | α degree | Z m | | |
| TH1 SI1 0° | 1 | Lower sec. | 0 | 0,60 | | |
| TH1 SI1 180° | 1 | Lower sec. | 180 | 0,60 | | |
| TH1 SI2 0° | 1 | Middle sec. | 0 | 2,00 | | |
| TH1 SI2 180° | 1 | Middle sec. | 180 | 2,00 | | |
| TH1 SI3 0° | 1 | Upper sec. | 0 | 3,40 | | |
| TH1 SI3 180° | 1 | Upper sec. | 180 | 3,40 | | |
| TH2 SI1 0° | 2 | Lower sec. | 0 | 0,60 | | |
| TH2 SI1 180° | 2 | Lower sec. | 180 | 0,60 | | |
| TH2 SI2 0° | 2 | Middle sec. | 0 | 2,00 | | |
| TH2 SI2 180° | 2 | Middle sec. | 180 | 2,00 | | |
| TH2 SI3 0° | 2 | Upper sec. | 0 | 3,40 | | |
| TH2 SI3 180° | 2 | Upper sec. | 180 | 3,40 | | |



Figur 4-2. Location of thermocouples inside (SI) and on (SE) the canisters

4.6 Instruments on the plug

Three force transducers and three displacement transducers have been placed on the plug to measure the force of the anchors and the displacement of the plug. The location of these transducers can be described in relation to Fig 4-3, which shows a schematic view of the plug with the slots, rods and cables.

The rods are numbered 1-9 anti-clockwise and number 1 is the northern rod 18 degrees from direction A. The force transducers are placed on rods 3, 6, and 9. The displacement transducers are placed between the rods on the steel ring in the periphery of the plug. They are fixed on the rock surface and measure thus the displacement relative to the rock.

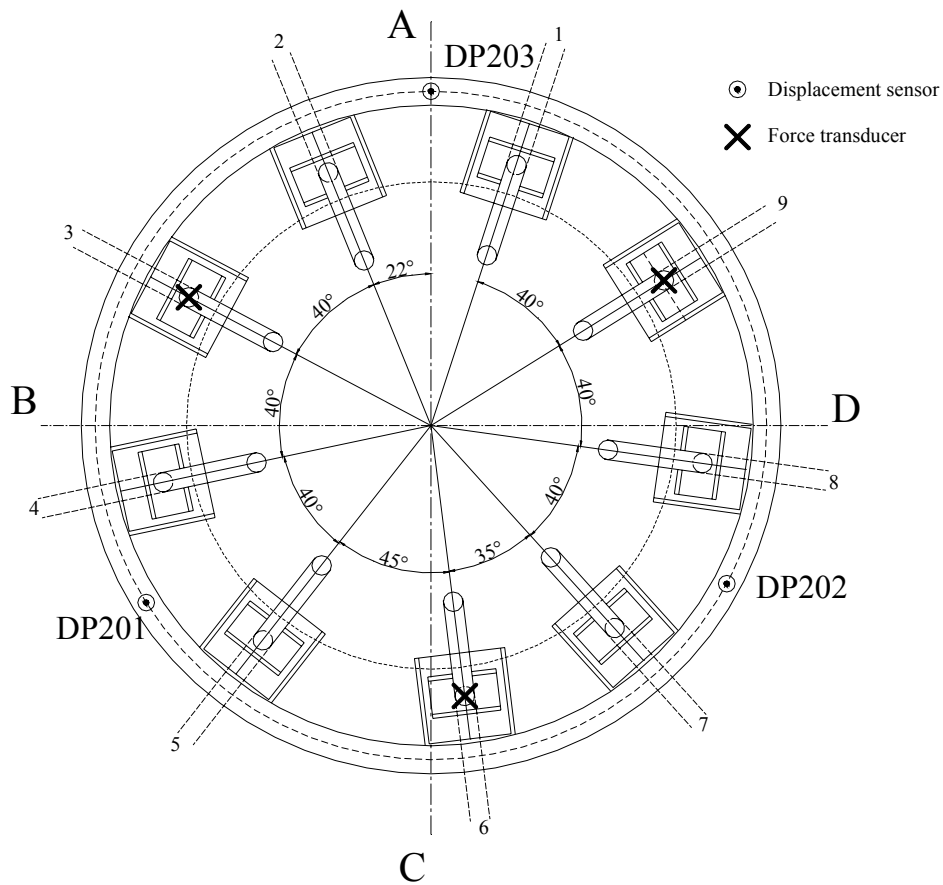


Figure 4-3. Schematic view showing the positions of the rods and the displacement and force transducers on the retaining plug.

5 Discussion of results

5.1 General

Below some results commented in chapter 2 are highlighted and discussed.

5.2 Total inflow of water

The sand filter located in the annular gap between the bentonite buffer and the surrounding rock was initially filled through four tubes ending at the bottom of the sand filter (injection level 1, c.f. Fig. 1-1). The accumulated water inflow up to day 82 was measured to 1.165 m³. The pressure in these tubes from day 50 until day 350 was measured to about 0.8 MPa (App.A\ page74). However, that pressure was not effective continuously, but dropped to zero at various times as shown in (App.A\ page74). At day 82, water began to flow through tubes connecting the uppermost parts of the sand filter with the atmosphere, indicating that the sand filter was filled after about 80 days. That outflow stopped spontaneously after a few days, indicating that some difficulty had developed in the water supply system or that the flow resistance of the system had increased.

On April 6 2004, i.e. after some 370 days, a major change in the injection system was made. The pressure was reduced to about 0.1 MPa and the four upper injection points (injection level 2, c.f. Fig. 1-1) were connected to that pressure (see Table 5-1). The intention was to apply a uniform boundary pressure along the height of the sand filter, rather than having a high pressure in the bottom and almost zero pressure in the top region, and with an uncertain pressure/height relation. The change (injection also from the top) gave a significant increase in inflow, indicating that the upper parts of the experiment had not been efficiently supplied with water during the time preceding the change.

Two hydraulic tests have thereafter been conducted. The first was executed in mid-June 2004, after which the pressure was increased to about 0.25 MPa, still engaging all injection tubes. The second was performed in mid-October 2004. After this, the pressure was again increased, this time to about 0.6 MPa. At the time of this event, pressure sensors were installed to each injection tube, enabling monitoring at closed and not pressurized points. After the second test, only two points were pressurized (AS 205 and 207), whereas the other points were closed. Approximately one month later, at November 10th 2004, the pressurization scheme was changed, so that all points were engaged except AS 203 and 207. The effect of these conditions on the flow rate can be observed in Figure 5-1.

At present (day 828, July 2005) approximately 2.8 m³ has been injected into the system. During the first 75 days the inflow was about 15 l/d. After 100 days the inflow had dropped to about 1.3 l/d, while it increased to about 8 l/d when the injection system was changed so that all 8 injection points were engaged. On average, the flow rate has dropped to 3 l/d, since the engagement of the upper injection points.

The pressurization scheme of the experiment has not been altered during the first six months of 2005 (see Table 5-1). During this period (starting December 25, 2004) the inflow increased considerably, from less than 1 litre per day to more than 8 litres per day at April 20, 2005 (see Figure 5-1). After this, the flow rate dropped to approximately 4 litres per day.

Table 5-3 shows the pore space available at the beginning of the test. The total injected water volume was 2.84 m³, at July 1, 2005. The calculated available pore volume has thereby been exceeded with 0.1 m³. This discrepancy can probably be ascribed to water flow into the rock, vapour leaks or perhaps other inaccuracies.

Table 5-1. Injection point pressurization scheme. The actual water pressure in the sand filter is only measured at those injection points that are closed to the atmosphere and not pressurized, during the first half of 2005 points AS203 and AS207.

| Intervals | Lower injection points | | | | Upper injection points | | | | p (MPa) |
|---|------------------------|-------|-------|-------|------------------------|-------------|-------------|-------------|---------|
| | 201 | 202 | 203 | 204 | 205 | 206 | 207 | 208 | |
| 030326 – 040406 <i>Day 0 - 377</i> | open | open | open | open | open atm | open atm | open atm | open atm | 0.8 |
| 040406 – 040615 <i>Day 377 - 447</i> | open | open | open | open | open | open | open | open | 0.1 |
| 040615 – 040616 <i>Day 447 - 448</i> | Hydraulic test I | | | | | | | | |
| 040616 – 041008 <i>Day 448 – 562</i> | open | open | open | open | open | open | open | open | 0.25 |
| 041008 – 041014 <i>Day 562 - 568</i> | Hydraulic test II | | | | | | | | |
| 041014 – 041110 <i>Day 568 - 595</i> | close | close | close | close | open | close | open | close | 0.6 |
| 041110 – 050701 <i>Day 595 - 828</i> | open | open | close | open | open | open | close | open | 0.6 |

Table 5-2. TBT Pore space.

| | Available at test start [m ³] | |
|----------------------------|---|------|
| Sand filter | 0.77 | |
| Pellets filling | 0.24 | 1.38 |
| Bentonite | 1.08 | |
| Heater/bentonite clearance | 0.06 | |
| Sand shield | 0.55 | |
| Total | 2.70 | |

5.2.1 Injection system behaviour

The change done to the injection system in early April 2004 resulted in significant changes in suction and stress evolution, in addition to increasing the inflow. This supported the notion that the upper part of the experiment had not been supplied with sufficient volumes of water in the time period preceding the change in water supply technique.

As mentioned above, two hydraulic test programs were conducted during 2004. Both tests confirmed that the flow capacity of the four lower injection points was much lower than the four upper injection points.

Equipment for measuring pressure at each injection point was installed at October 8, 2004. Since then, it has been possible to monitor the pressure at injection points closed to the atmosphere. The pressure in the two such points (AS203 and AS207) has varied significantly during the 7 months since installation. The measured values are still almost identical. These values are also very similar to measured pore pressures in the peripheral part of Ring 9 (see App.A\page 72). Since these three points are located at very different levels in the experiment, it now seems clear that these pressures represent the actual pressure in the sand filter. The pressure drop between the injection pressure and the sand filter pressure can therefore be ascribed to the filter cups. Data on pressure drops and flow rate enable a quantification of the hydraulic conductivity of the pressurized filter cups. Results from such a calculation are shown in Figure 5-2. This was based on an assumed 1-dimensional flow, with a flux area of 5 cm² and a 1 mm thickness.

Decreasing hydraulic conductivities of these cups can be explained by precipitations or particle accumulation. Recorded developments during the beginning of 2005 imply *increasing* conductivities however. No explanation for such a change has yet been proposed.

Pressurization and flow rate (041008-050701)

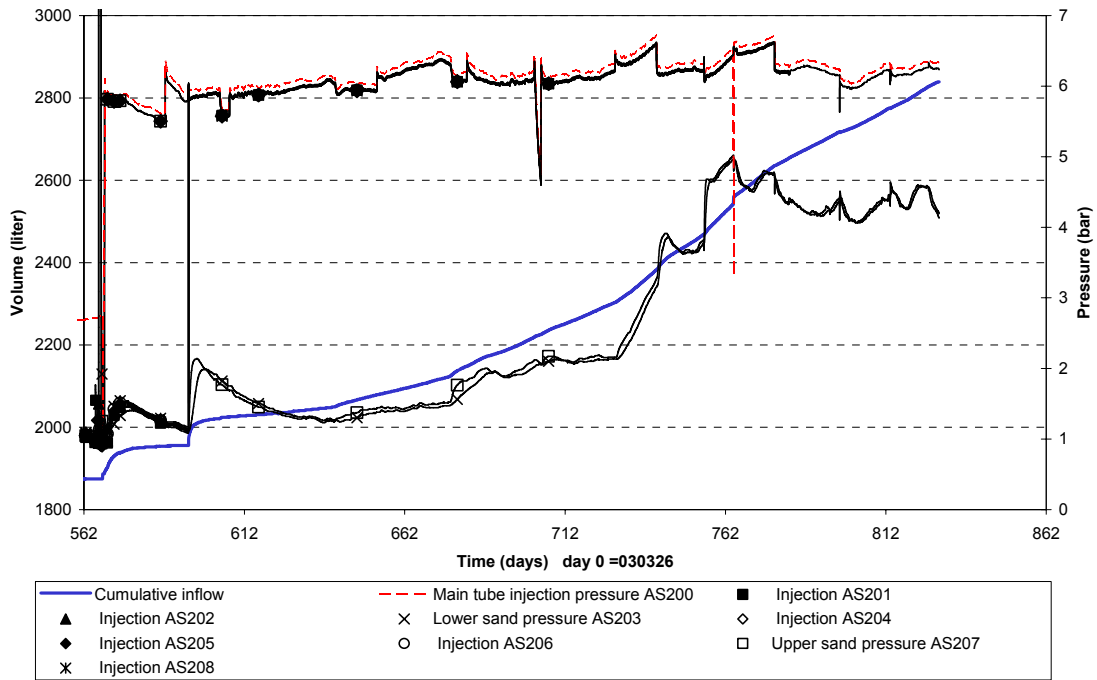


Figure 5-1. Pressurization and flow rate after the second hydraulic test mid-October 2004. AS200 is the main tube. AS201 – AS 208 is individual injection tubes. The actual water pressure in the sand filter was only measured at points AS203 and AS207 during the first half of 2005.

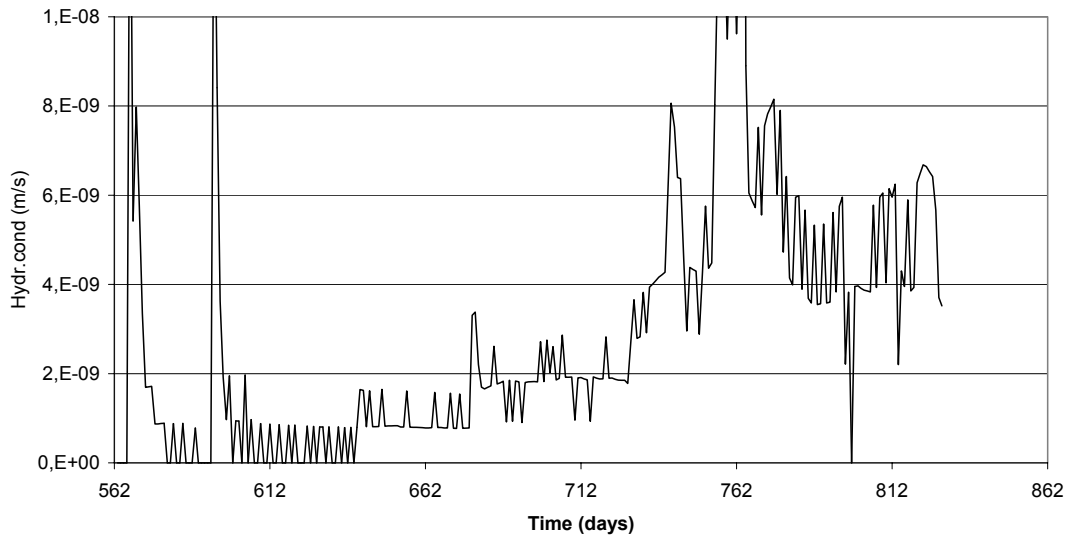


Figure 5-2. Apparent hydraulic conductivity of filter cups.

5.3 Temperatures

Temperatures are monitored by use of thermocouples in three cylinders (C1, C2 and C3) and two rings (R4 and R10), cf. Fig. 1-1. In addition, temperature readings are provided by the capacitance-type relative humidity (RH) sensors. In general, the temperature results exhibit consistent trends up to maximum values after about 200 days (App.A\ pages 79-84). A few exceptions have occurred for inner parts in Cyl 2 and the inner sand shield at Ring 10, where the maximum temperatures were reached after only about 40 and 60 days, respectively (App.A\pages 81-82).

A minor temperature decrease has also been recorded at the innermost points in these sections. Similar trends are found on the heater surfaces and in the interior of the heaters (App.A\Pages 82-92). For the upper heater the trend is very clear and can be explained by the delayed wetting of the upper parts of the sand filter (not completed until after 80 days). The gentle decrease in heater temperature after completion of the sand filter saturation may be due to compression of the sand shield and following increase in sand shield thermal conductivity. Details in these trends may be due to successive and slow changes in the heat flow organization around the heaters. In contrast to these declining trends, a seasonal variation can be observed in Cylinder 3 close to the tunnel floor (see App.A\page 84). The tunnel temperature can apparently influence the uppermost part of the experiment.

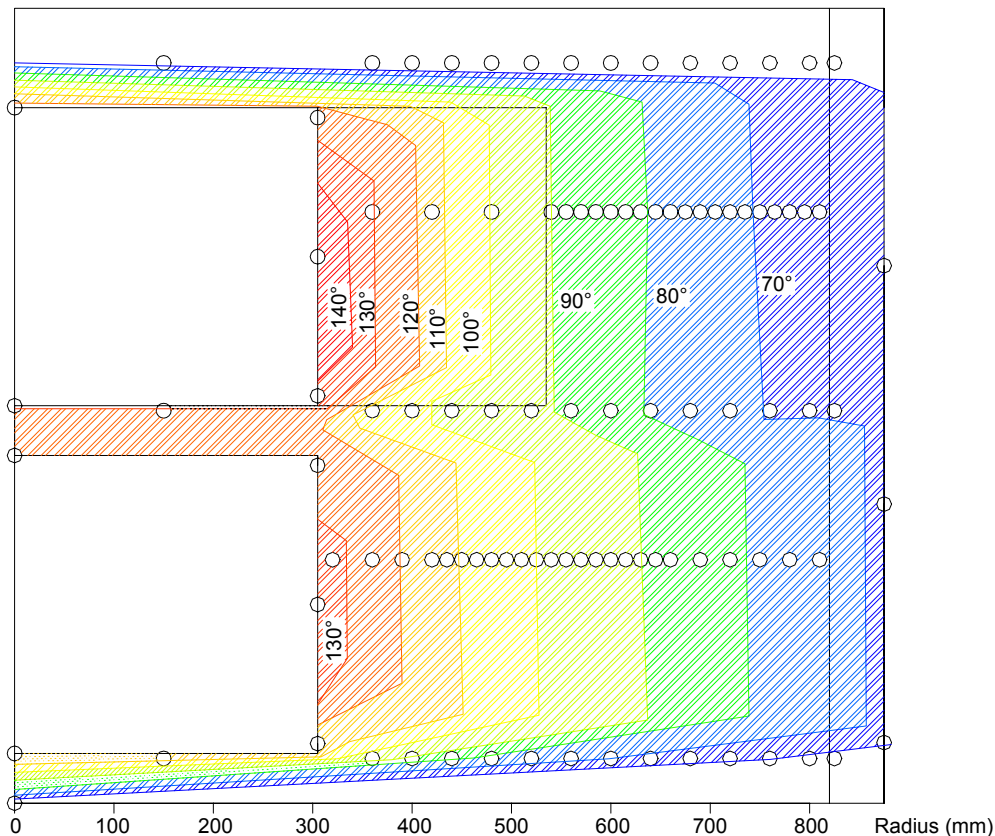


Figure 5-3. Temperature distribution at July 1, 2005.

The temperature readings from July 1 2005 are compiled in Figure 5-3. It can be noted that the highest temperatures in the bentonite blocks are found in Ring 4, whereas the lowest can be found in cylinder C3. It can also be noted that the temperatures in Cylinder 2 at radius 350 – 450 mm is significant lower than in Ring 4 and Ring 10 at corresponding radii.

The TBT experiment is located 6 m from the CRT experiment. The latter was initiated approximately 850 days before the start of the TBT experiment and has therefore affected the surrounding rock temperature. In general, recorded temperatures in the rock follow the same trend as in the bentonite blocks, but on a lower level (App.A\pages 85-88). A compilation of the initial and the recently measured temperatures at different levels, depths and azimuths is presented in Table 3-4 below. It can be noted that the current rock surface temperatures towards the CRT (Az 10°) are up to 5°C higher than the corresponding temperatures on the opposite side (Az 170°). The initial difference was not more than 3°C. This is consistent with the overlapping thermal fields of the CRT and the TBT. Recent power failures of the CRT heaters are reflected in the latest temperature readings in the rock around the TBT experiment.

Table 5-3. Rock temperatures at wall and at 1.5 m depth.

| Time (d) | Level (m) | Temp.(°C) - rock surface | | Temp.(°C) - 1,5 m in rock | |
|----------|-----------|--------------------------|---------|---------------------------|---------|
| | | Az:10° | Az:170° | Az:10° | Az:170° |
| 0 | 5,41 | 21 | 19 | 24 | 17 |
| | 3,01 | 22 | 19 | 26 | 18 |
| | 0,61 | 22 | 19 | 25 | 18 |
| 295 | 5,41 | 64 | 63 | 44 | 38 |
| | 3,01 | 71 | 66 | 47 | 40 |
| | 0,61 | 61 | 57 | 41 | 35 |
| 645 | 5,41 | 65 | 66 | 44 | 39 |
| | 3,01 | 73 | 68 | 47 | 40 |
| | 0,61 | 62 | 59 | 42 | 36 |
| 828 | 5,41 | 64 | 65 | 42 | 38 |
| | 3,01 | 72 | 67 | 46 | 41 |
| | 0,61 | 61 | 59 | 40 | 36 |

Azimuth 0° is toward the CRT experiment.

Sporadic irregularities in the temperature trends, especially around the lower heater, can be attributed to a number of brief heater power failures (App.A\ pages93-96).

Figure 5-4 shows Azimuth 90° temperatures measured in Ring 4 and 10. The effect of the wetting of the sand filter outside Ring 10 is obvious: Within the first 60 days of heating, the temperature drop across the filter had discernibly decreased, as would be expected in a system that had become water saturated and had potentially undergone some swelling pressure – induced compression.

Figure 5-3 and 5-4 below illustrate changes in apparent thermal conductivity. The results are based on the slopes of temperature-distance curves derived from thermocouple readings in rings 10 and 4 (Fig. 5-4), and on the assumption of constant radial heat output at heater mid-height. There are systematic increases that indicate that saturation may be proceeding at a reasonably high rate. Among the latest results this is most apparent in the innermost part of Ring 4. There is also an apparent increase in the sand shield conductivity, in particular in the period between 60 and 145 days.

In general, Figure 5-3 and 5-4 should be interpreted with some caution: some of the changes may be due to variation of the mid-height heat flux, and some may be due to dislocation of individual sensors. No changes are therefore shown for the latest time interval (day 645-825). There is also the likelihood that the sand-filled regions of the two sections of the TBT have undergone some degree of compression due to the swelling pressure generated by the saturated portions of the buffer.

More specifically, the calculated conductivities in Ring 10 appear to systematically reach higher values in the outer part (Figure 5-4). This is probably an effect of cooling from the tunnel floor and since the heat flux is assumed to be radial in these calculations. This assumption appears however not to be completely valid in this part.

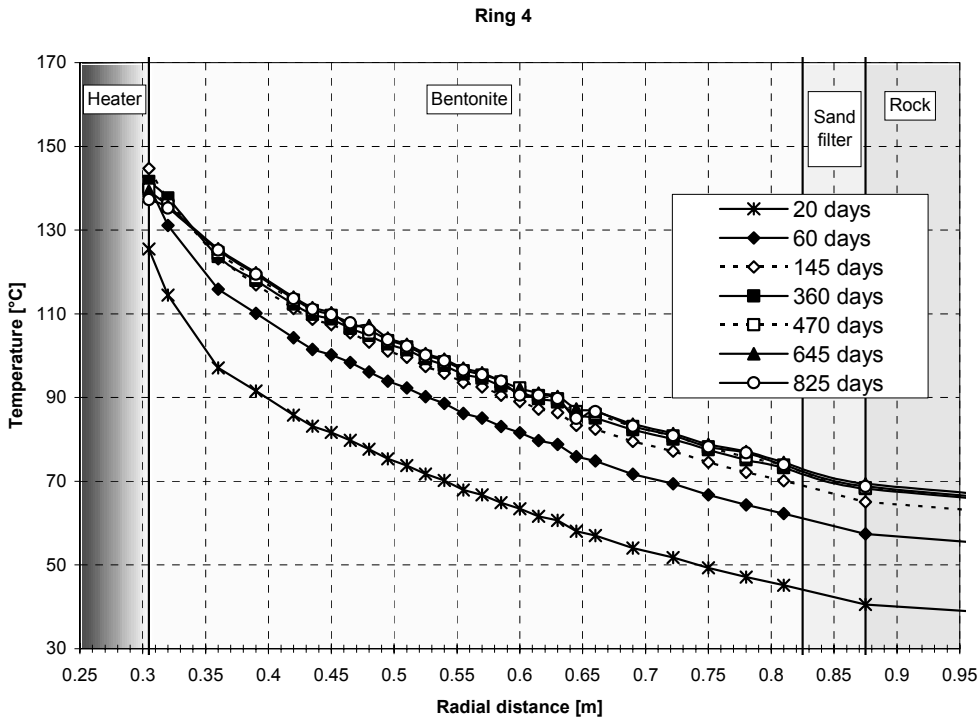


Figure 5-4. Temperatures measured at mid-height of heater 1 (Ring 4) and heater 2 (Ring 10).

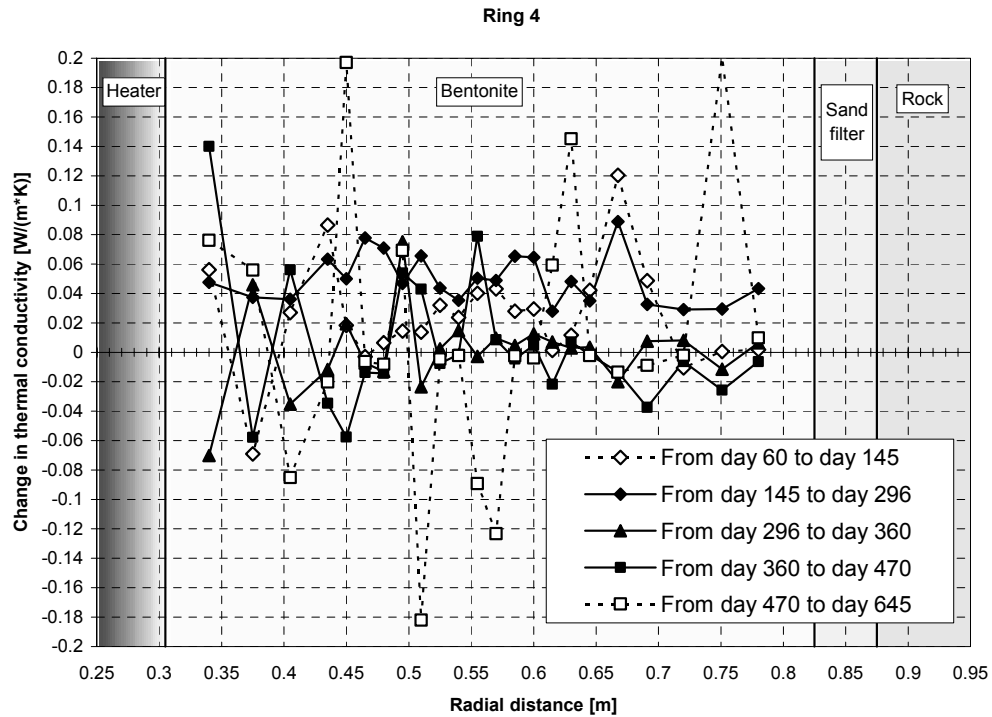
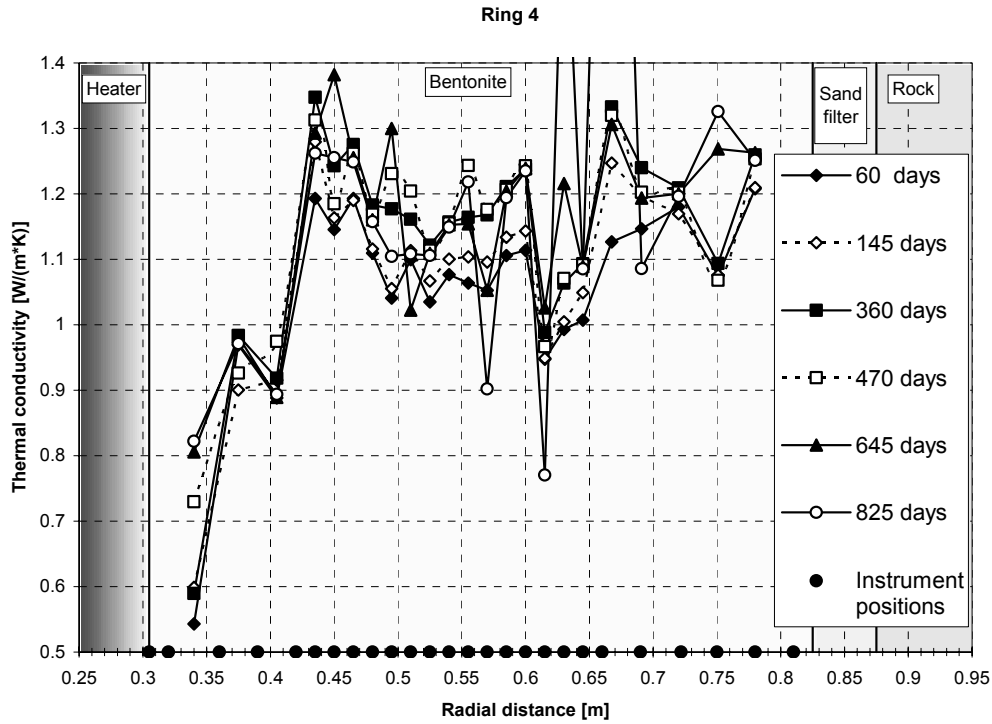


Figure 5-5. Upper: Thermal conductivity in ring 4 as computed from slopes of distance-temperature relation. Lower: Change in thermal conductivity during four time intervals. Day 60 data are slightly affected by the transient heating effect.

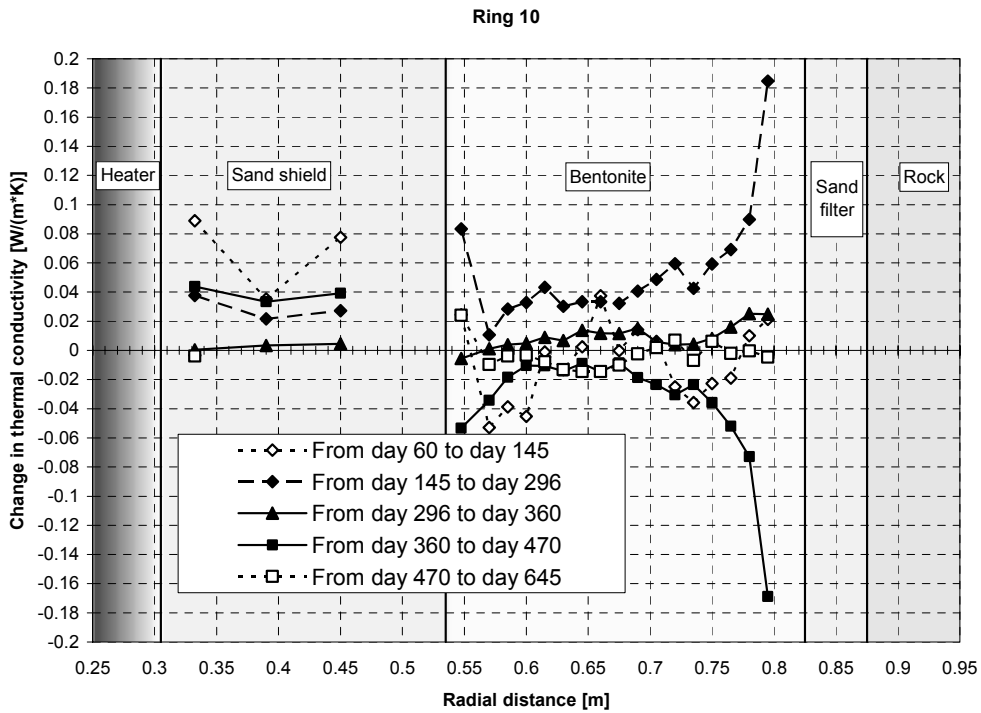
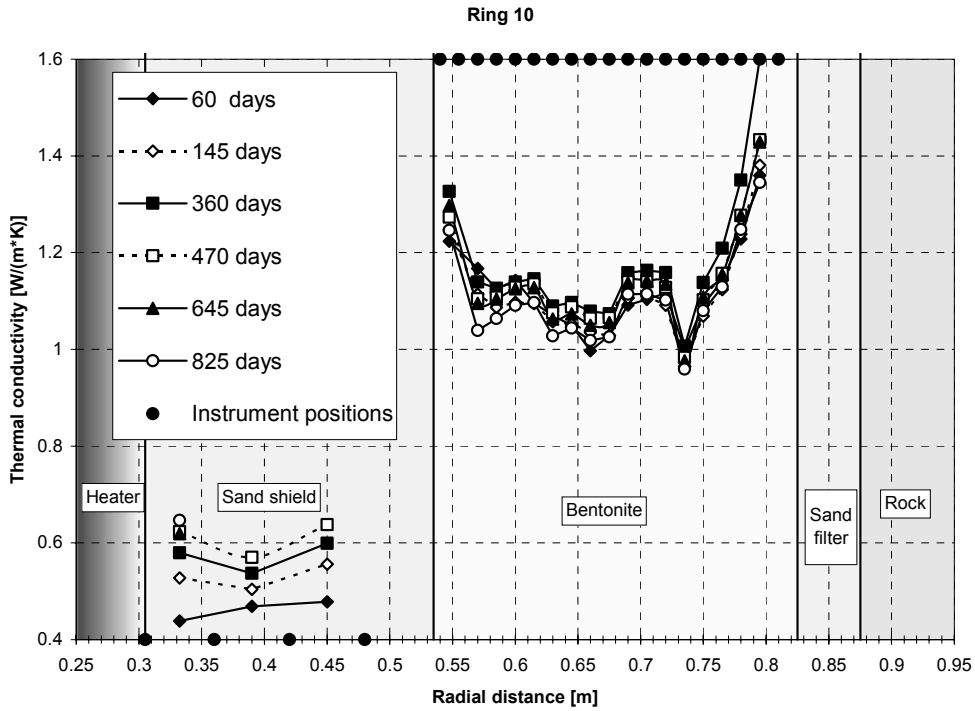


Figure 5-6. Upper: Thermal conductivity in ring 10 and in sand shield as computed from slopes of distance- temperature relation. Lower: Change in thermal conductivity during four time intervals.

5.4 Relative humidity/suction

Recorded RH values and suctions indicate that moisture contents generally increase: RH from 72 to maximum 100 % (App.A\pages 65-70); suction between 6 and 1 MPa (App.A\pages 60-64).

A significant exception is the suction increase in Ring 10 at radius 785 and 735 mm after day 225 (App.a\page 63). Although this increase correlated with a general decrease in stresses in parts of Ring 9, it was most likely caused by a shortage in water supply, resulting in a localized desiccation cycle to occur. The trend was also reversed when water injection through the upper tubes was introduced (see Section 5.2), which supports the water supply explanation for these observations.

A compilation of saturation events are compiled in Figure 5-5. Events are here arranged in periods of 60 days. As can be noted, the greatest penetration of the saturation front after 480 days of TBT operation is 420 mm in Cylinder 2. The sensor at the same radius in Cylinder 3 was saturated after day 840. An observation that can be made is that Cylinder 2, closely followed by Ring 4, seems to have gone through a rapid saturation of the outermost parts. The relatively fast saturation here may be an effect of vapor diffusing outwards from the hot, desaturated, parts close to the heater. It can also be caused by a relatively high reduction of water viscosity at higher temperature steps.

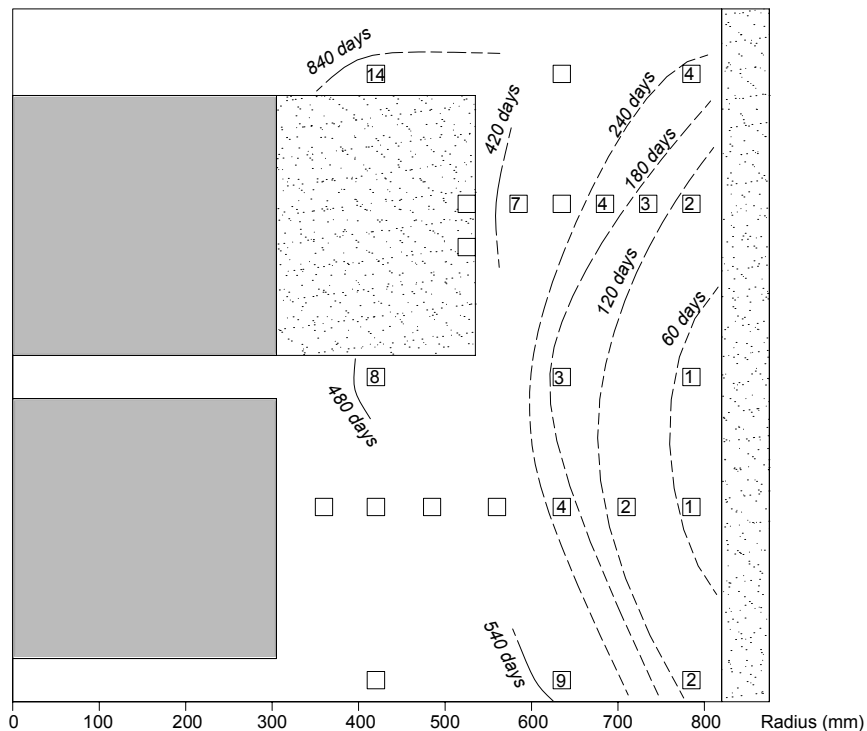


Figure 5-7. Occurrences of saturation as indicated by $RH \approx 100\%$ and active Wescor sensors ($RH > 95\%$). Number denote periods of 60 days.

Data from the innermost RH-sensor of Ring 4 (radius 360 mm) has recently been re-evaluated (App.A\page 66). This sensor was thought to have failed after day 120, since subsequent signals have exhibited an unstable behaviour. Recent data indicate however that the sensor is still functional. Results indicate stable conditions at a RH level of 62 %. The notion of dry conditions in the inner part of Ring 4 is supported by apparent thermal conductivities as well as low swelling pressures in this part.

5.5 Total pressure

Results from pressure monitoring are shown in (App.A\pages 51-59). A compilation of recent total pressures is shown in Figure 5-7. From this a number of observations can be made. The highest pressure levels occur in the lower peripheral part and around the upper heater. The conditions in the lower zone is quite isostatic, while upper zone is characterized by significant deviatoric stresses. The lowest pressure levels occur in the upper cylinders. The axial stresses close to the lower heater is also quite low.

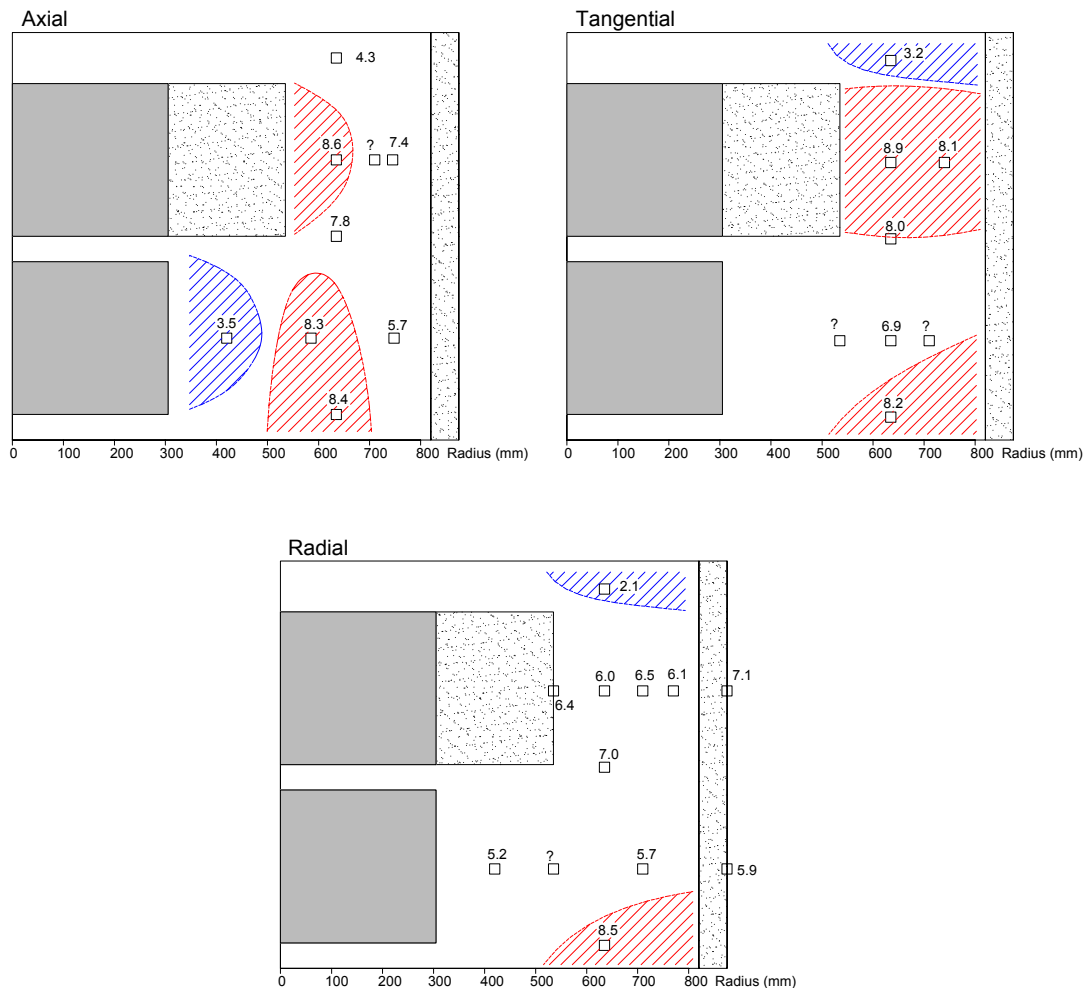


Figure 5-7. Current total pressure overview in MPa (data from 050701). Levels above 8 MPa marked red; below 4 MPa marked blue.

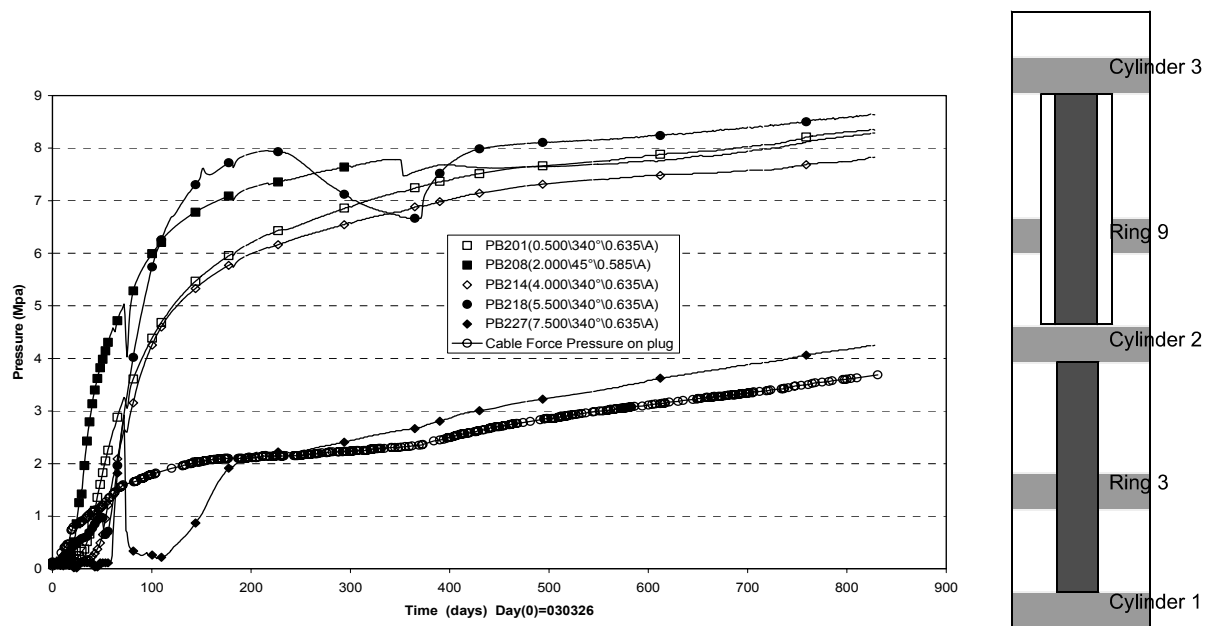


Figure 5-8. Axial pressure measured in different sections. Sensor in Ring 9 failed after about 300 days.

Recent axial pressures, shown in Figure 5-7, appear to be quite similar in a band between radius 550 and 650 mm from Cylinder 1 to Ring 10. In contrast, the axial pressure in Cylinder 3 is significantly lower. This relation is further illustrated in Figure 5-8 in which results are shown from axial pressure sensors all located at radii 585 - 635 mm. Moreover, measured cable forces are here shown after conversion to pressures under the assumption that the forces are evenly distributed over the entire rock hole area (2.40 m^2).

A fairly clear-cut grouping can be observed, which suggests that the vertical forces are predominantly transferred in a section corresponding to the buffer rings around the upper heater. The stress levels around the heaters and in the lower cylinders is approximately twice as high as in the upper part of the experiment, which suggest that the area engaged in the top is twice as high as in lower part.

This is further illustrated in Figure 5-9. In this, the vertical force is calculated at three levels: at the top of Ring 9, Cylinder 3 and the concrete plug, respectively. Differences in vertical forces between two sections can be attributed to shear forces at the rock wall. With the chosen approach, these shear forces are relatively small, which can be expected given sufficient time.

The chosen approach also implies that the axial forces through the heaters are negligible. This may have been an oversimplification in the beginning of the test when the thermal expansion of the heaters were significant. A 100°C temperature increase will result in about 7 mm increase in total heater length. But the total displacement of the plug at present amount to 14 mm, which would imply that the thermal expansion of the heaters is not limited in vertical direction by the buffer package. At the beginning of the test however, the plug force exhibited a more rapid build-up than the axial pressures in the buffer, which may be attributed to the thermal expansion.

Apart from these all-embracing observations, other more exclusive trends are also of interest:

- After about 225 days, most stresses in Ring 9 began to decrease very significantly. This decrease has been found to be a result of insufficient water supply to the upper parts of the experiment. When the four upper injection points were connected in early April 2004, the stresses recovered.
- There was a sudden (local) loss of axial stress in Cylinder 3 after about 80 days. This was probably an effect of brittle block failure. It could also be caused by a temporary malfunctioning of the total pressure sensor, as none of the two other sensors in Cylinder 3 indicated anything at that time.
- Some 100 or 120 days after test start, the axial stress in Ring 9 did not increase any further, at least not significantly. This is true for the tangential stress as well, App.A\page 57. This apparent cut-off of axial and tangential stresses is probably due to plastic shear strains, which occur at certain deviatoric stresses levels, according to the BBM-model. Such conditions arise if the buffer can expand in radial direction during build-up of swelling pressure, so that the radial stresses will be notably lower than the axial and tangential stresses.

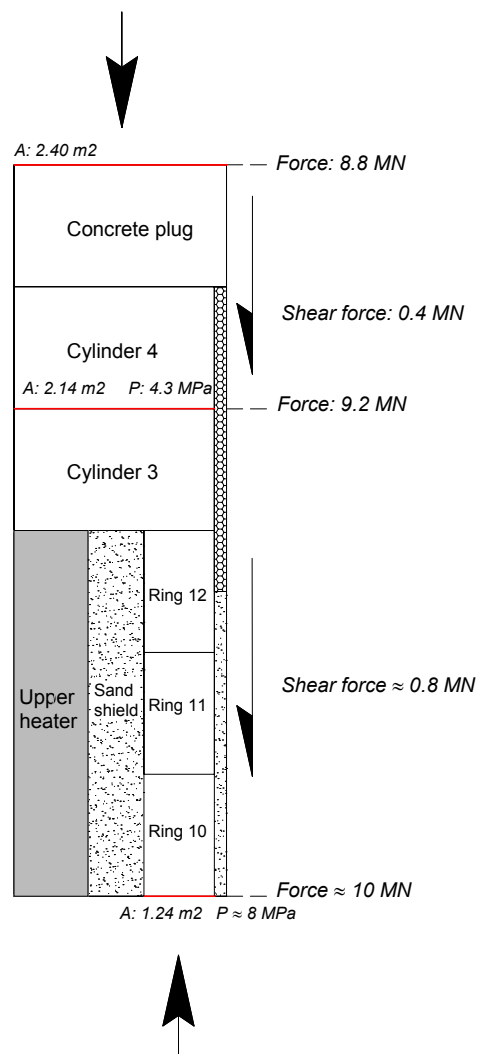


Figure 5-9. Schematic of vertical forces acting on the upper part of the package.

References

/4-1/ Sandén T and Börgesson L. Report on instruments and their positions for THM measurements in buffer and rock and preparation of bentonite blocks for instruments and cables. Temperature Buffer Test, Report R5 , 2002. SKB ITD-02-05

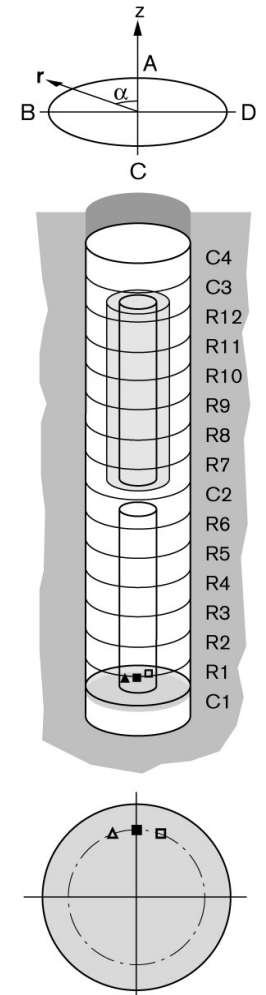
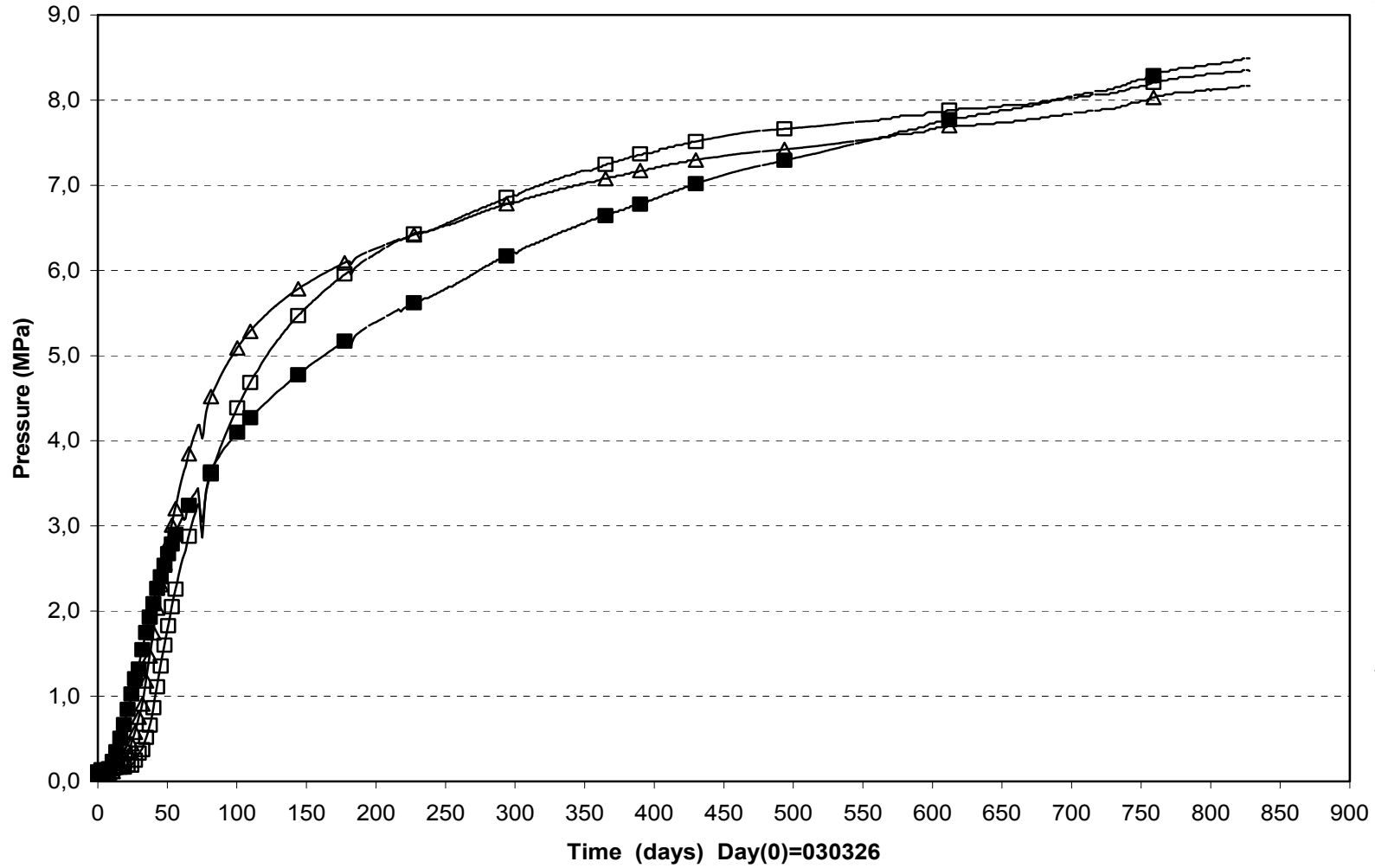
/4-2/ Garcia-Sineriz, J.L and Fuentes- Cantillana. Feasibility study for the heating system at the TBT test carried out at the Äspö HRL in Sweden. Temperature Buffer Test , October 2002. SKB IPR-03-18

/5-1/ Sandén T., De Combarieu M., Hökmark H. Description of the instrumentation installed in Temperature Buffer Test. Sitges Workshop on large-scale field experiments in granite. 2003. UPC, Barcelona.

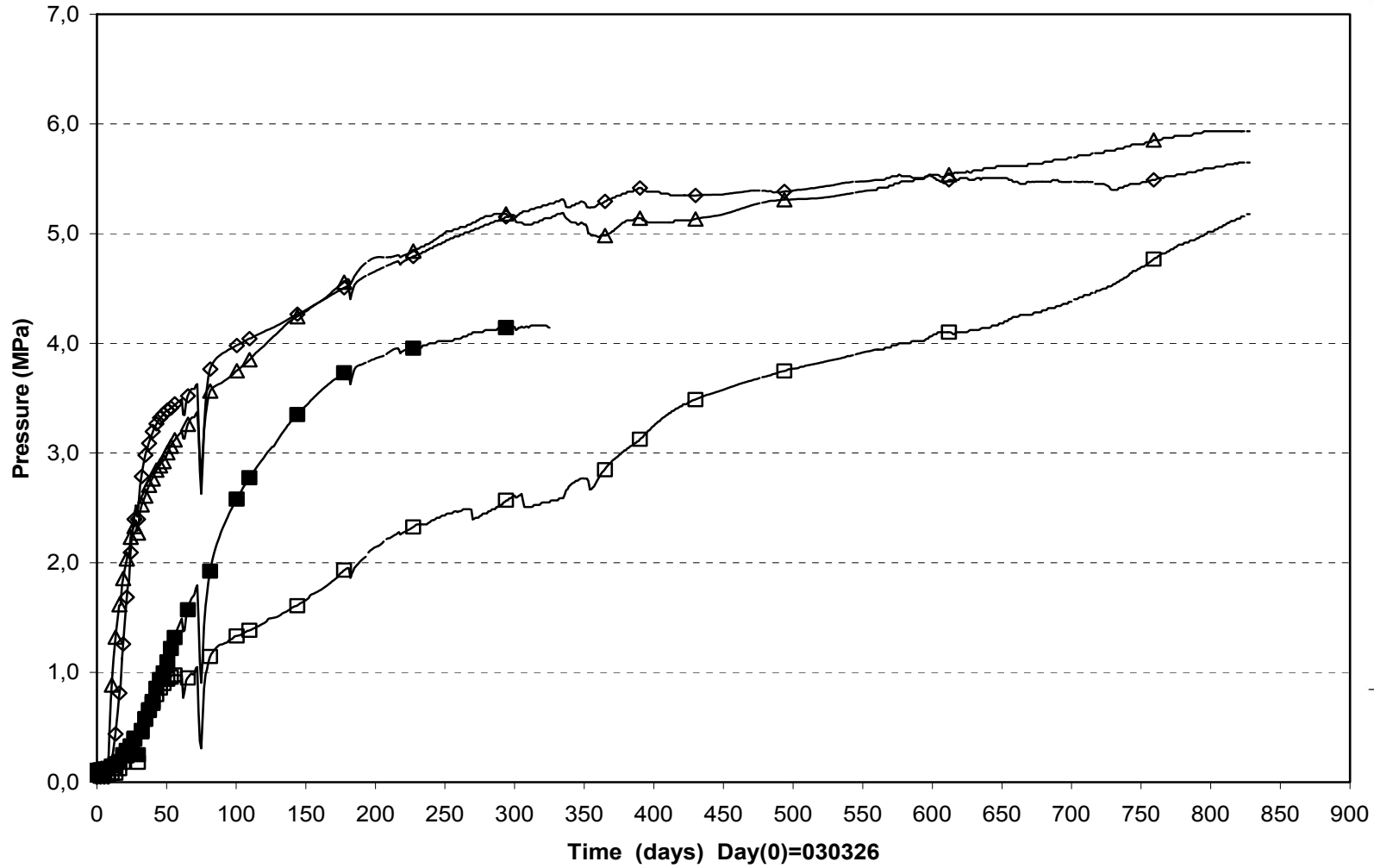
Appendix A

Measured data

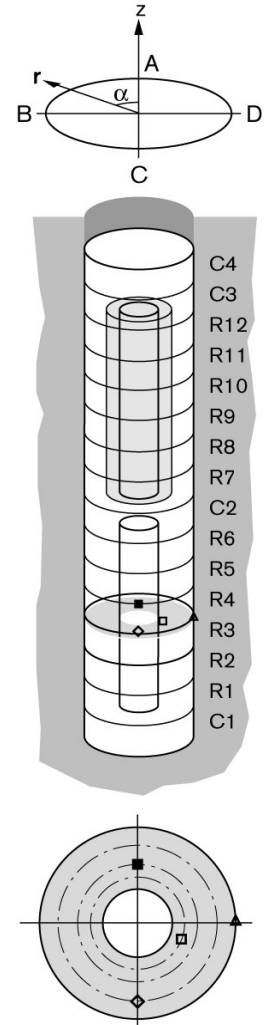
Total pressure/Cyl.1 (030326-050701)
Geokon



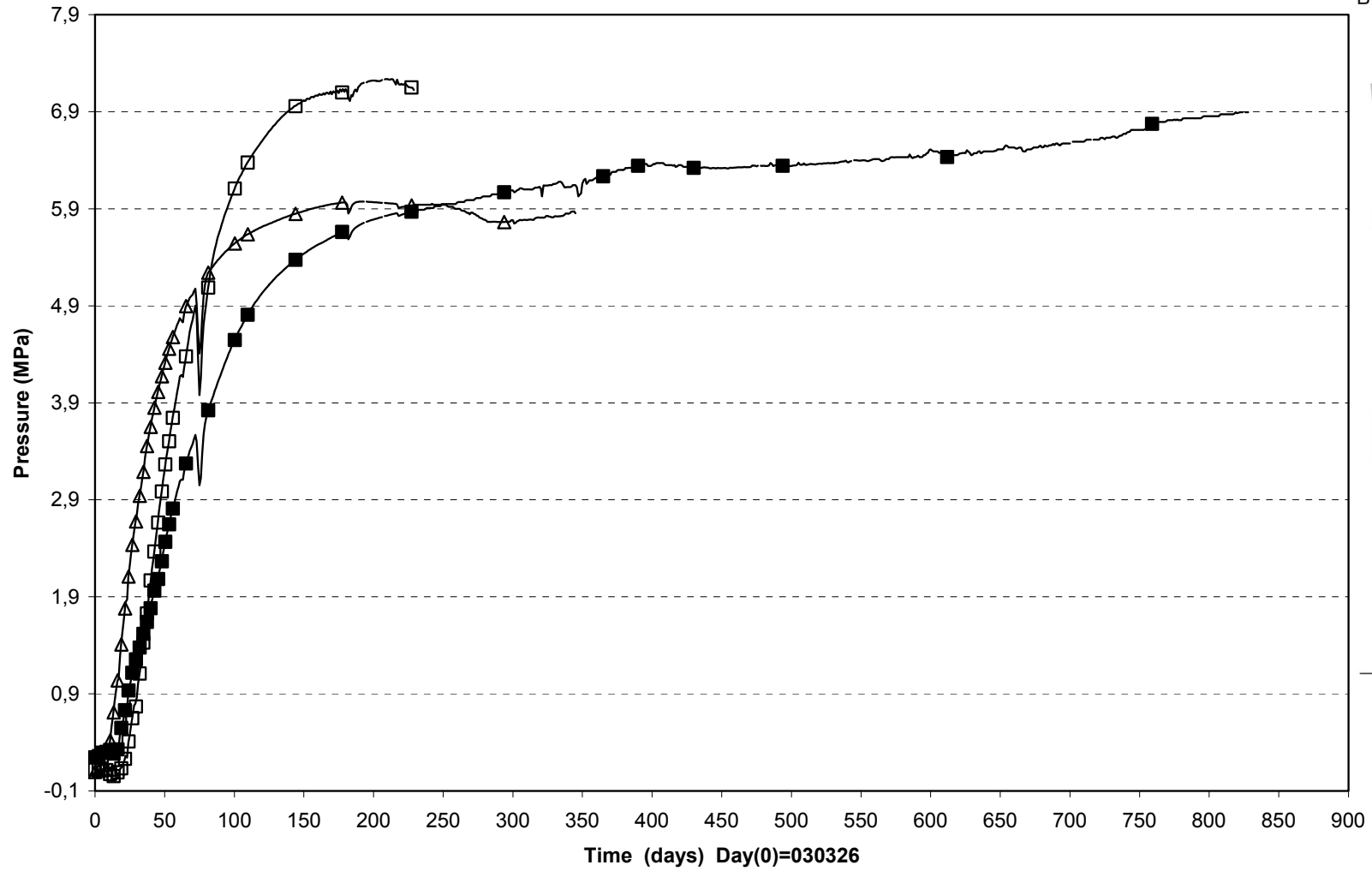
**Total pressure/Ring 3 (030326-050701)
Geokon**



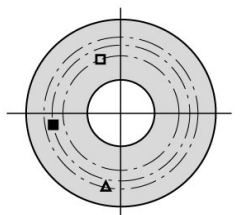
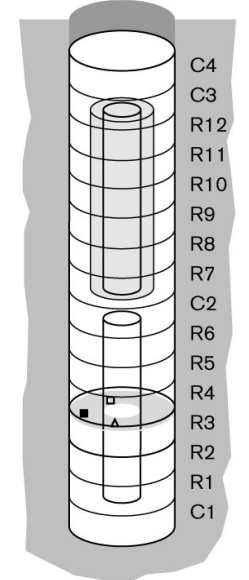
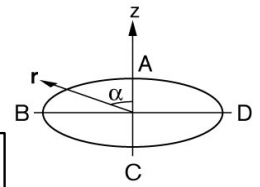
□ PB204(1.950\250°\0.420\R) ■ PB206(1.950\8°\0.535\R) ◇ PB211(1.950\180°\0.710\R) △ PB213(1.950\270°\0.875\R)



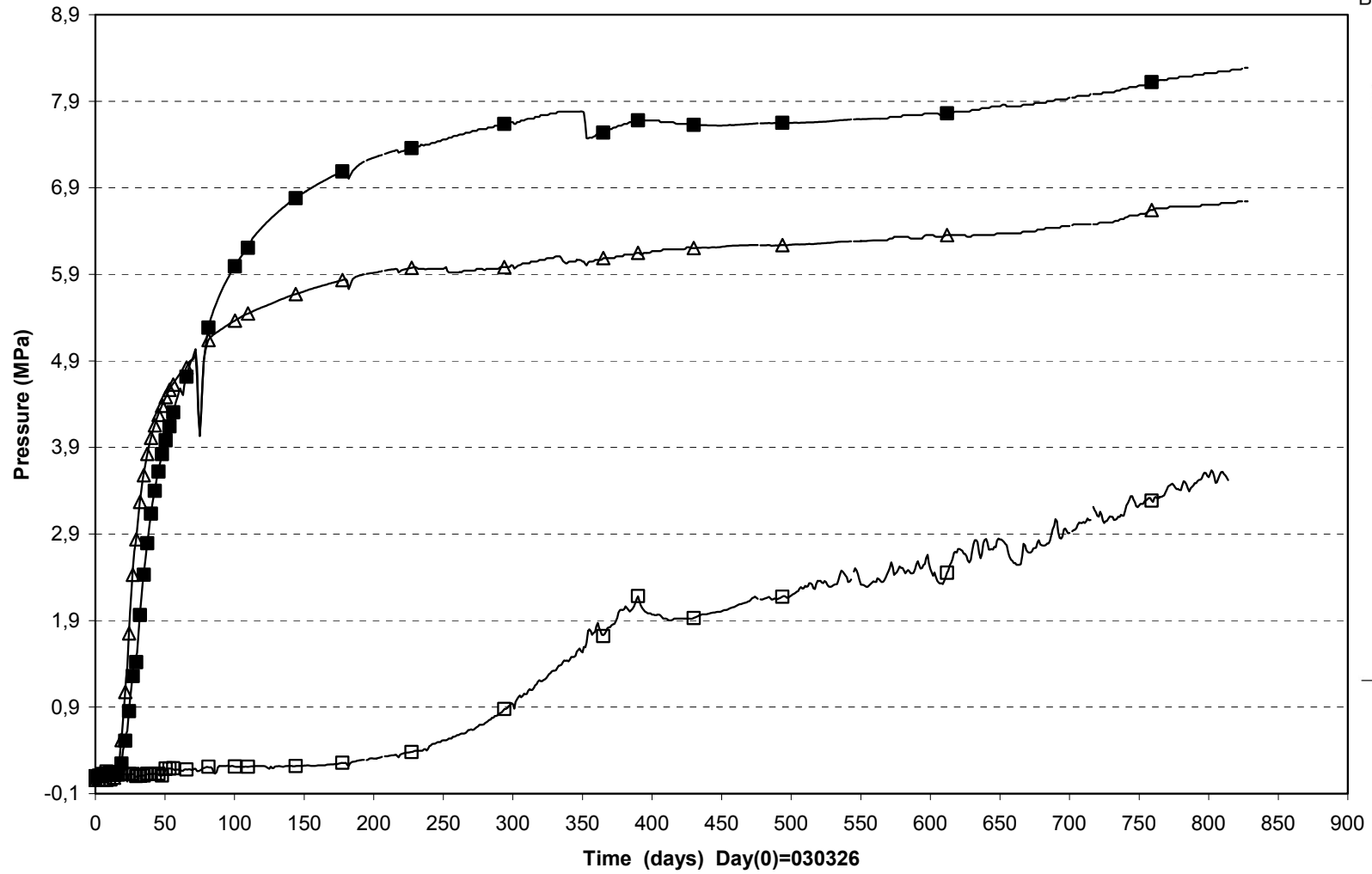
Total pressure/R3 (030326-050701)
Geokon



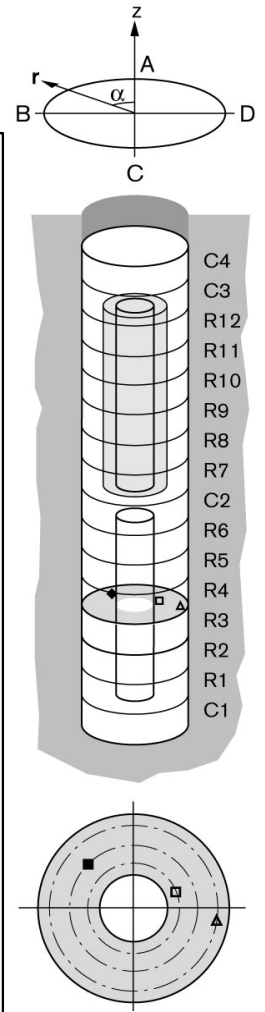
□ PB207(1.950\20°\0.535\T) ■ PB209(1.950\100°\0.635\T) △ PB210(1.950\170°\0.710\T)



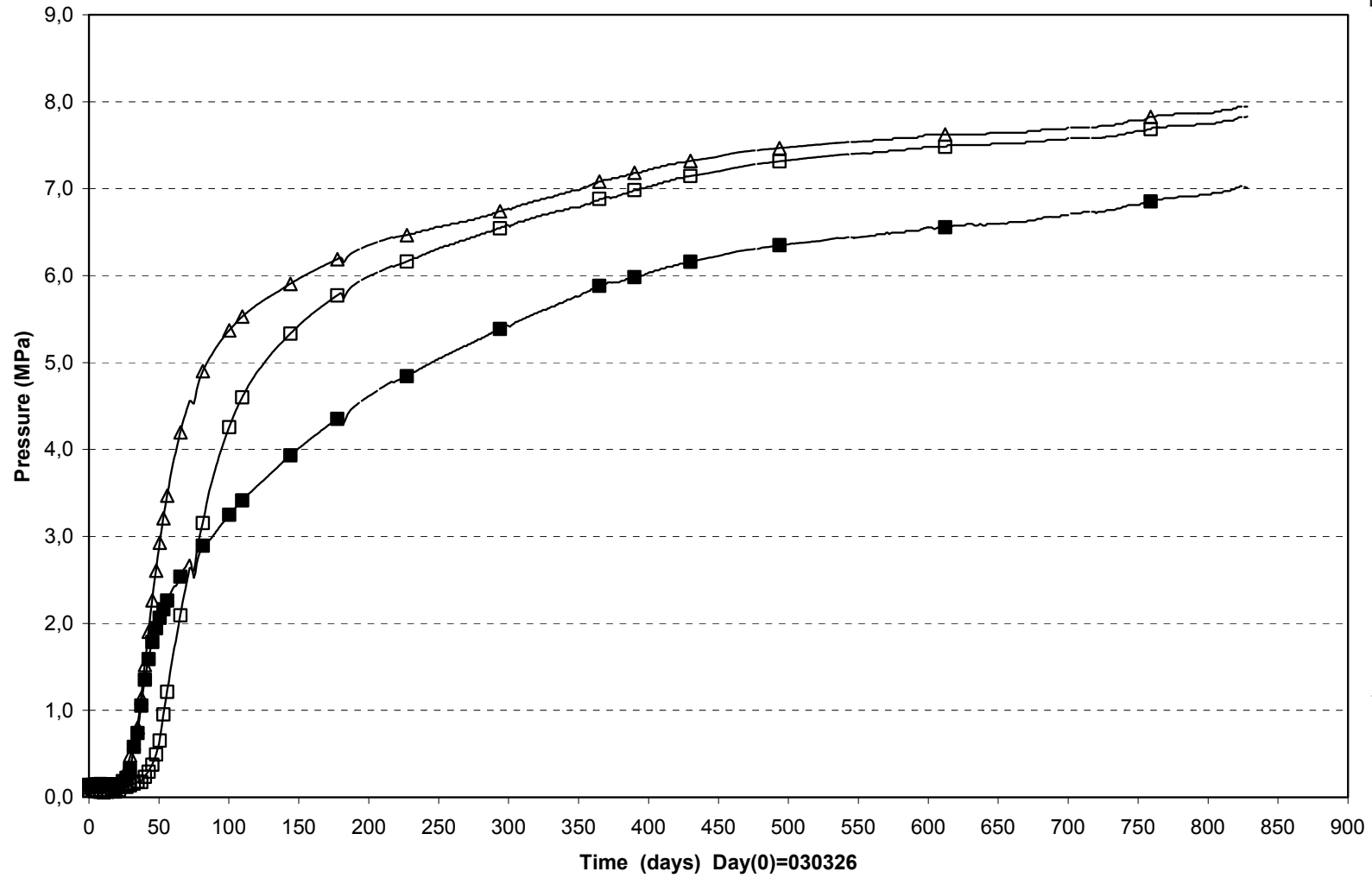
Total pressure/R3 (030326-050701)
Geokon



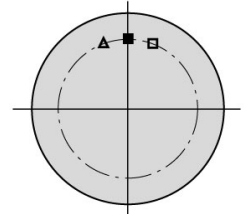
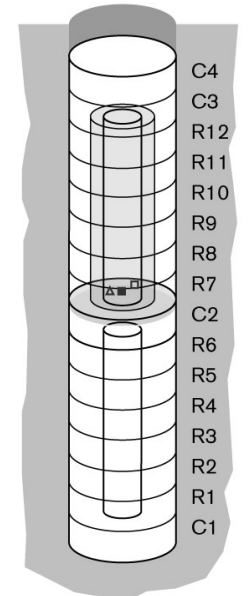
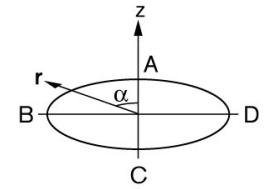
□ PB205(2.000\290°\0.420\A) ■ PB208(2.000\45°\0.585\A) △ PB212(2.000\260°\0.748\A)



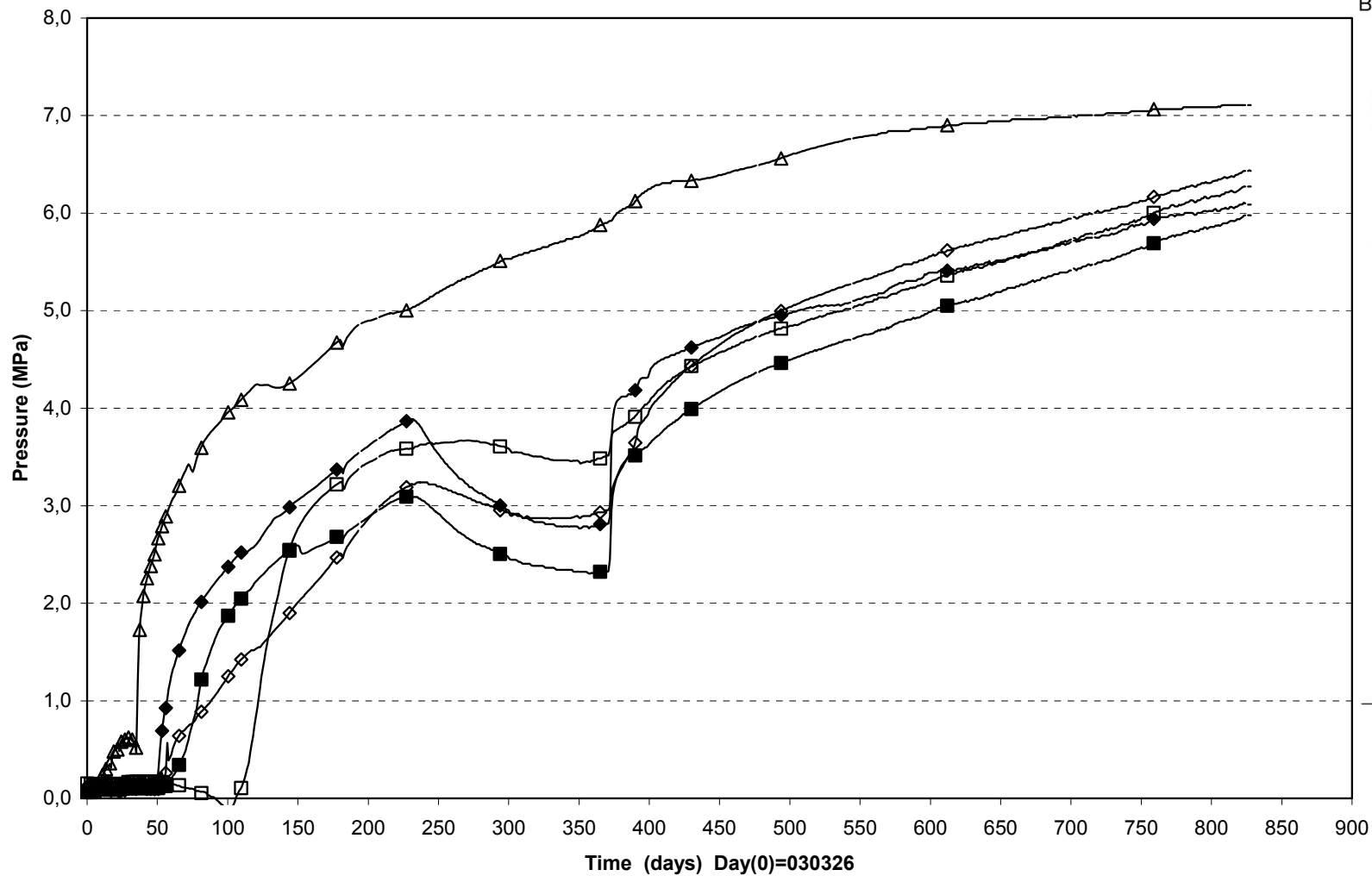
Total pressure/Cyl.2 (030326-050701)
Geokon



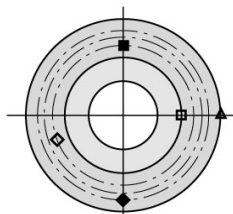
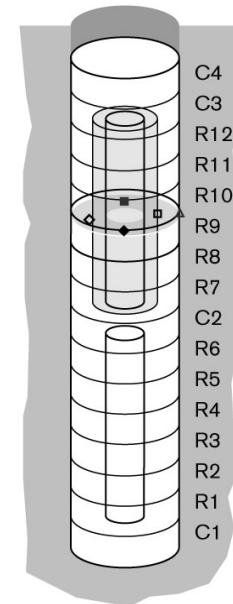
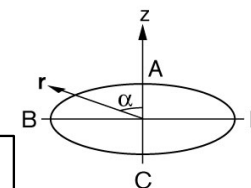
□ PB214(4.000\340°\0.635\A) ■ PB215(3.950\0°\0.635\R) Δ PB216(3.950\20°\0.635\T)



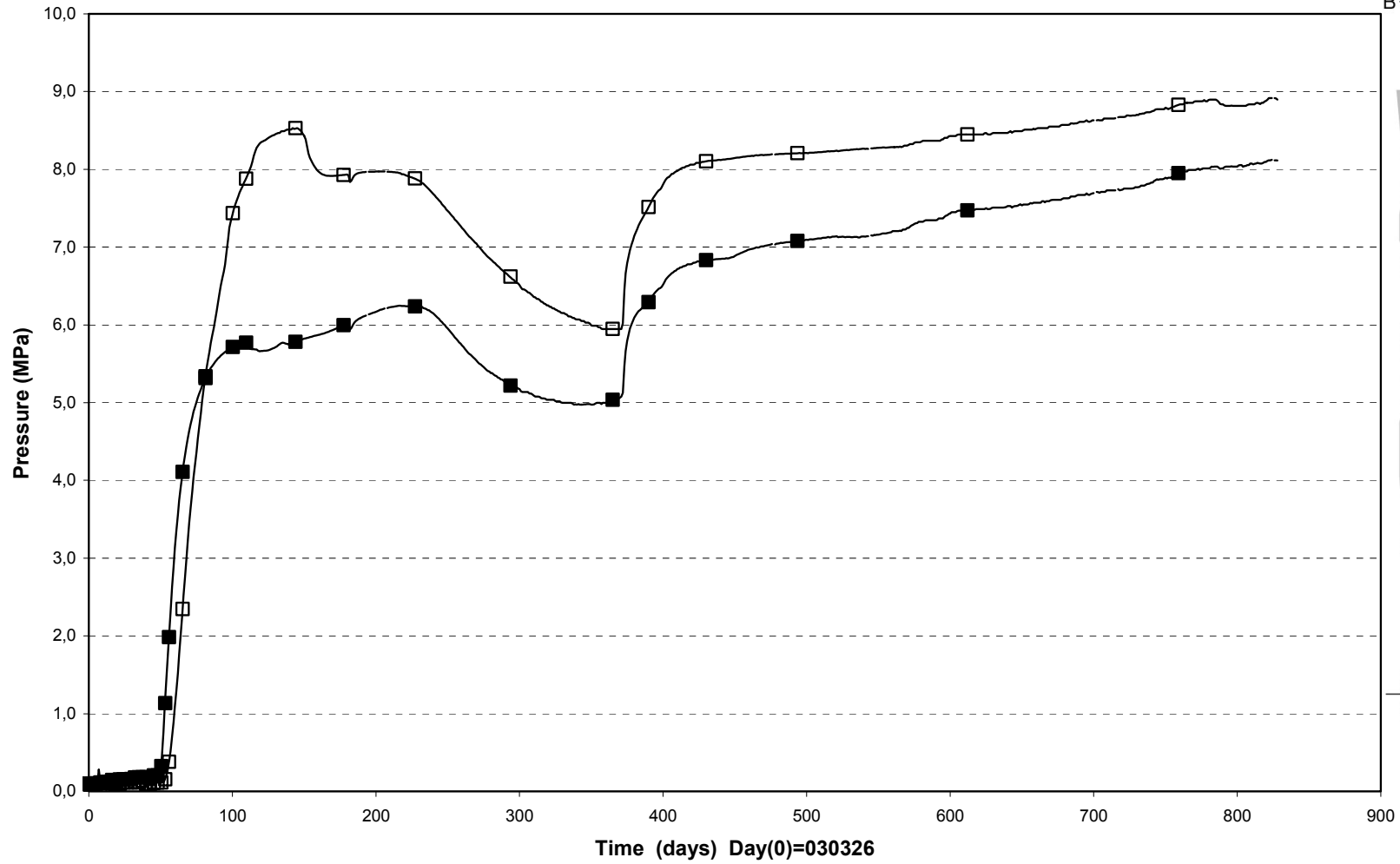
Total pressure/Ring 9 (030326-050701)
Geokon



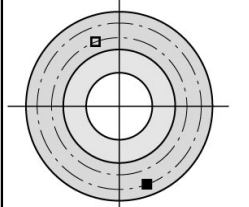
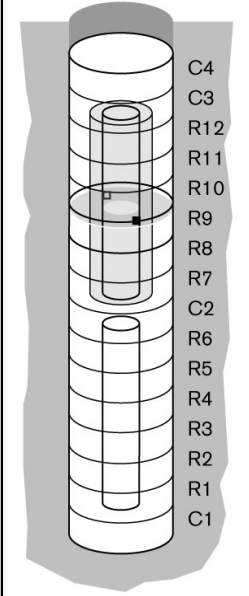
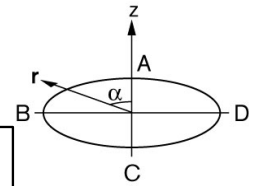
□ PB217(5.450\270°\0.535\R) ■ PB219(5.450\0°\0.635\R) ◇ PB222(5.450\110°\0.710\R) ◆ PB224(5.450\180°\0.770\R) △ PB226(5.450\270°\0.875\R)



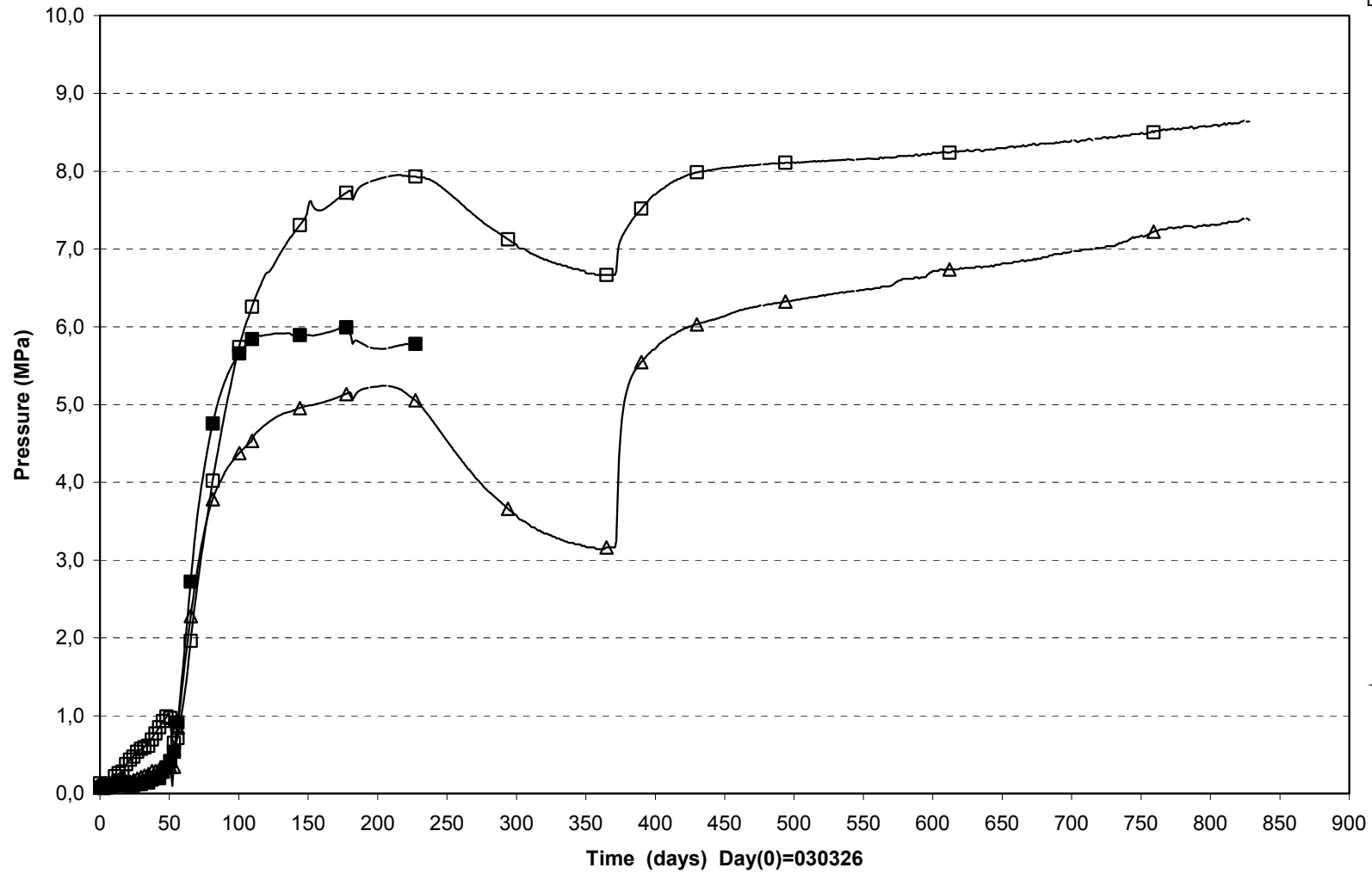
Total pressure/Ring 9 (030326-050701)
Geokon



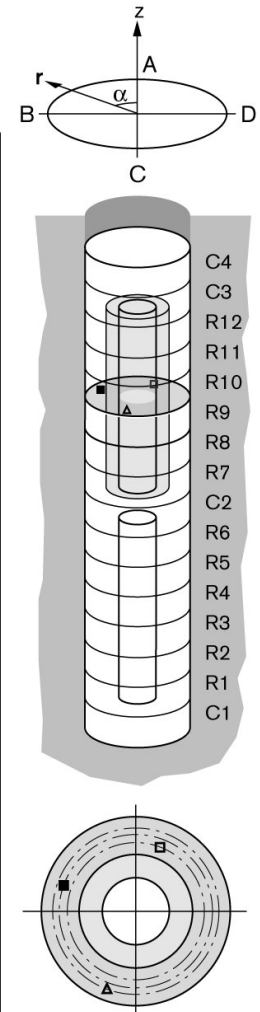
□ PB220(5.450\20°\0.635\T) ■ PB225(5.450\200°\0.740\T)



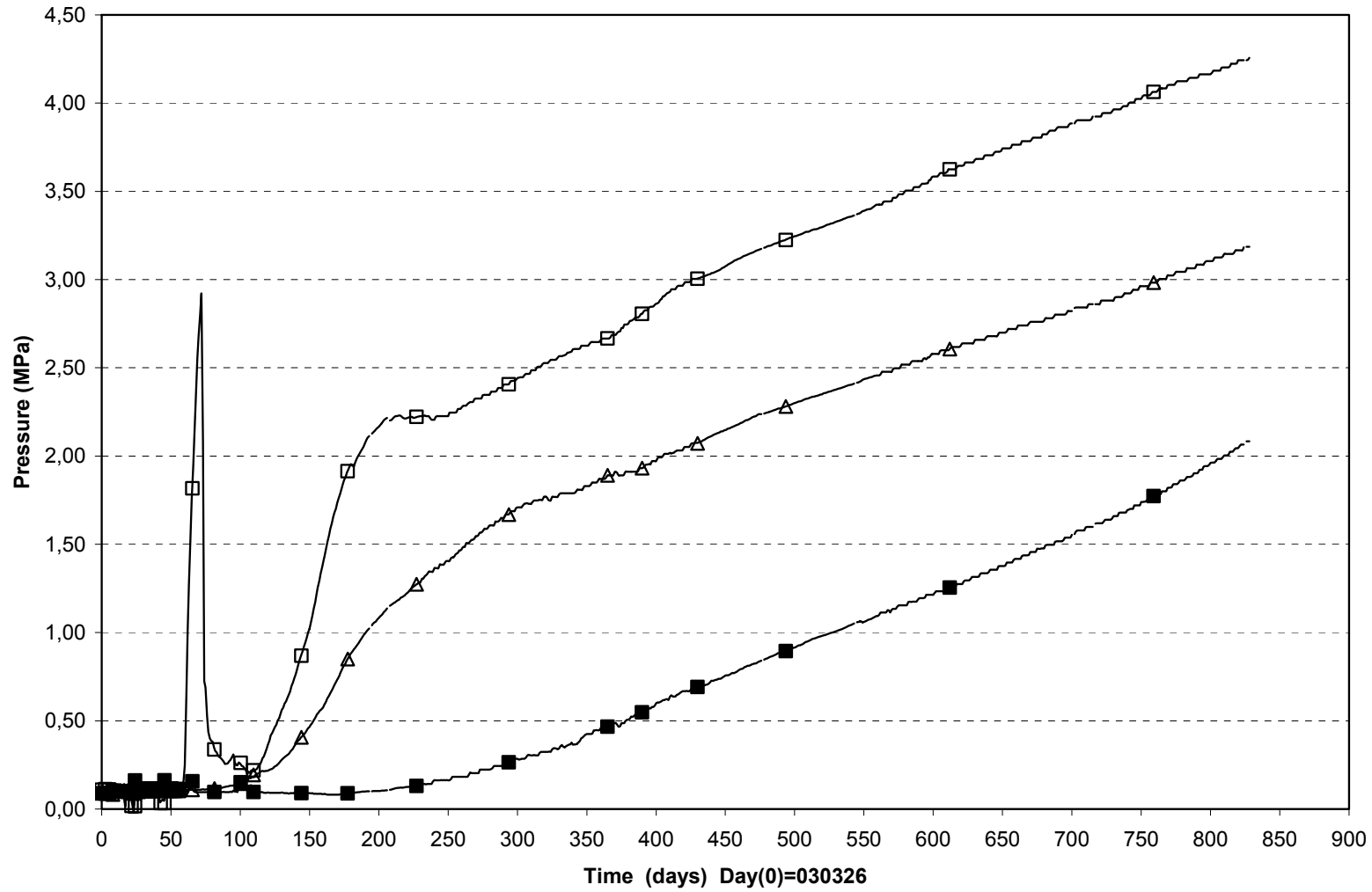
Total pressure/R9 (030326-050701)
Geokon



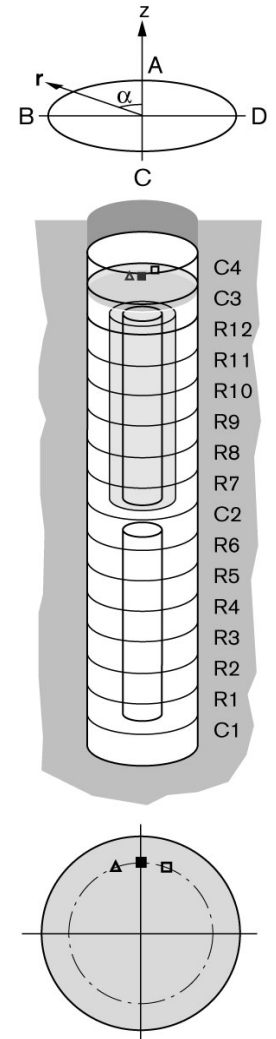
□ PB218(5.500\340°\0.635\A) ■ PB221(5.500\70°\0.710\A) △ PB223(5.500\160°\0.745\A)



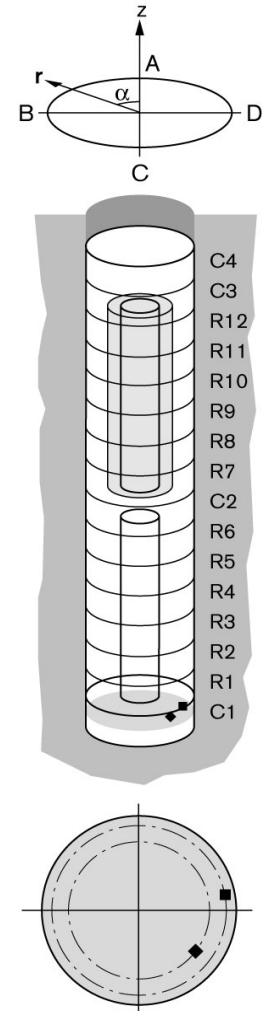
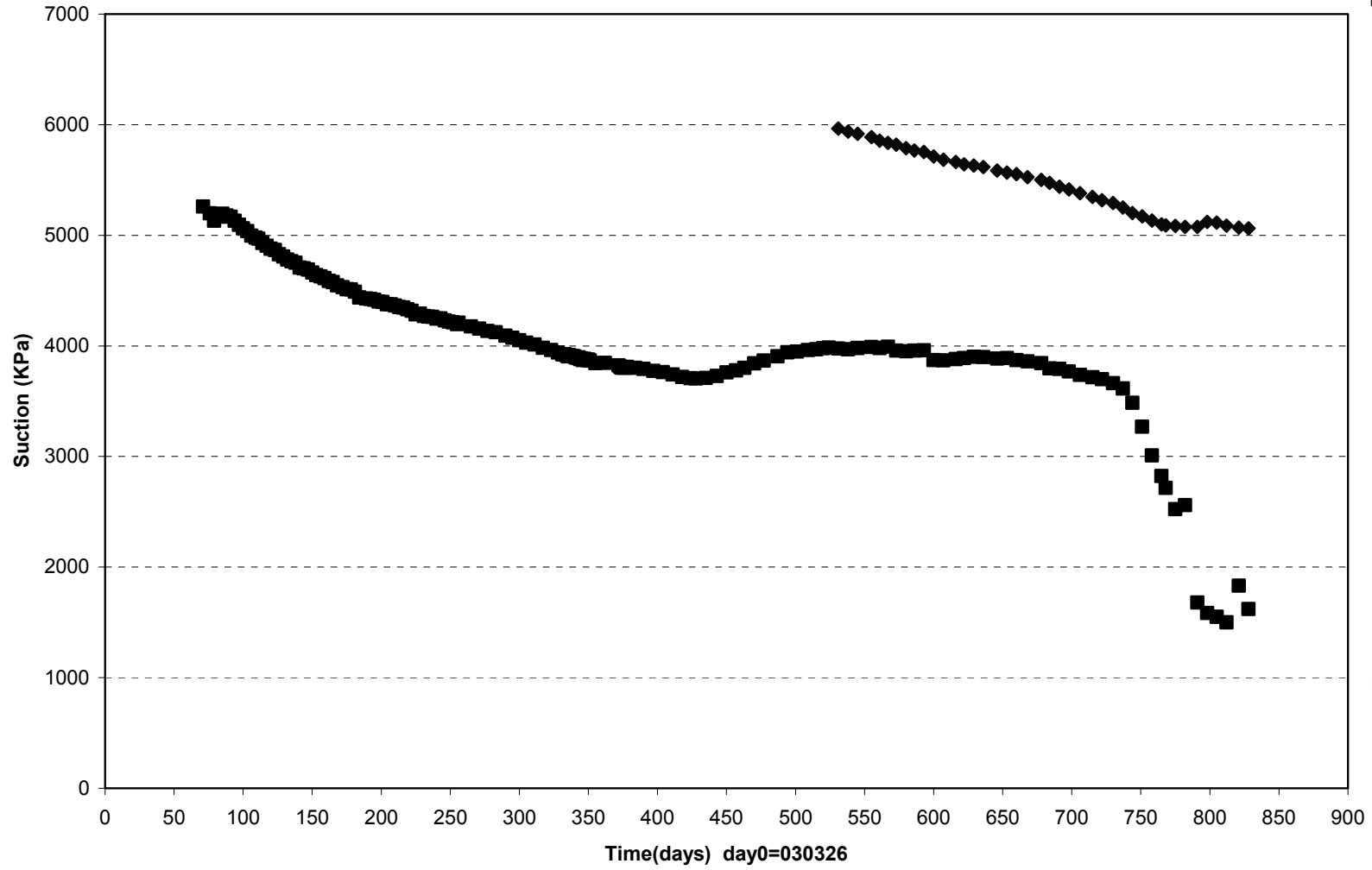
**Total pressure/Cyl.3 (030326-050701)
Geokon**



□ PB227(7.500\340°\0.635\A) ■ PB228(7.450\0°\0.635\R) △ PB229(7.450\20°\0.635\T)

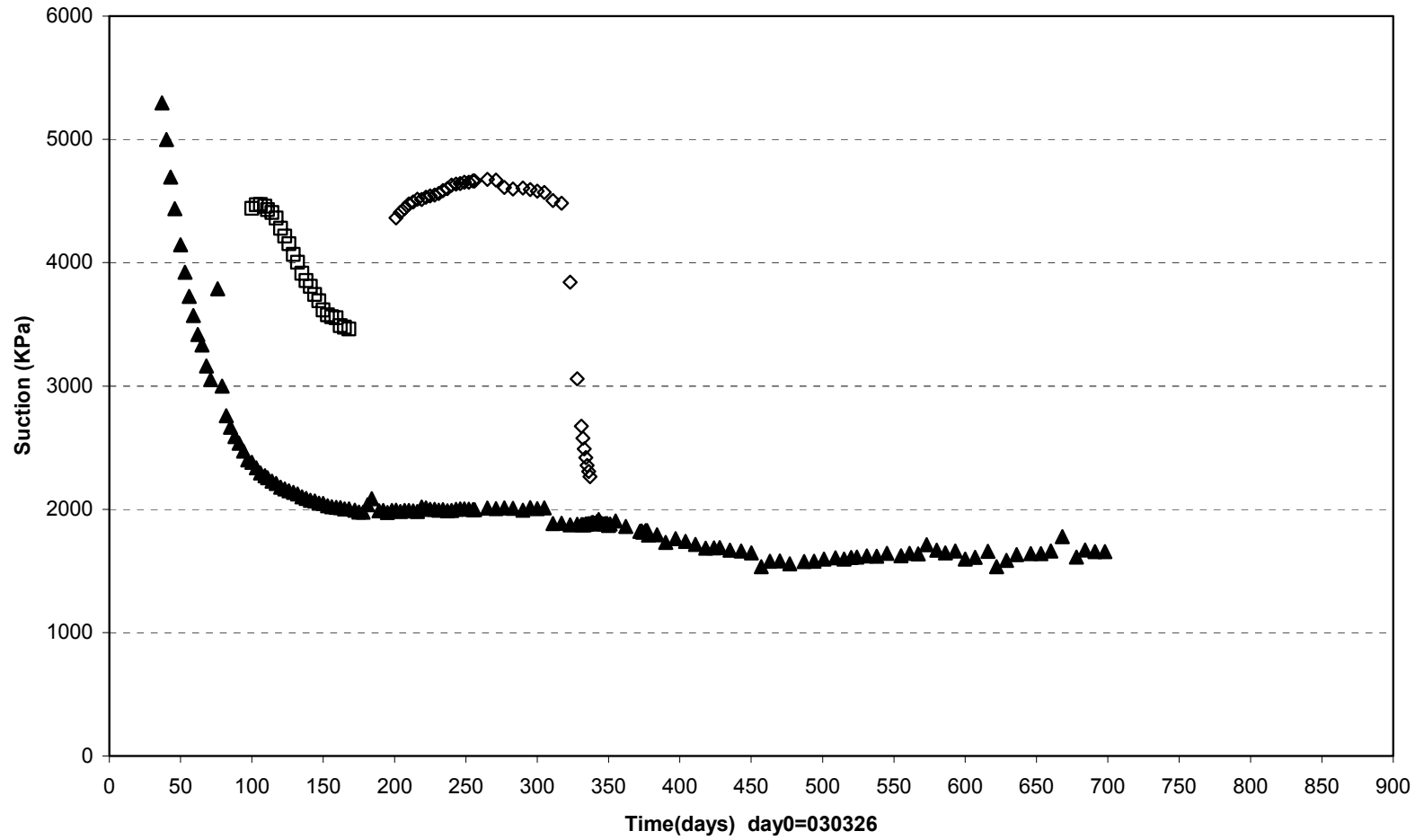


TBT\ Cyl.1 (030326-050701)
Suction - Wescor

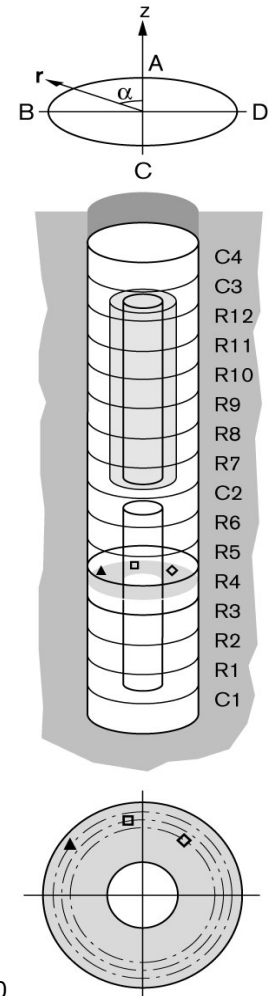


◆ WB203(250\235°\635) ■ WB205(250\280°\785)

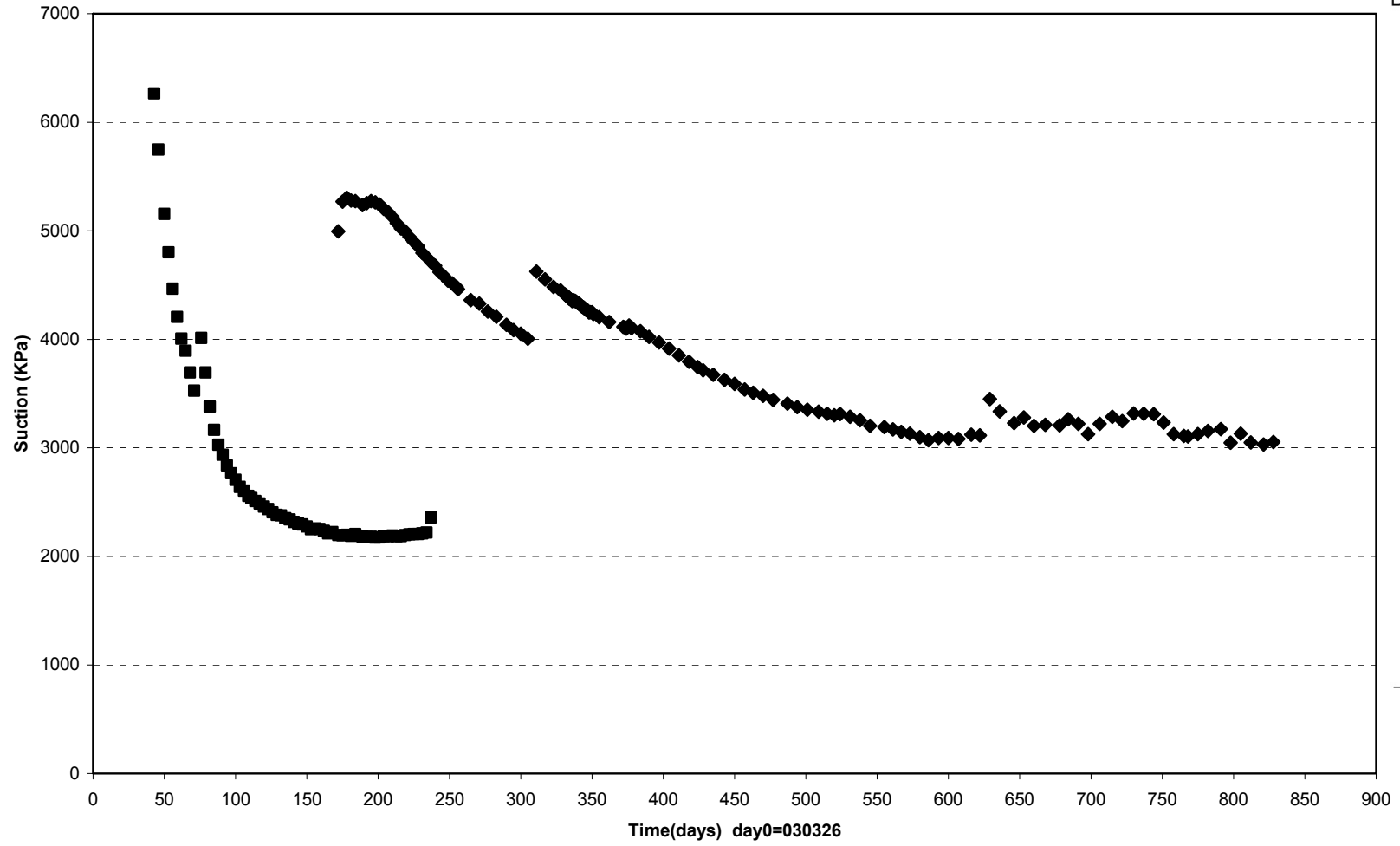
TBT\ Ring 4 (030326-050701)
Suction - Wescor



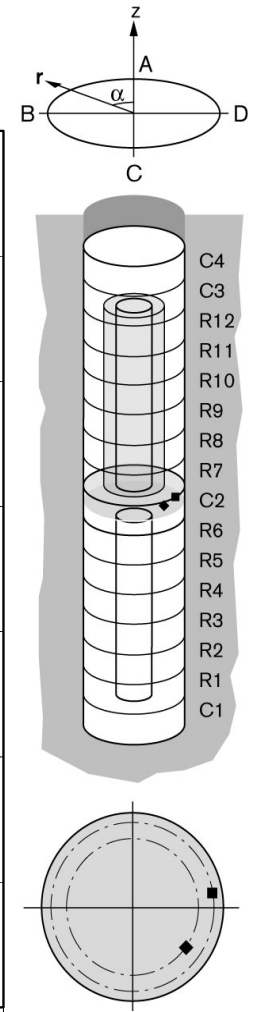
◇ WB211(2250\325°\635) □ WB213(2250\10°\710) ▲ WB215(2250\55°\785)



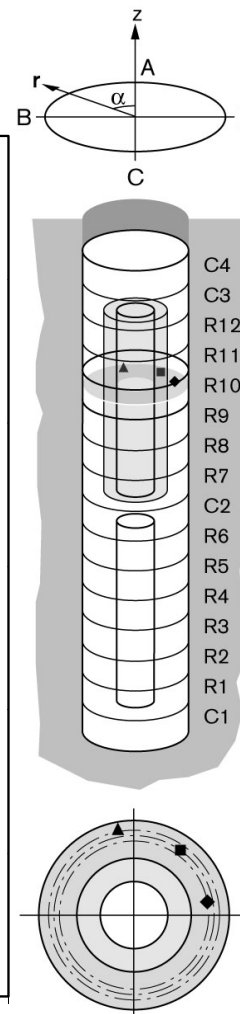
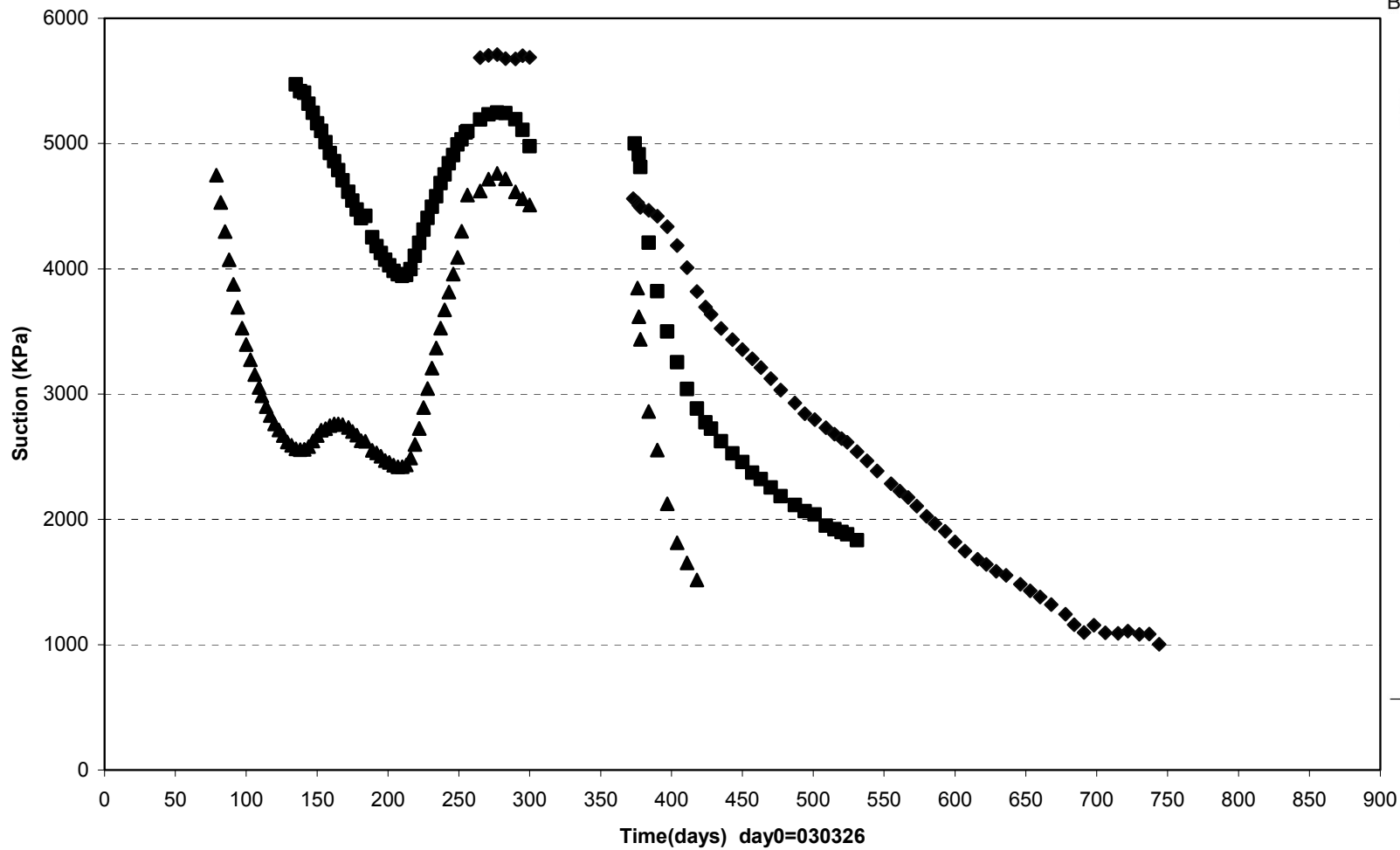
TBT\ Cyl.2 (030326-050701)
Suction - Wescor



◆ WB218(3750\235°\635) ■ WB220(3750\280°\785)

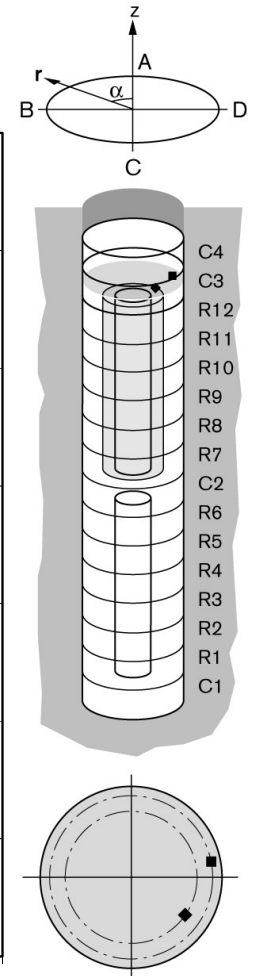
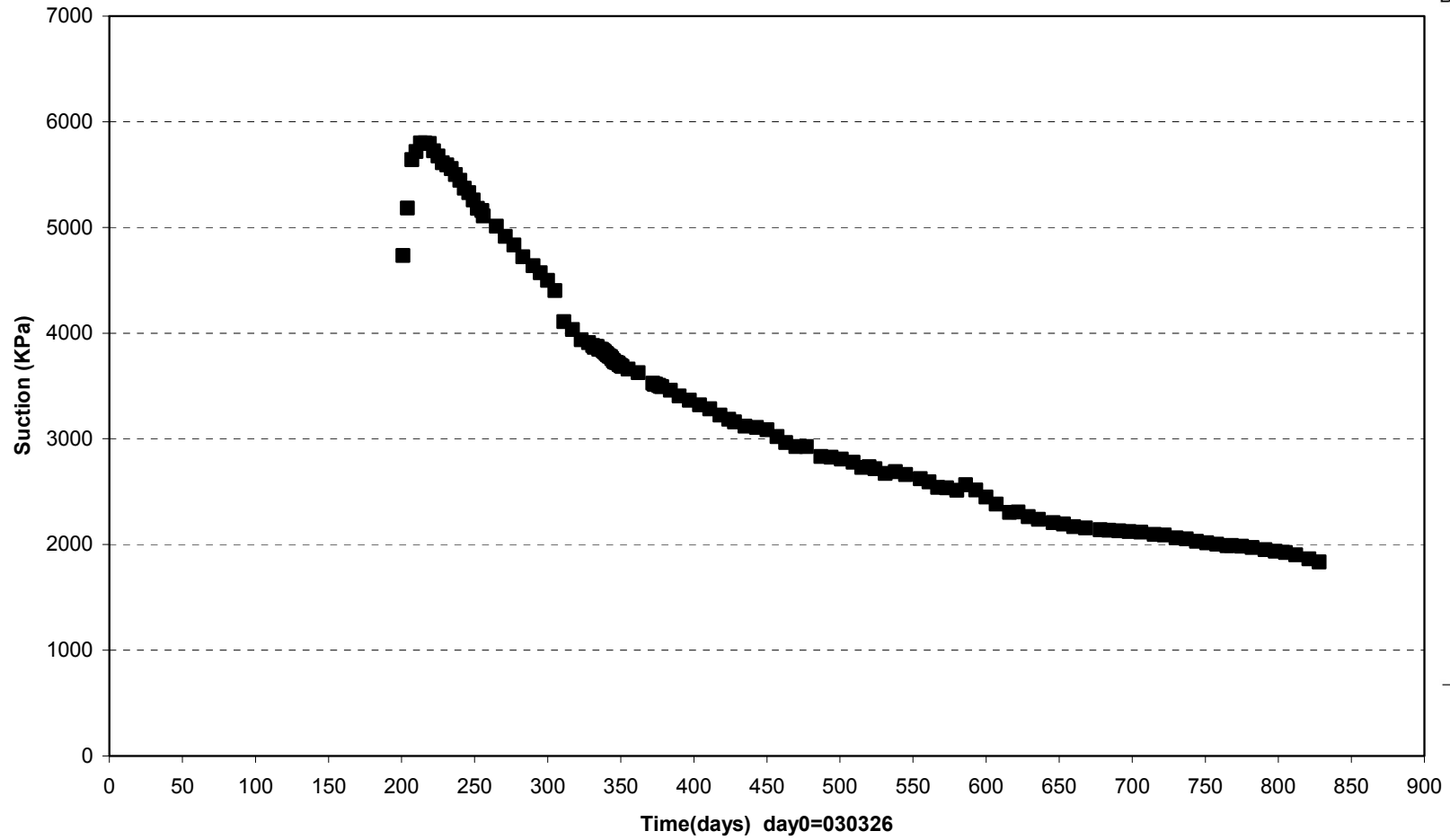


TBT\ Ring 10 (030326-050701)
Suction - Wescor



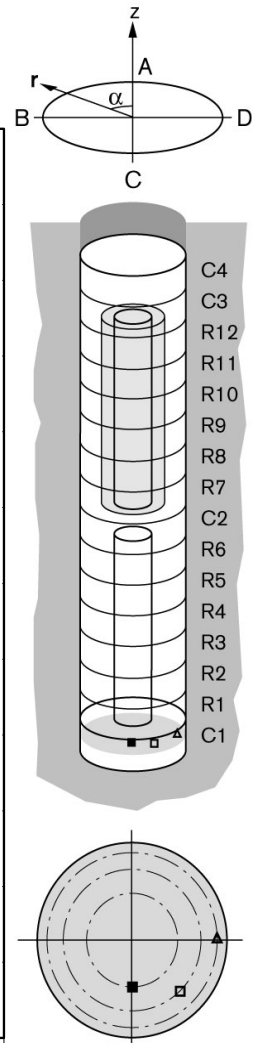
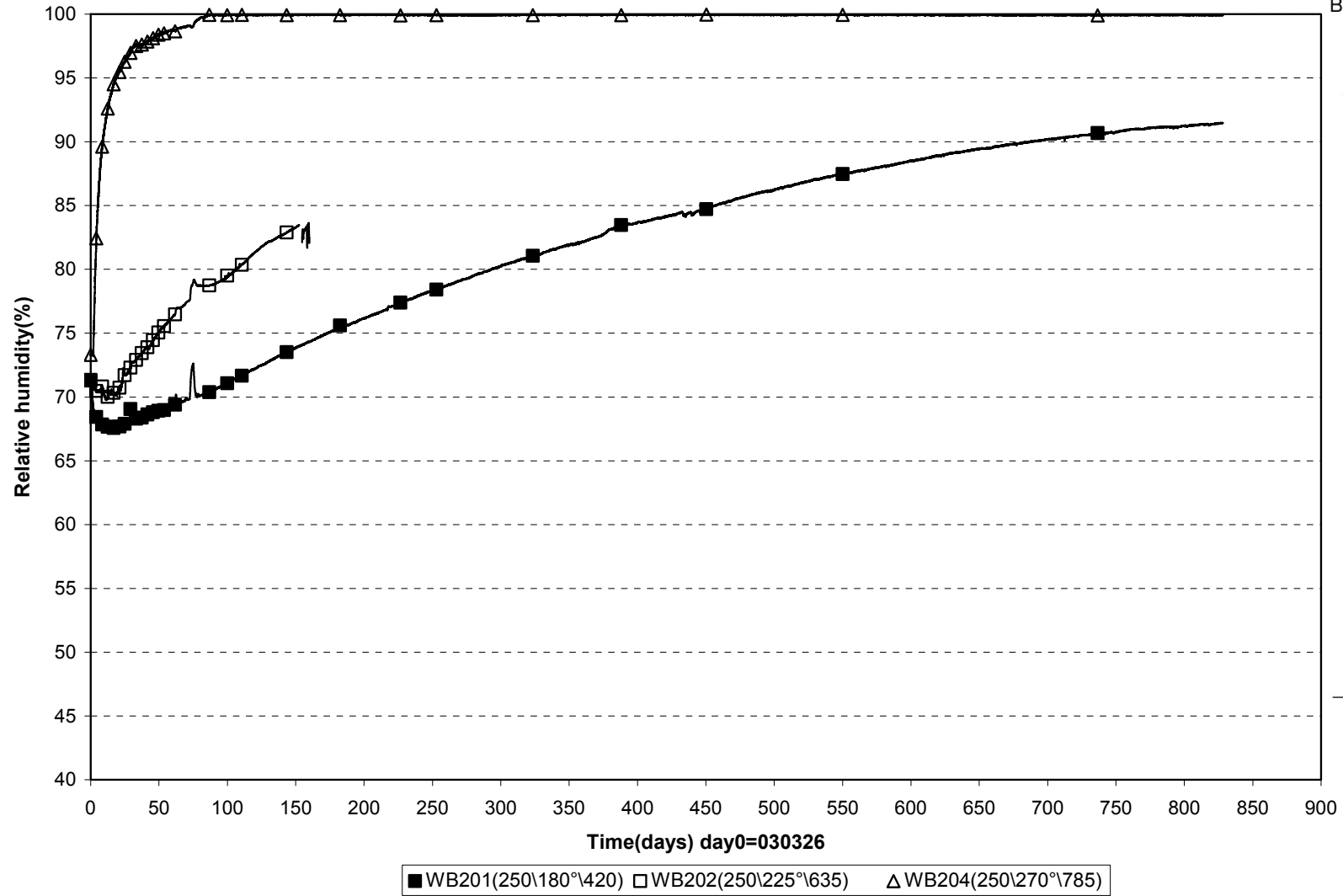
◆ WB226(5750\280°\685) ■ WB228(5750\325°\735) ▲ WB230(5750\10°\785)

TBT Cyl.3 (030326-050701)
Suction - Wescor

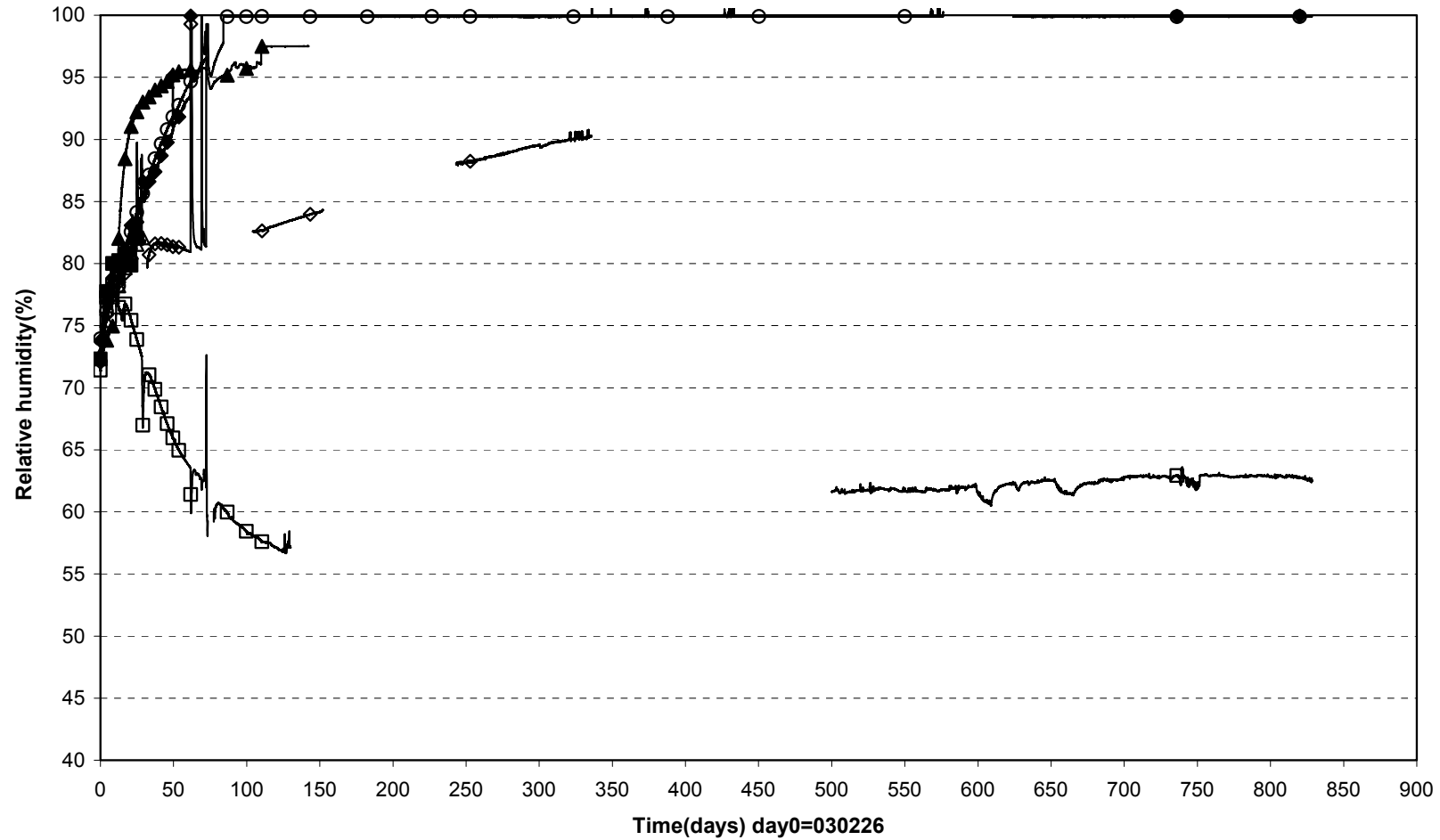


◆ WB233(7250\235°\635) ■ WB235(7250\280°\785)

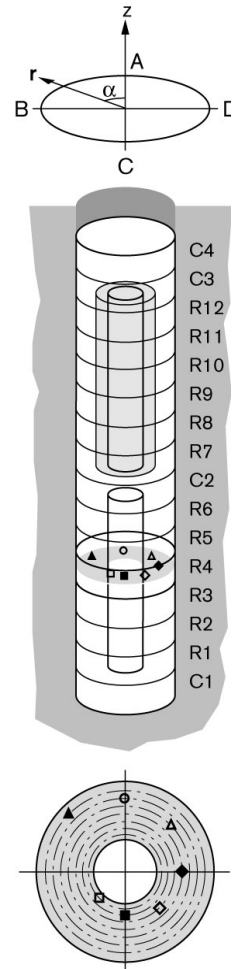
TBT\Cyl.1 (030326-050701)
 Relative humidity - Vaisala & Rotronic

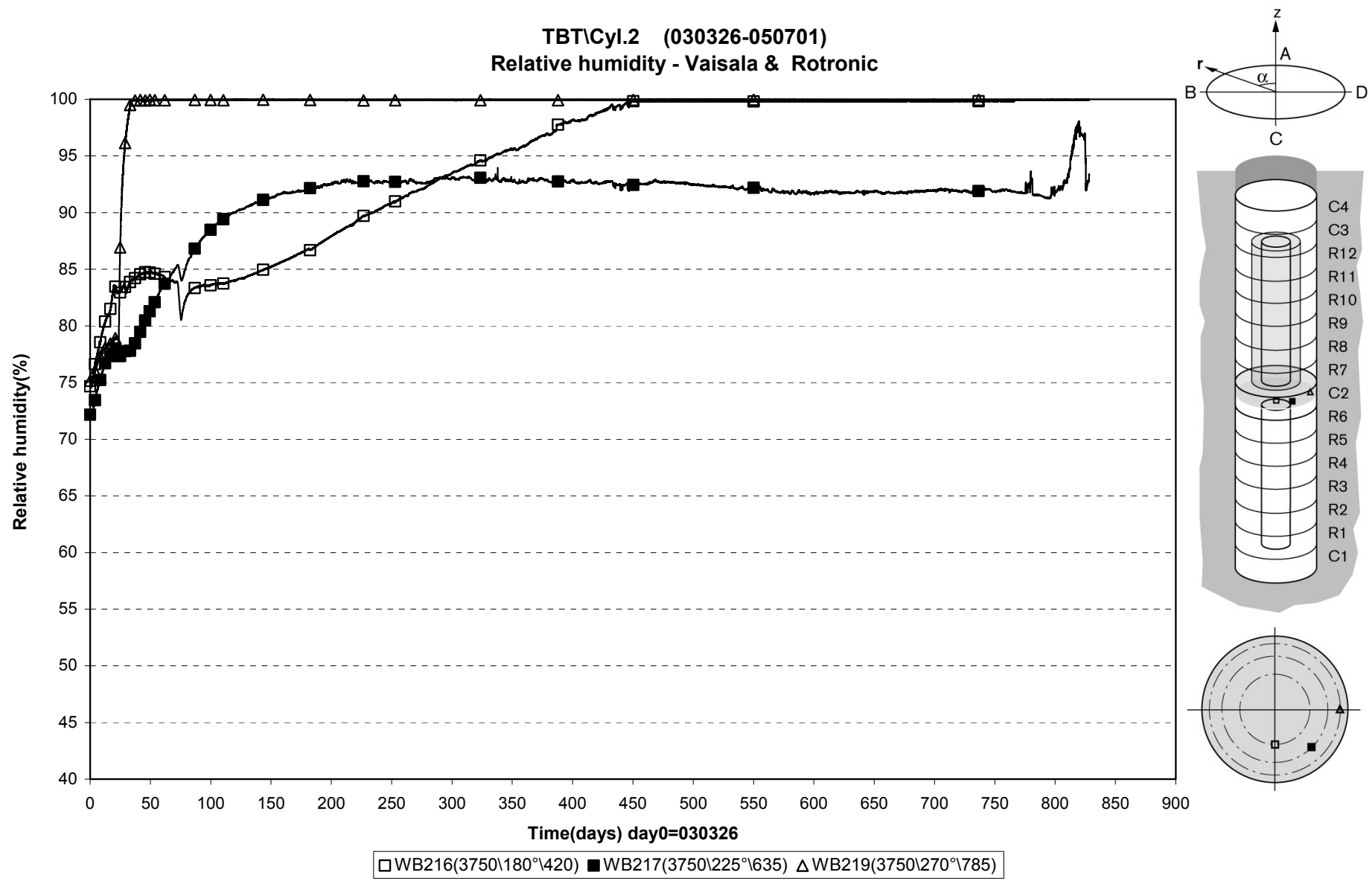


TBT\ Ring 4 (030326-050701)
 Relative humidity - Vaisala & Rotronic

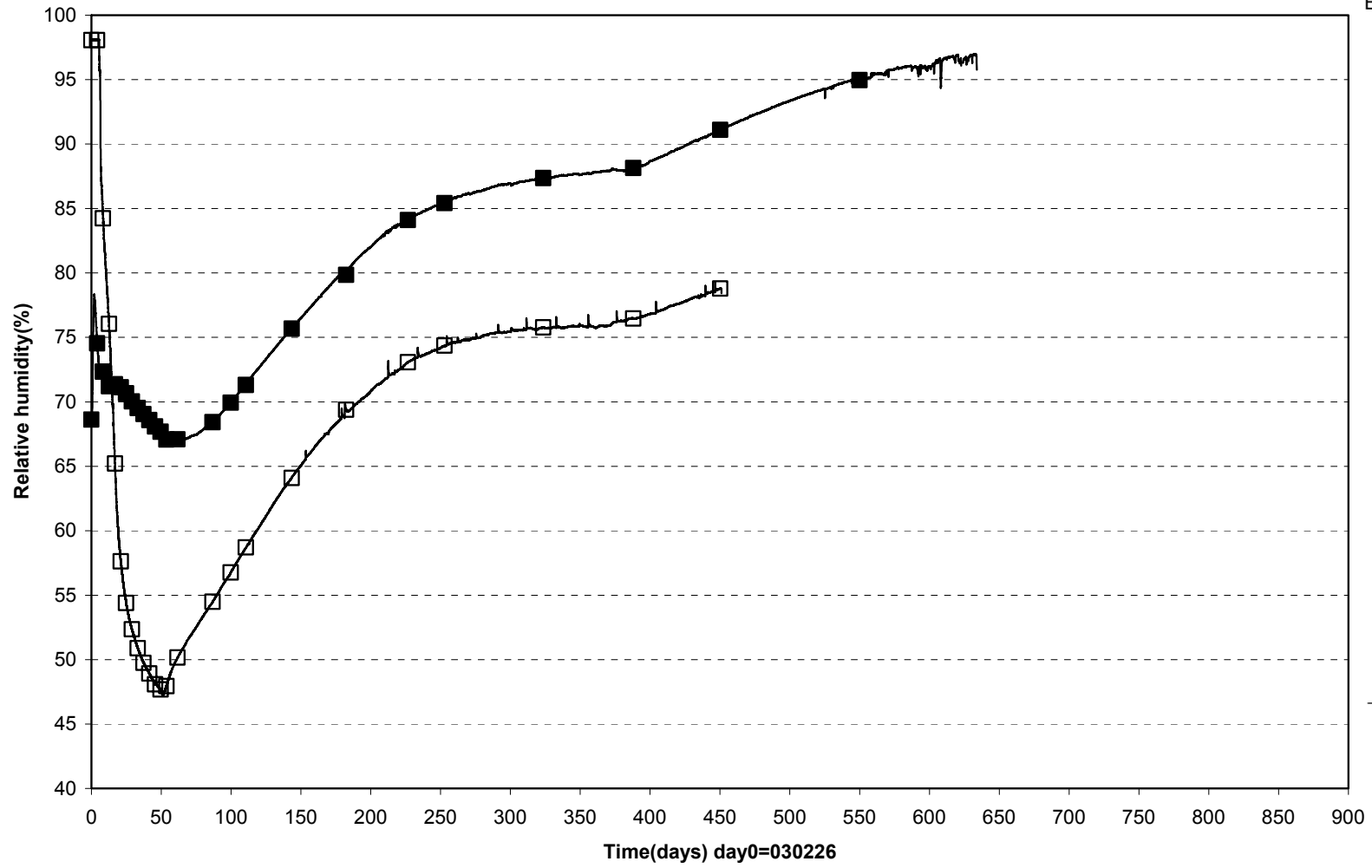


□ WB206(2250\135°\360) ■ WB207(2250\180°\420) ◇ WB208(2250\225°\485) ◆ WB209(2250\270°\560) △ WB210(2250\315°\635)
 ○ WB212(2250\0°\710) ▲ WB214(2250\45°\785)

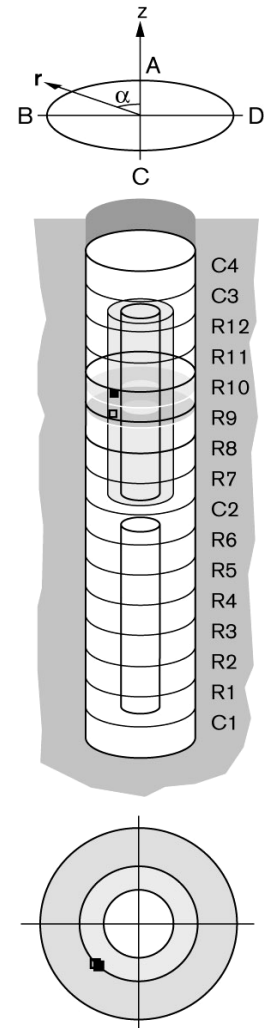




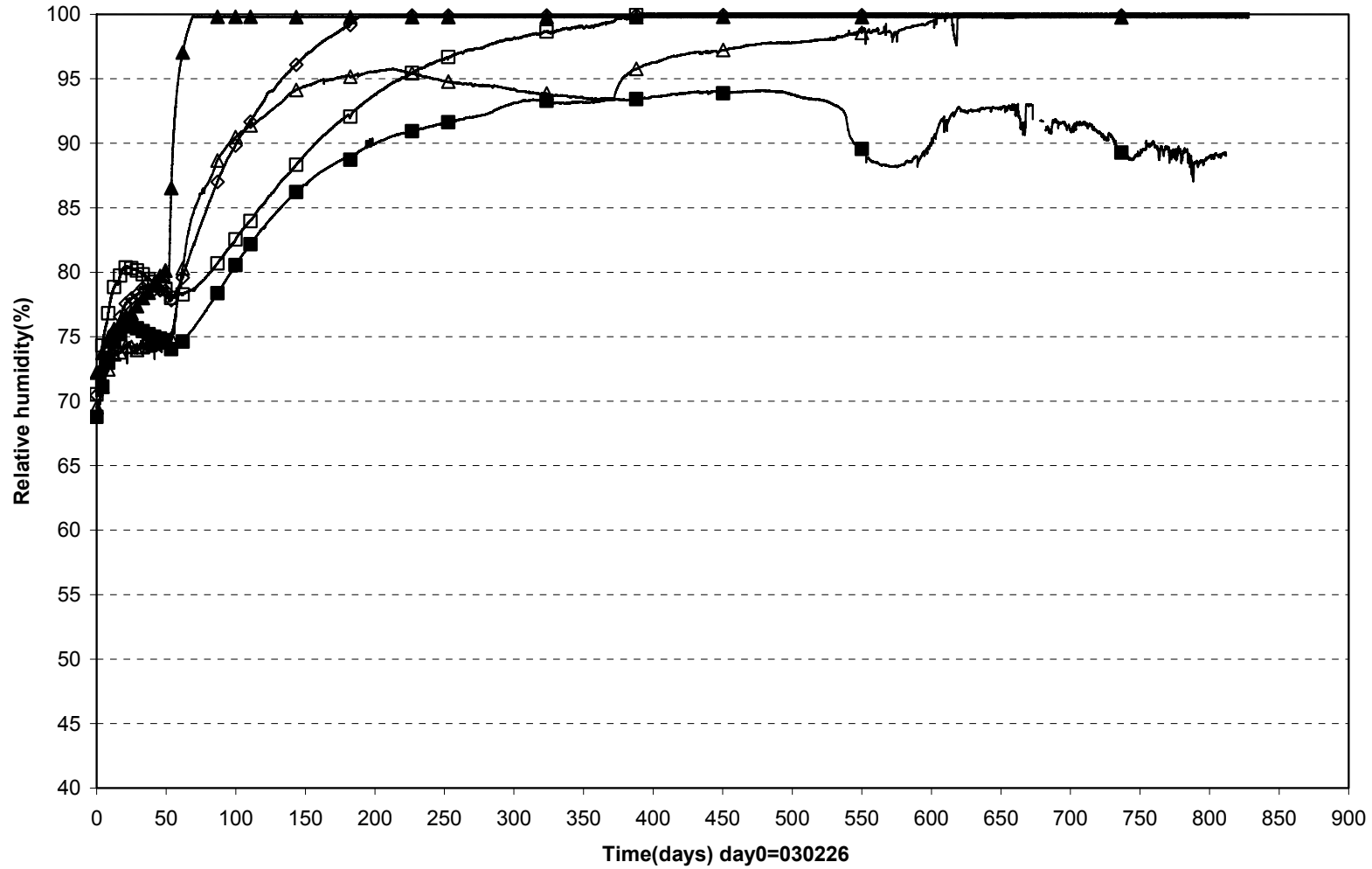
TBT\ Ring 9-10 (030326-050701)
 Relative humidity - Vaisala & Rotronic



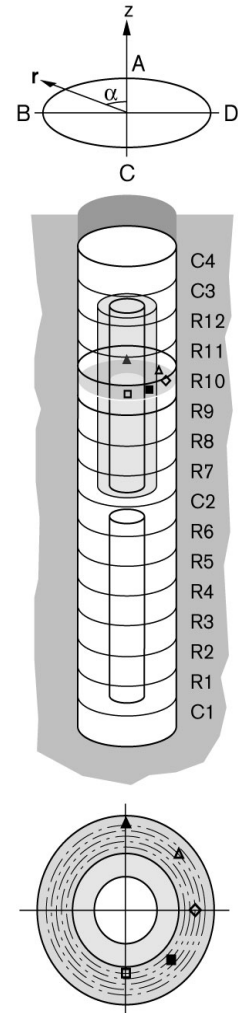
□ WB221(5250\135°\525) ■ WB222(5750\135°\525)



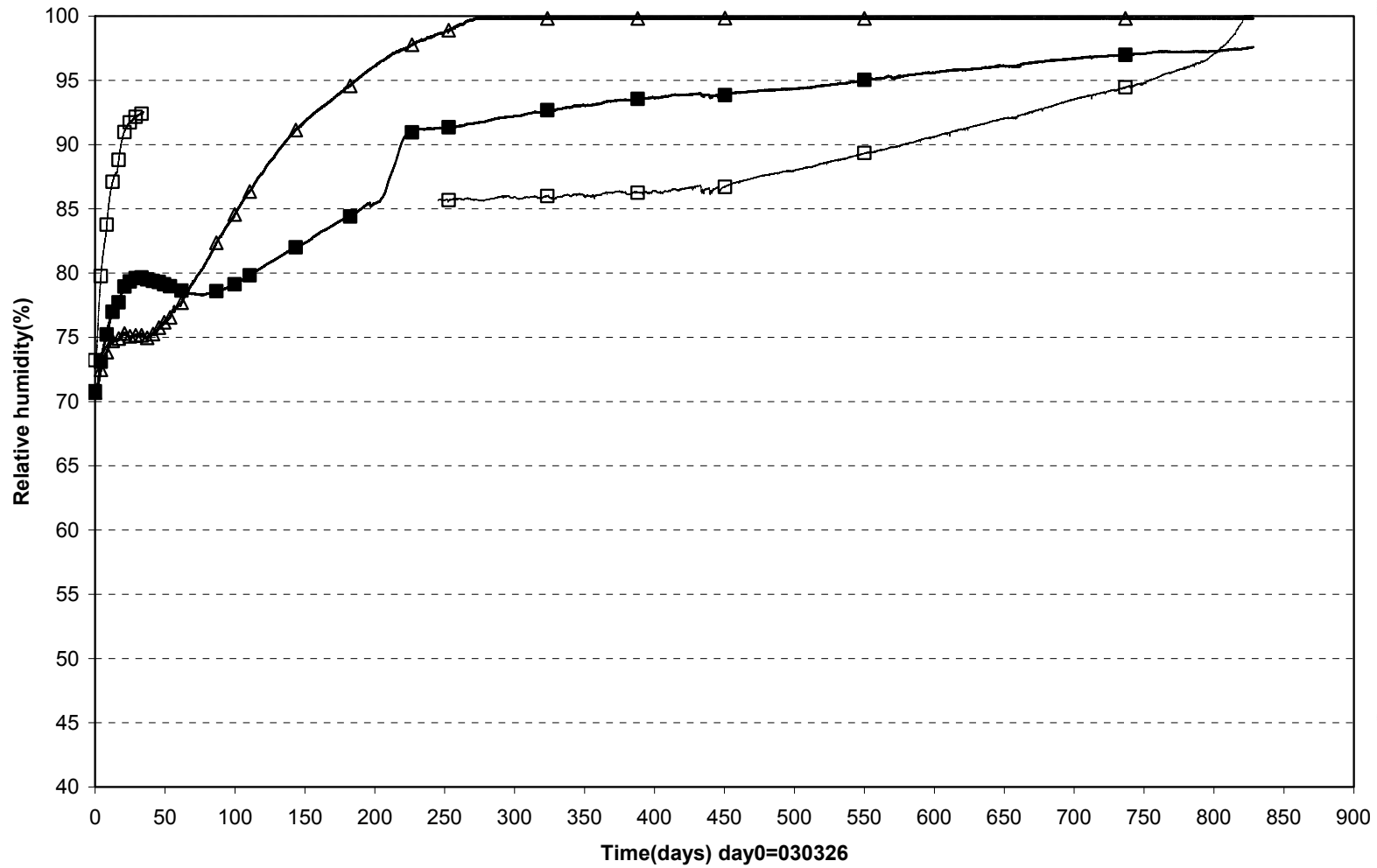
TBT\ Ring 10 (030326-050701)
Relative humidity - Vaisala & Rotronic



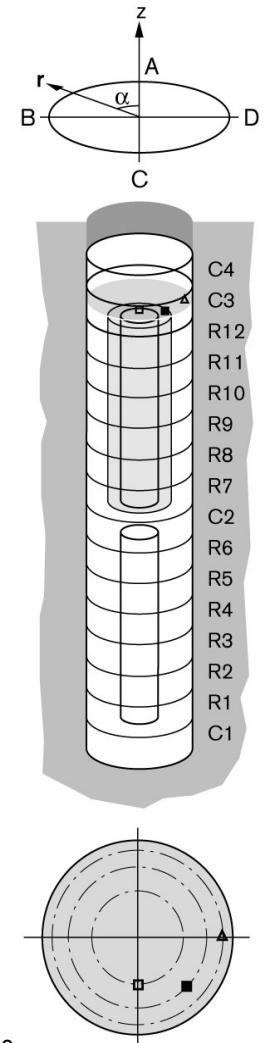
□ WB223(5750\180°\585) ■ WB224(5750\225°\635) ◇ WB225(5750\270°\685) △ WB227(5750\315°\735) ▲ WB229(5750\0°\785)



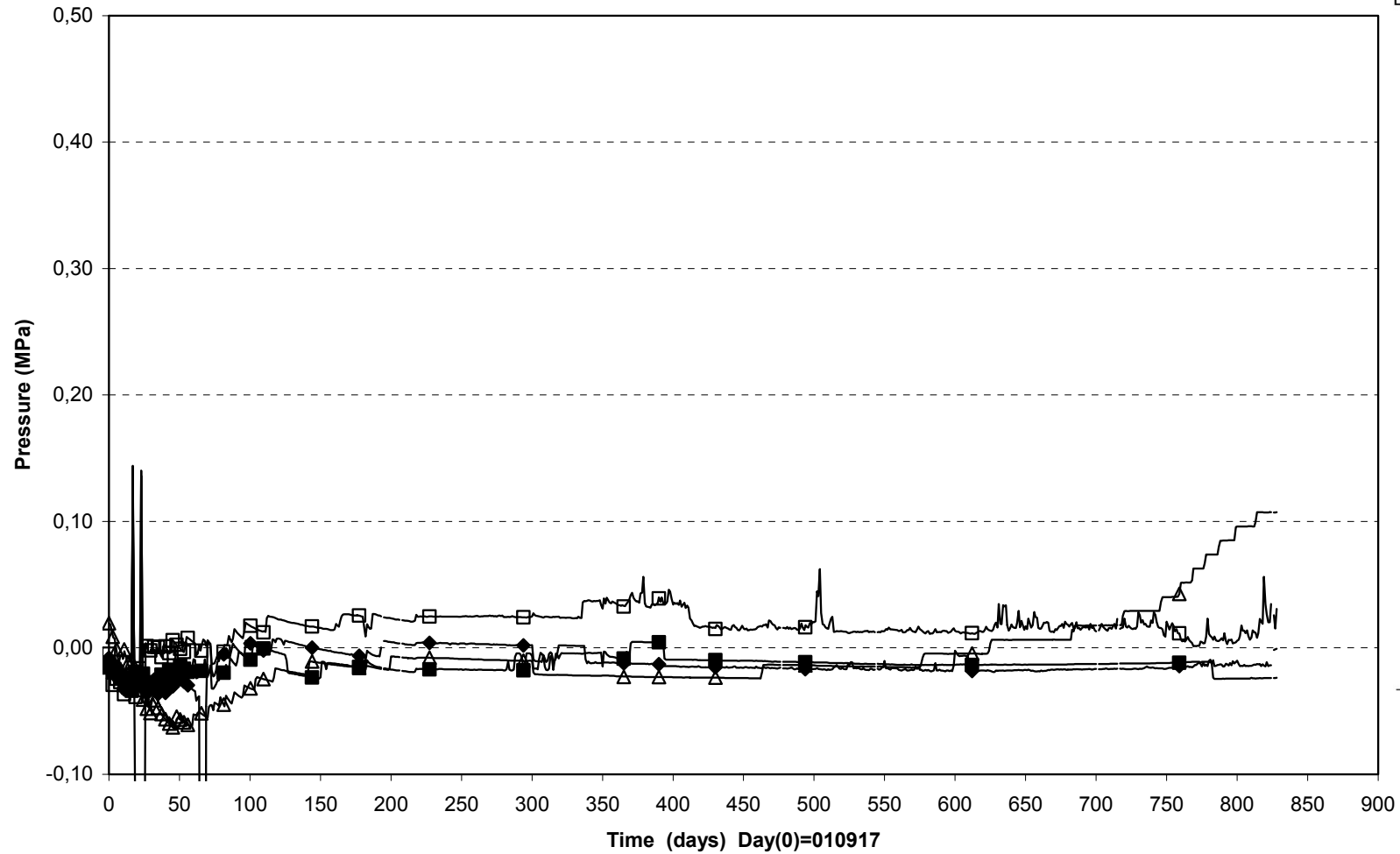
TBT\Cyl.3 (030326-050701)
 Relative humidity - Vaisala & Rotronic



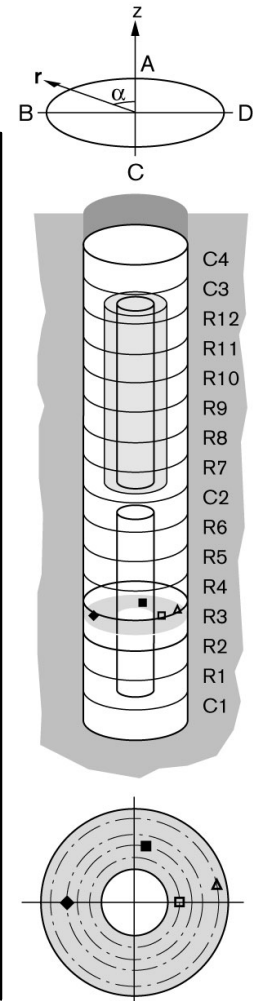
□ WB231(7250\ 180°\ 420) ■ WB232(7250\ 225°\ 635) △ WB234(7250\ 270°\ 785)



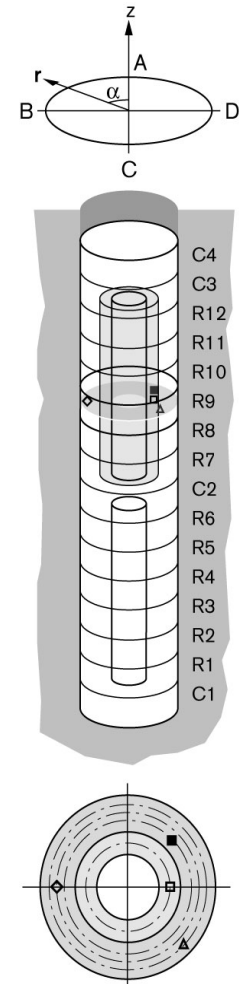
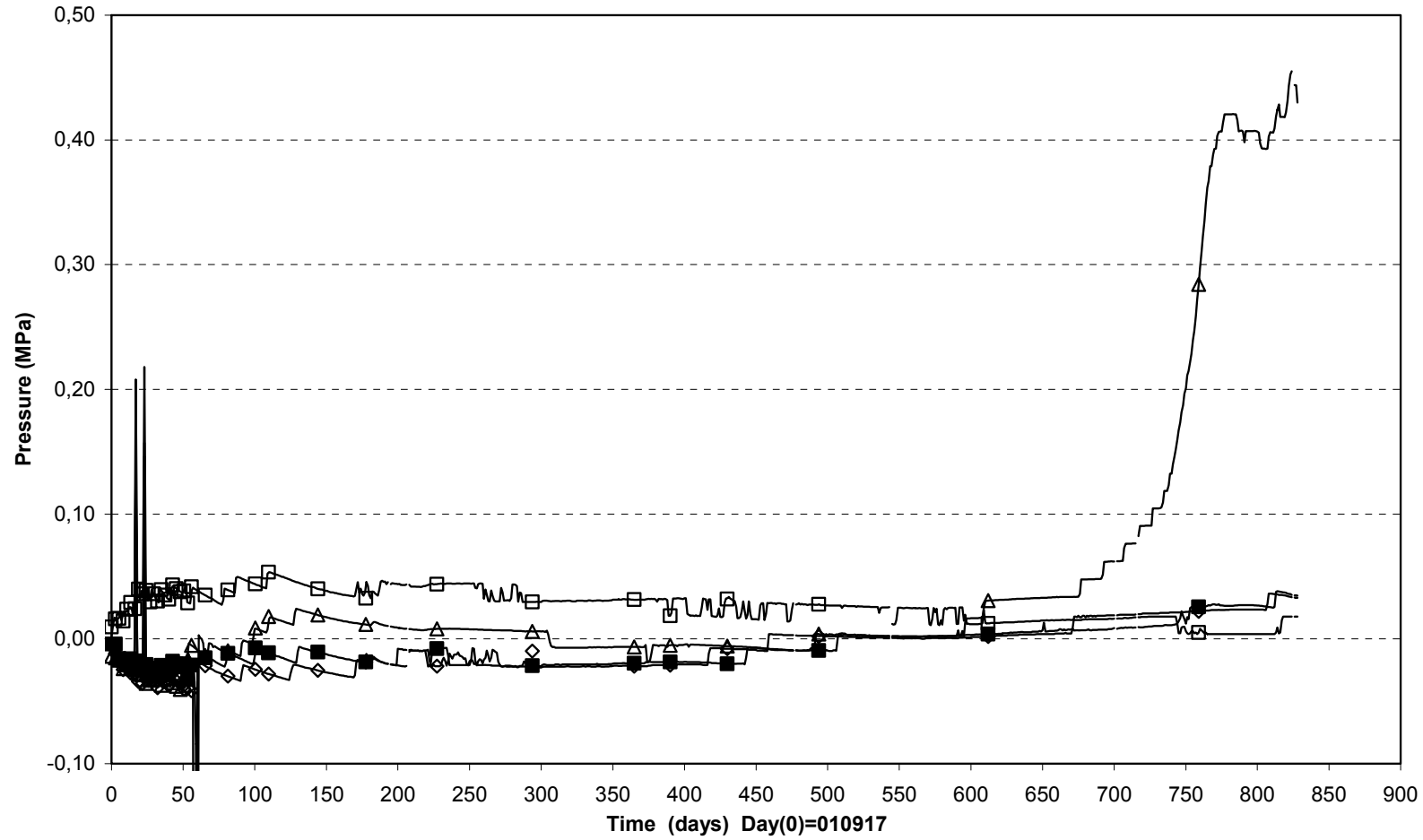
Pore pressure/Ring 3 (030326-050701)
Geokon



□ UB201(1.750\270°\0.420\R) ■ UB202(1.750\350°\0.535\R) ◆ UB203(1.750\90°\0.635) △ UB204(1.750\280°\0.785)

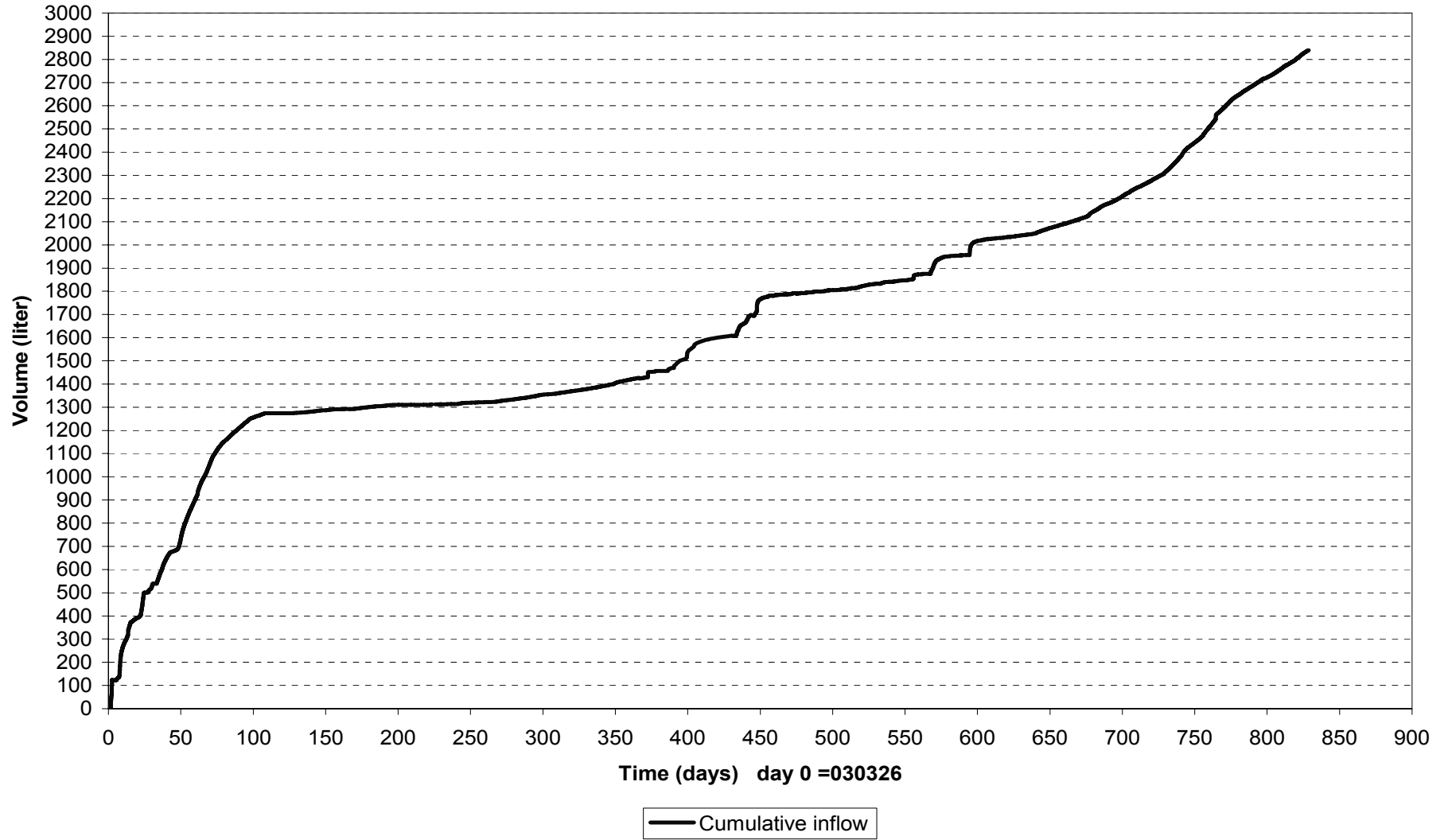


Pore pressure/Ring 9 (030326-050701)
Geokon

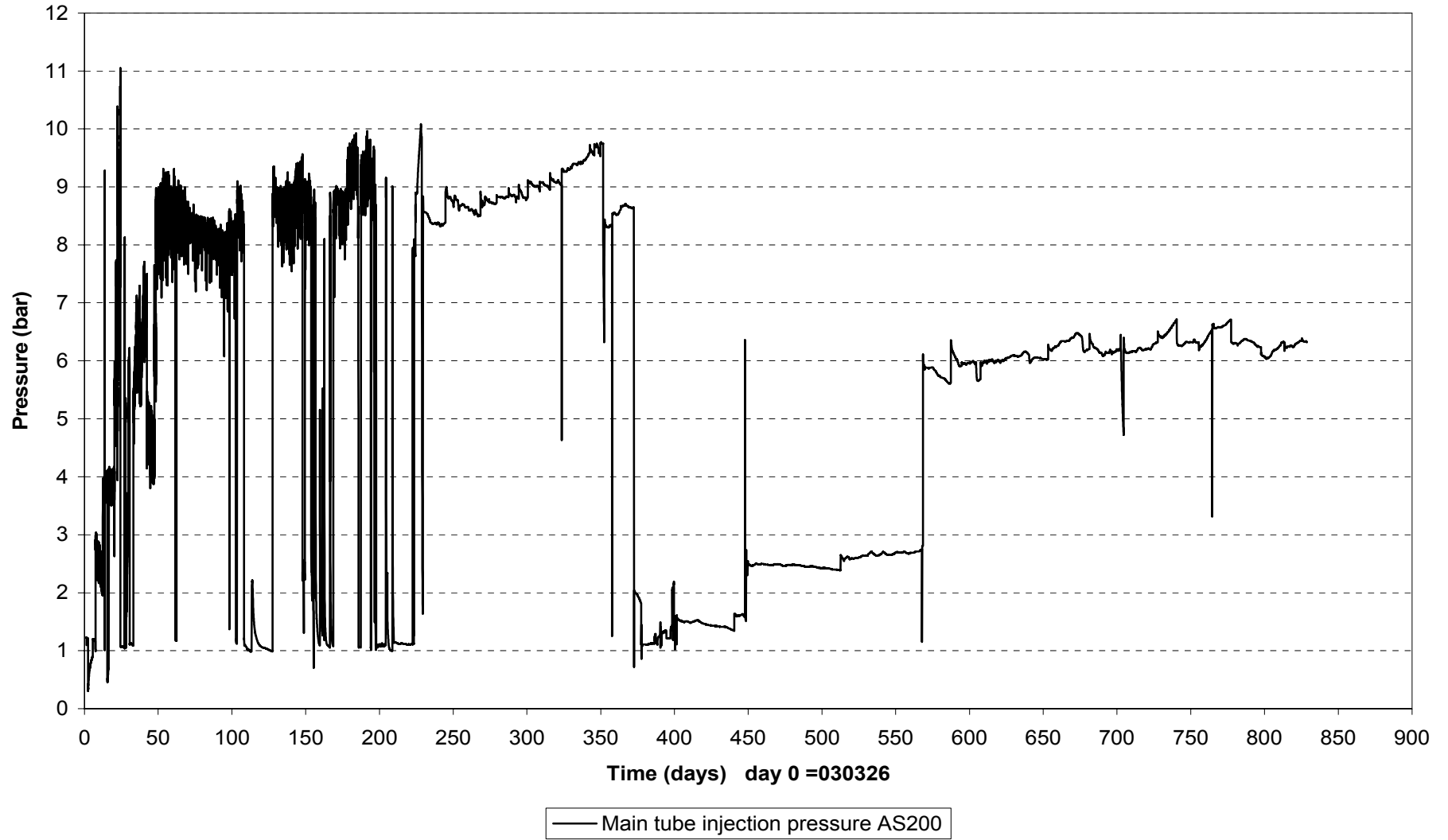


□ UB205(5.250\270°\0.420) ■ UB206(5.250\315°\0.635) ◇ UB207(5.250\90°\0.710) △ UB208(5.250\225°\0.785)

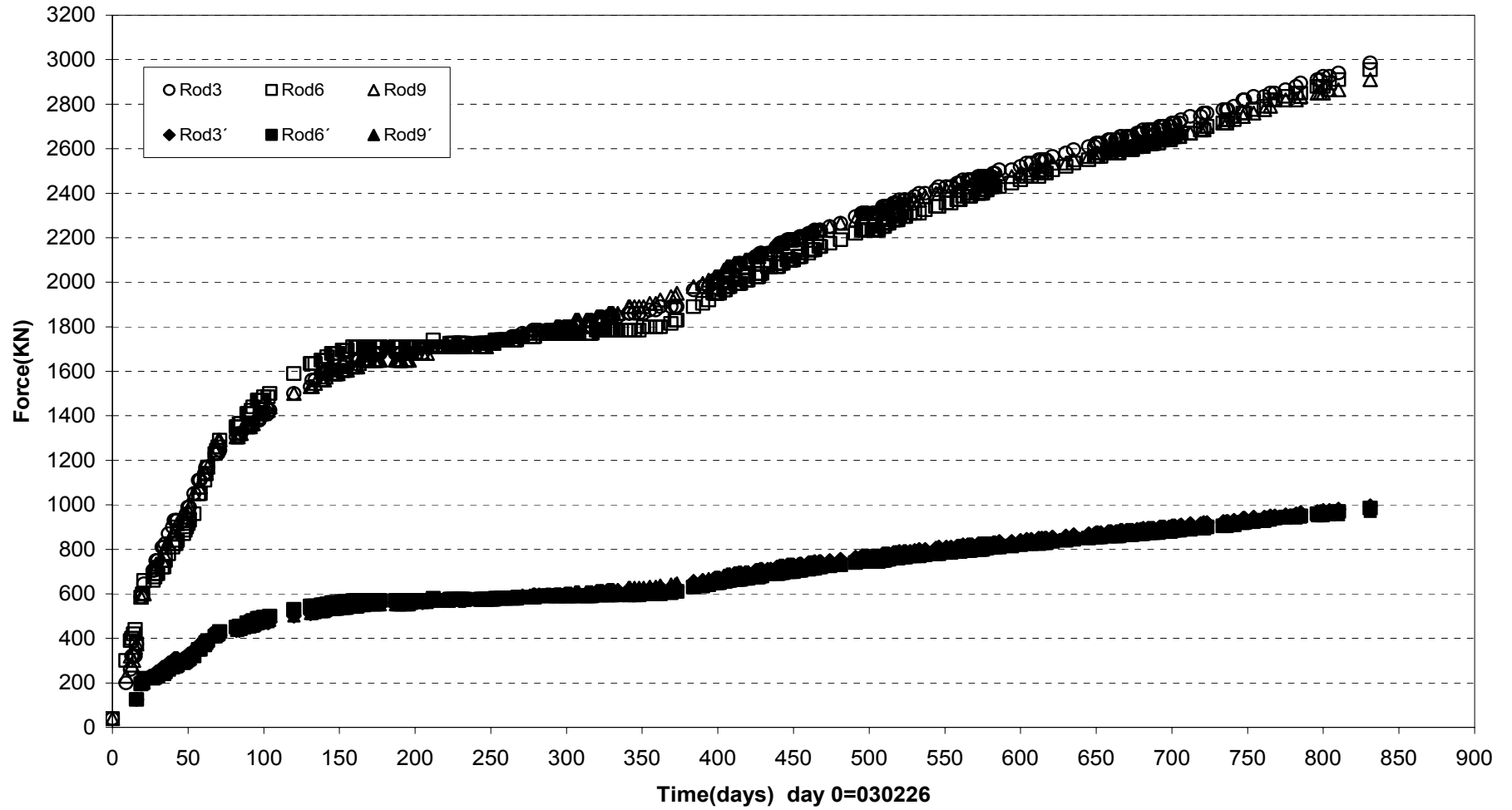
Inflow of water (030326-050701)



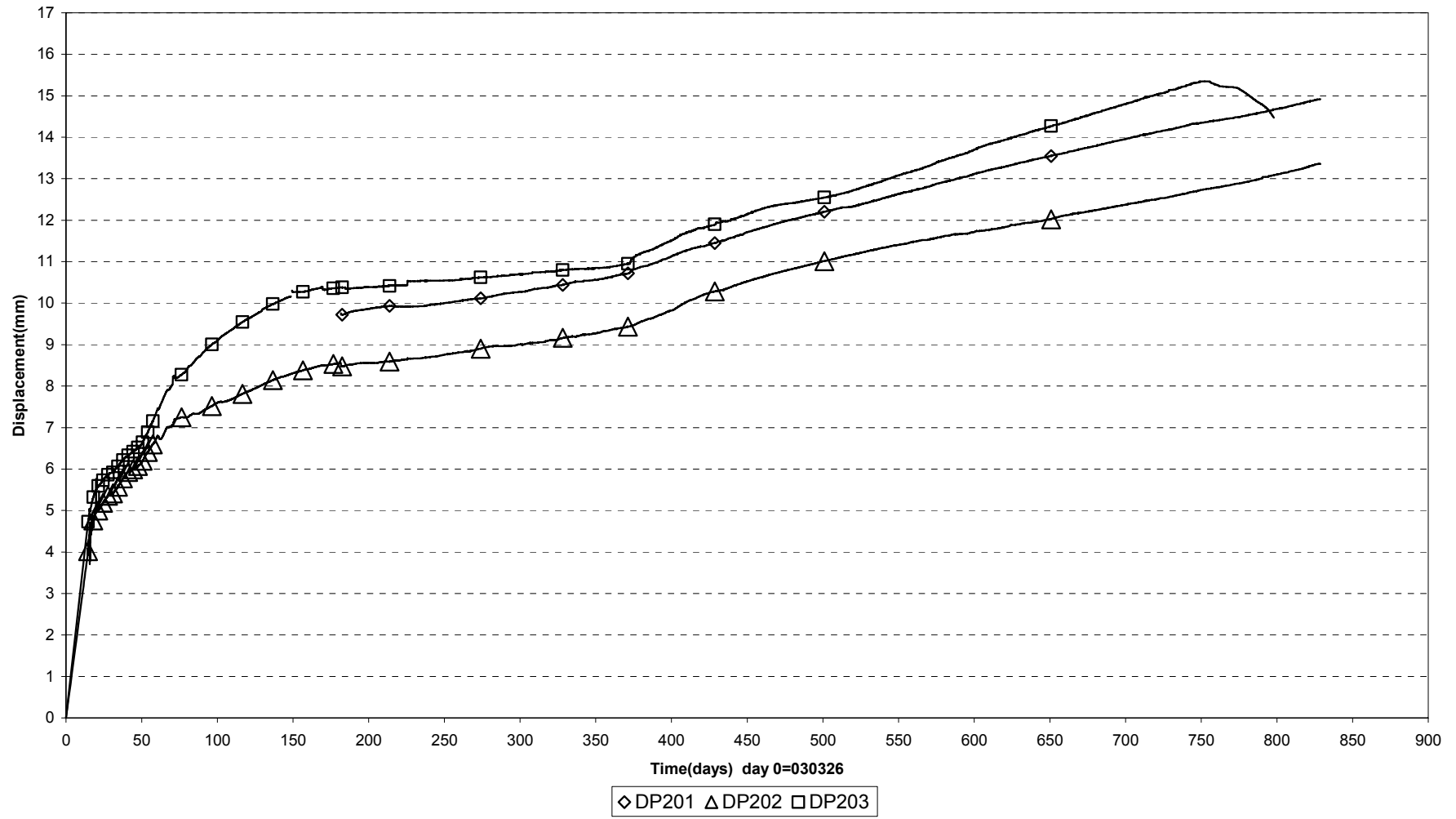
Injection pressure upstream the filter tips (030326-050701)



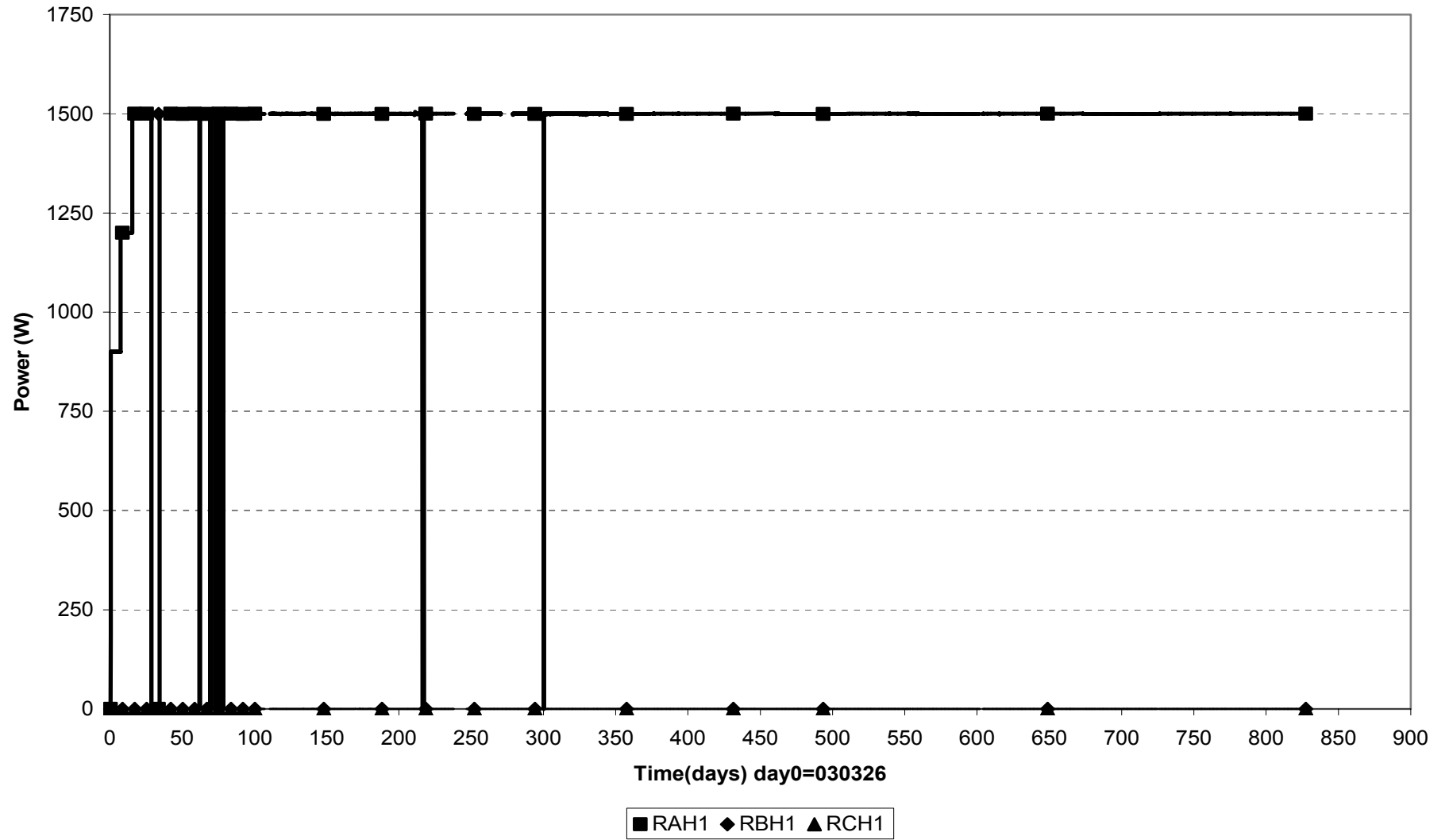
Forces on plug (030326-050704)



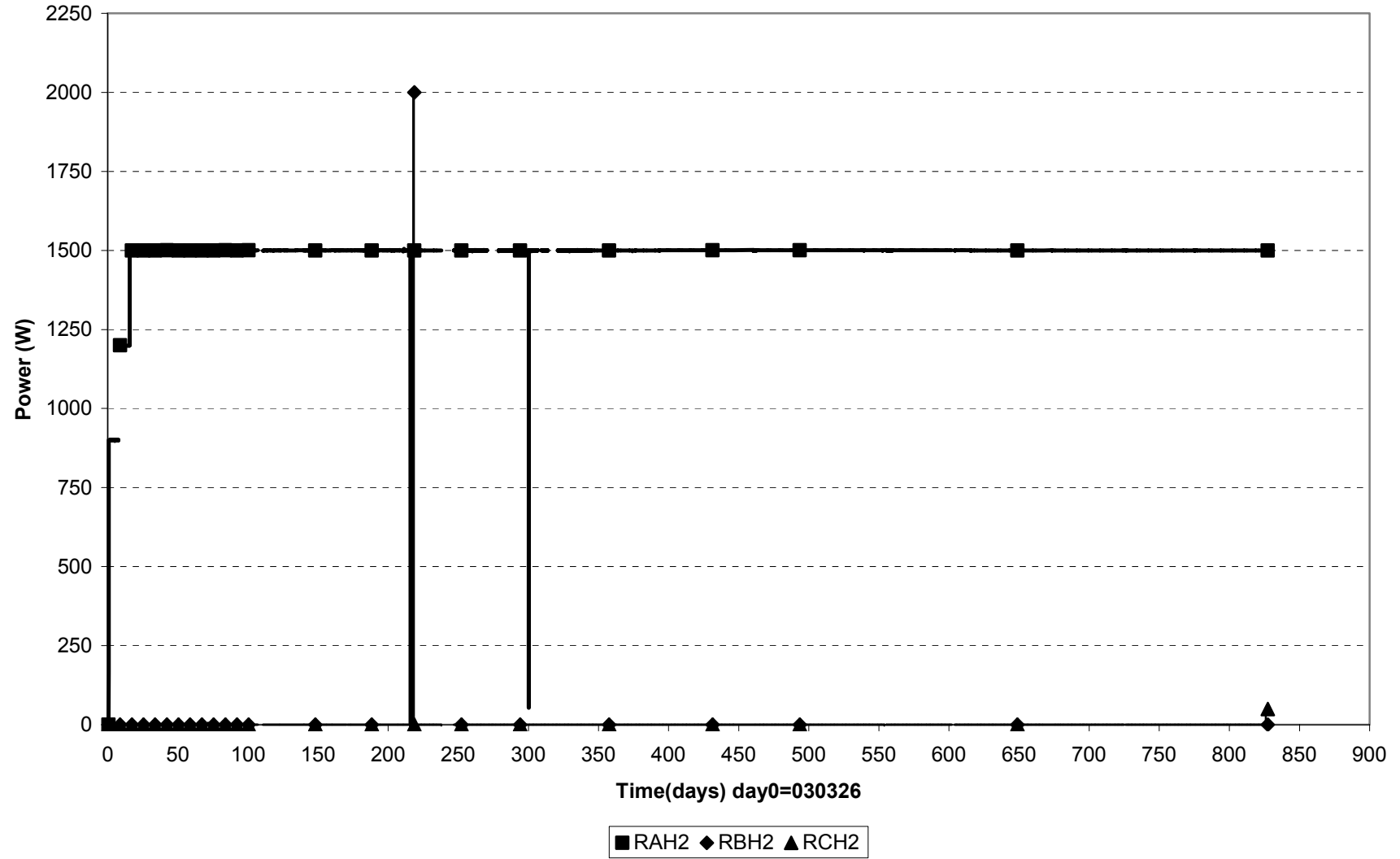
Displacement of plug (030326-050701)



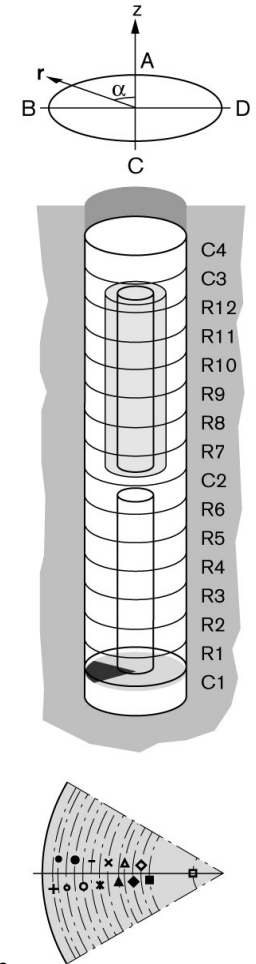
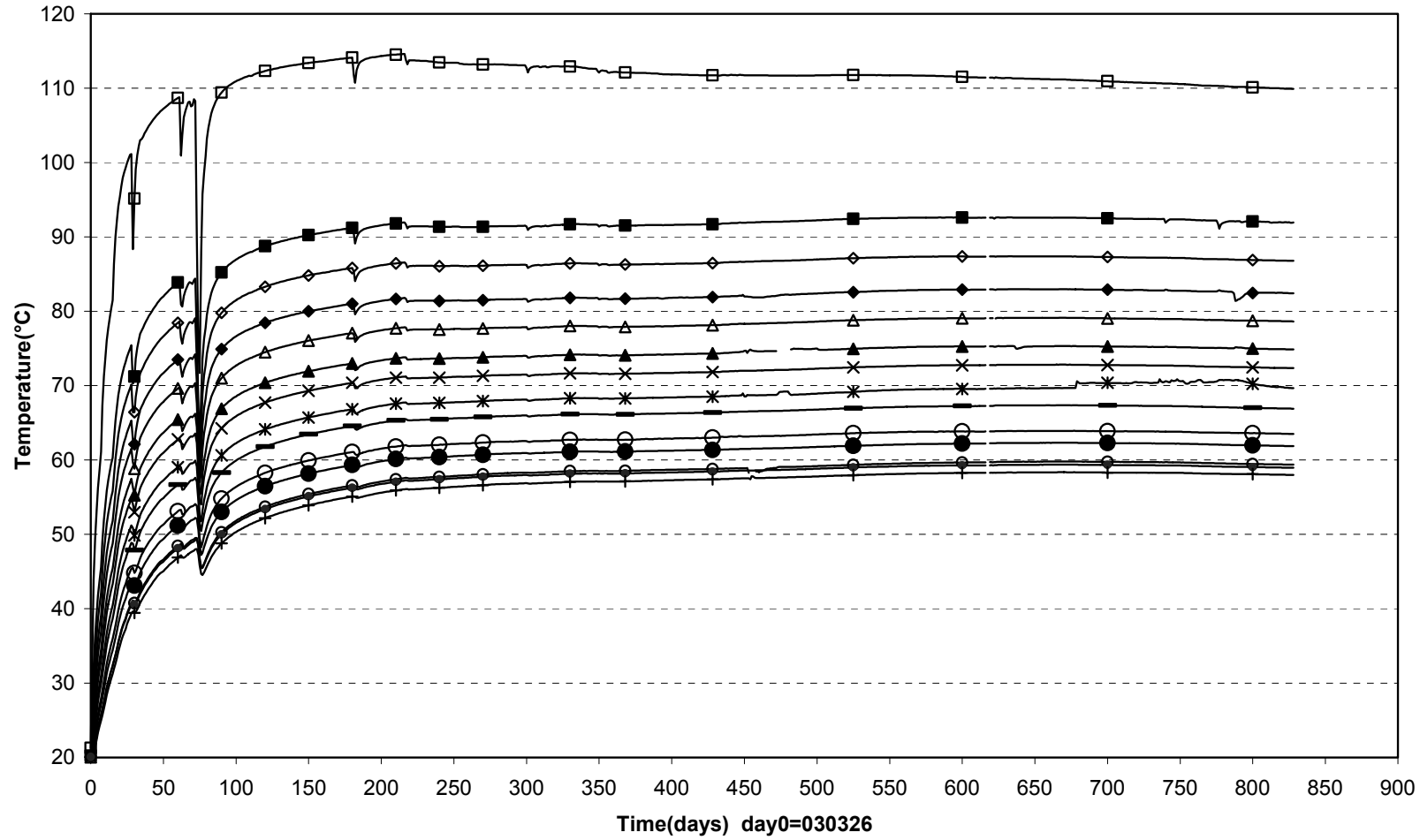
Power Heater 1 (030326-050701)



Power Heater 2 (030326-050701)

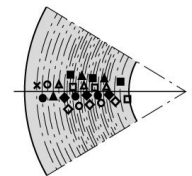
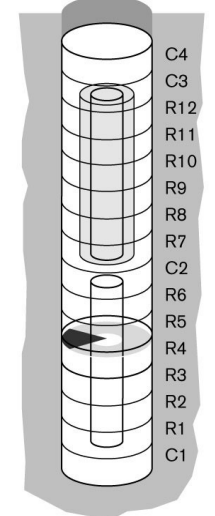
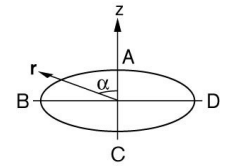
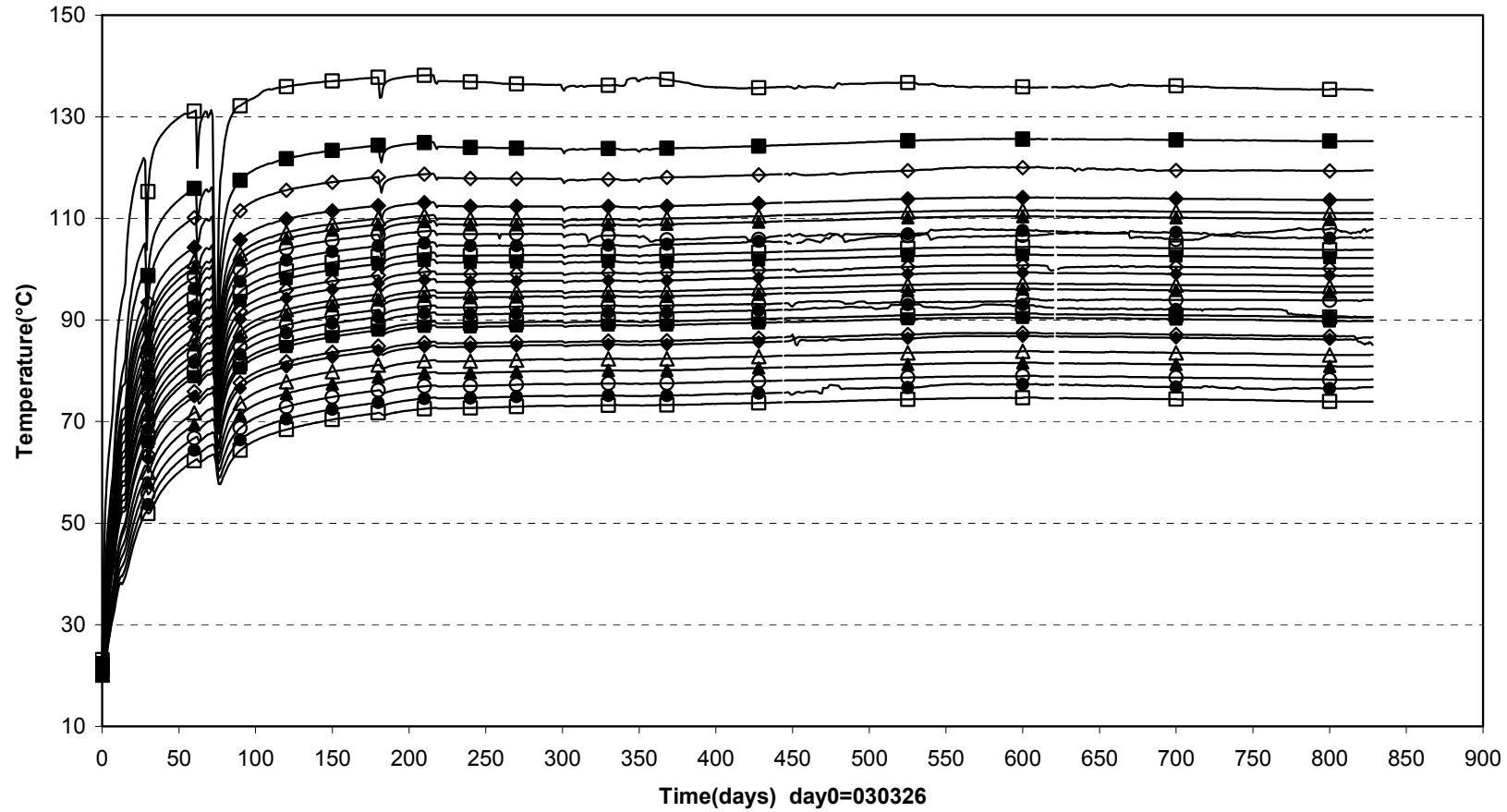


TBT\Cyl.1 (030326-050701)
 Temperature - Pentronic



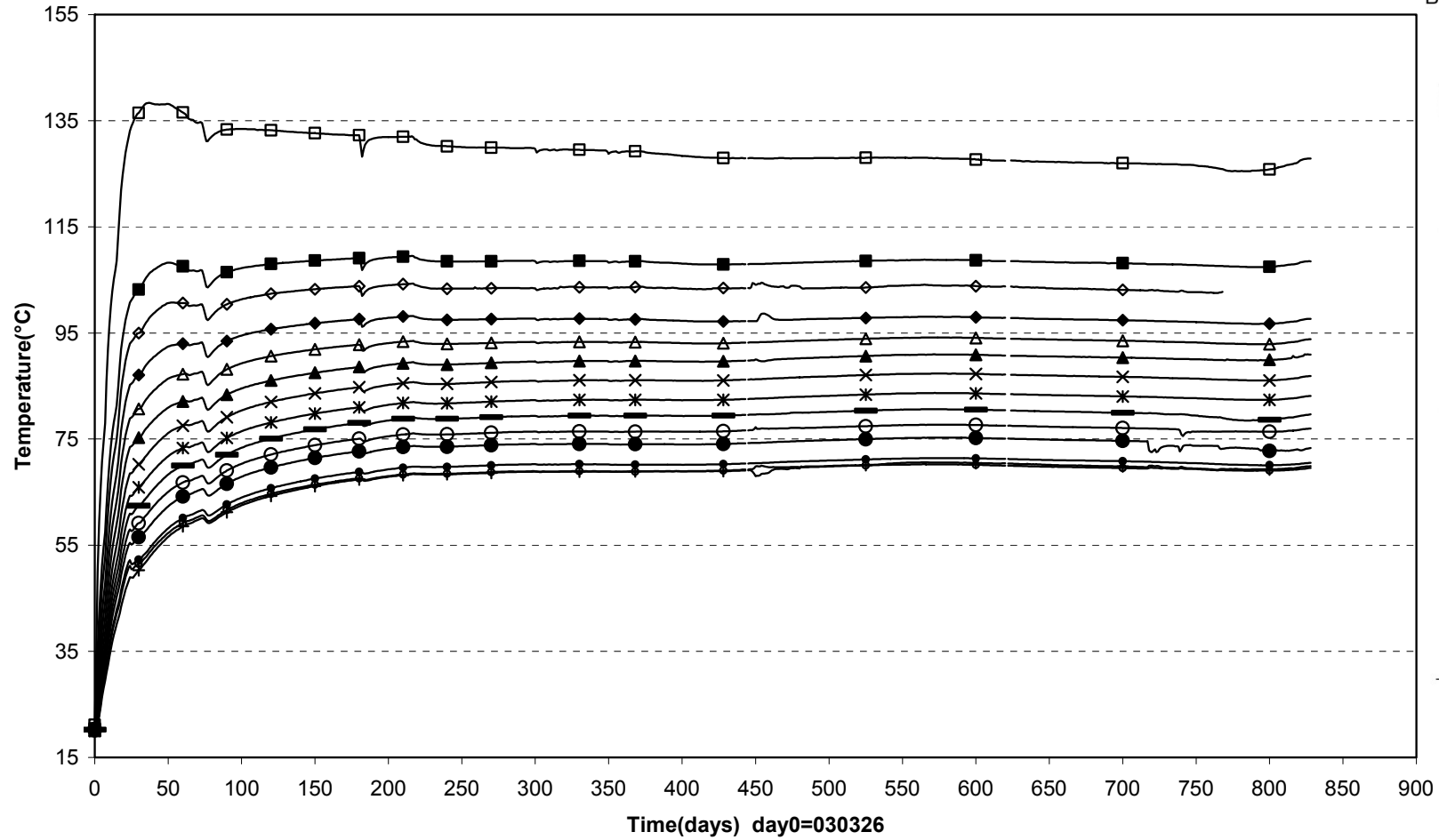
□ TB201(450\90°\150) ■ TB202(450\95°\360) ◇ TB203(450\85°\400) ◆ TB204(450\95°\440) △ TB205(450\85°\480) ▲ TB206(450\95°\520) × TB207(450\85°\560)
 ✖ TB208(450\95°\600) — TB209(450\85°\640) ○ TB210(450\95°\680) ● TB211(450\85°\720) ◌ TB212(450\95°\760) • TB213(450\85°\800) + TB214(450\95°\825)

TBT \Ring4 (030326-050701)
Temperature - Pentronic



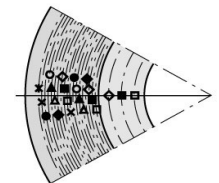
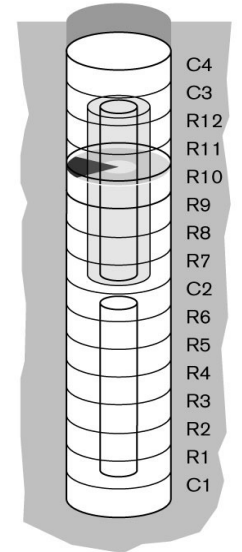
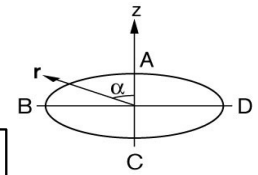
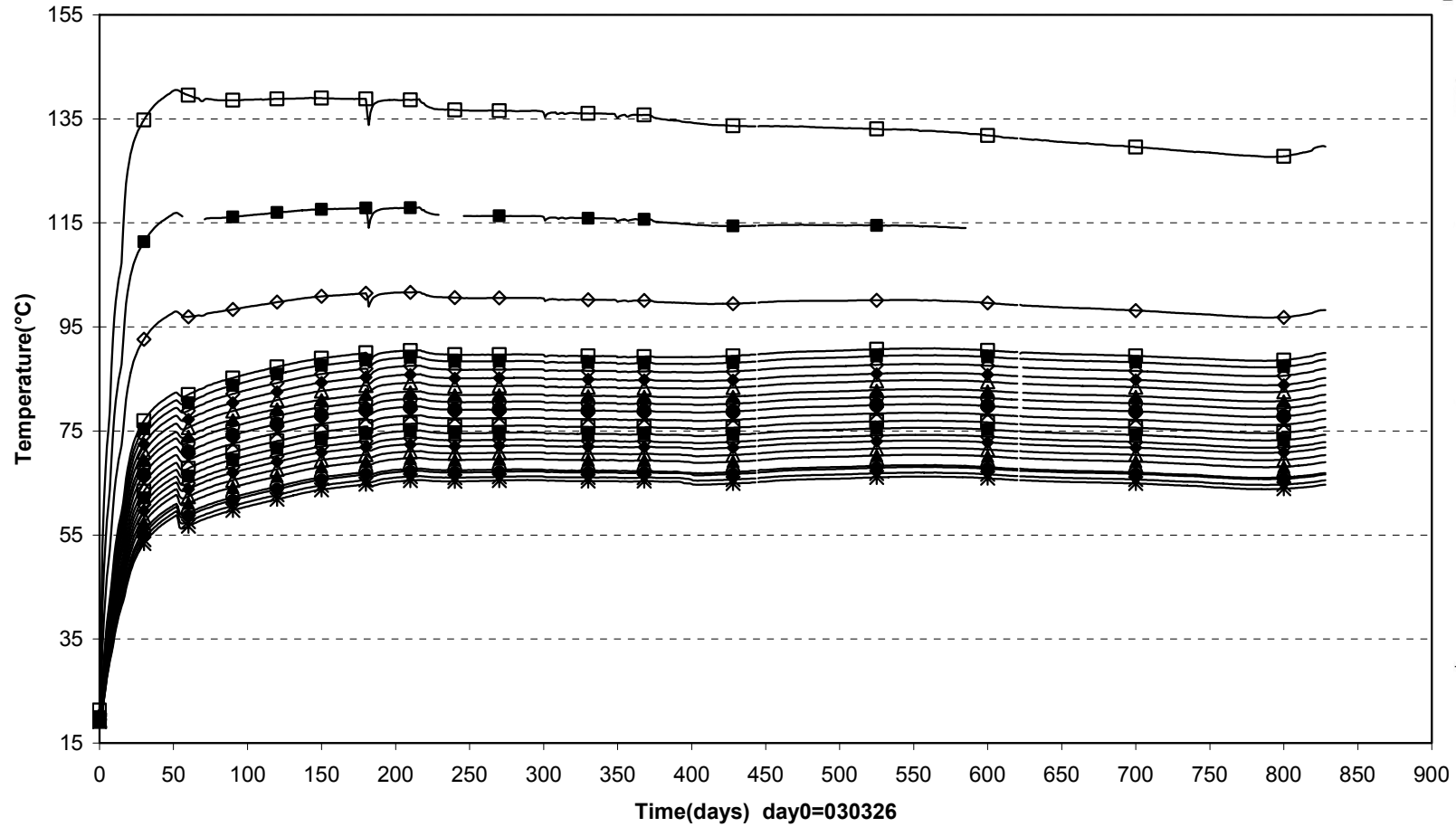
- TB215(2450\97,5°\320) ■ TB216(2450\82,5°\360) ◇ TB217(2450\97,5°\390) ◆ TB218(2450\92,5°\420) △ TB219(2450\87,5°\435)
- ▲ TB220(2450\82,5°\450) ○ TB221(2450\97,5°\465) ● TB222(2450\92,5°\480) □ TB223(2450\87,5°\495) ■ TB224(2450\82,5°\510)
- ◇ TB225(2450\97,5°\525) ◆ TB226(2450\92,5°\540) △ TB227(2450\87,5°\555) ▲ TB228(2450\82,5°\570) ○ TB229(2450\97,5°\585)
- TB230(2450\92,5°\600) □ TB231(2450\87,5°\615) ■ TB232(2450\82,5°\630) ◇ TB233(2450\97,5°\645) ◆ TB234(2450\92,5°\660)
- △ TB235(2450\87,5°\690) ▲ TB236(2450\92,5°\720) ○ TB237(2450\87,5°\750) ● TB238(2450\92,5°\780) □ TB239(2450\87,5°\810)

TBT\Cyl.2 (030326-050701)
 Temperature - Pentronic



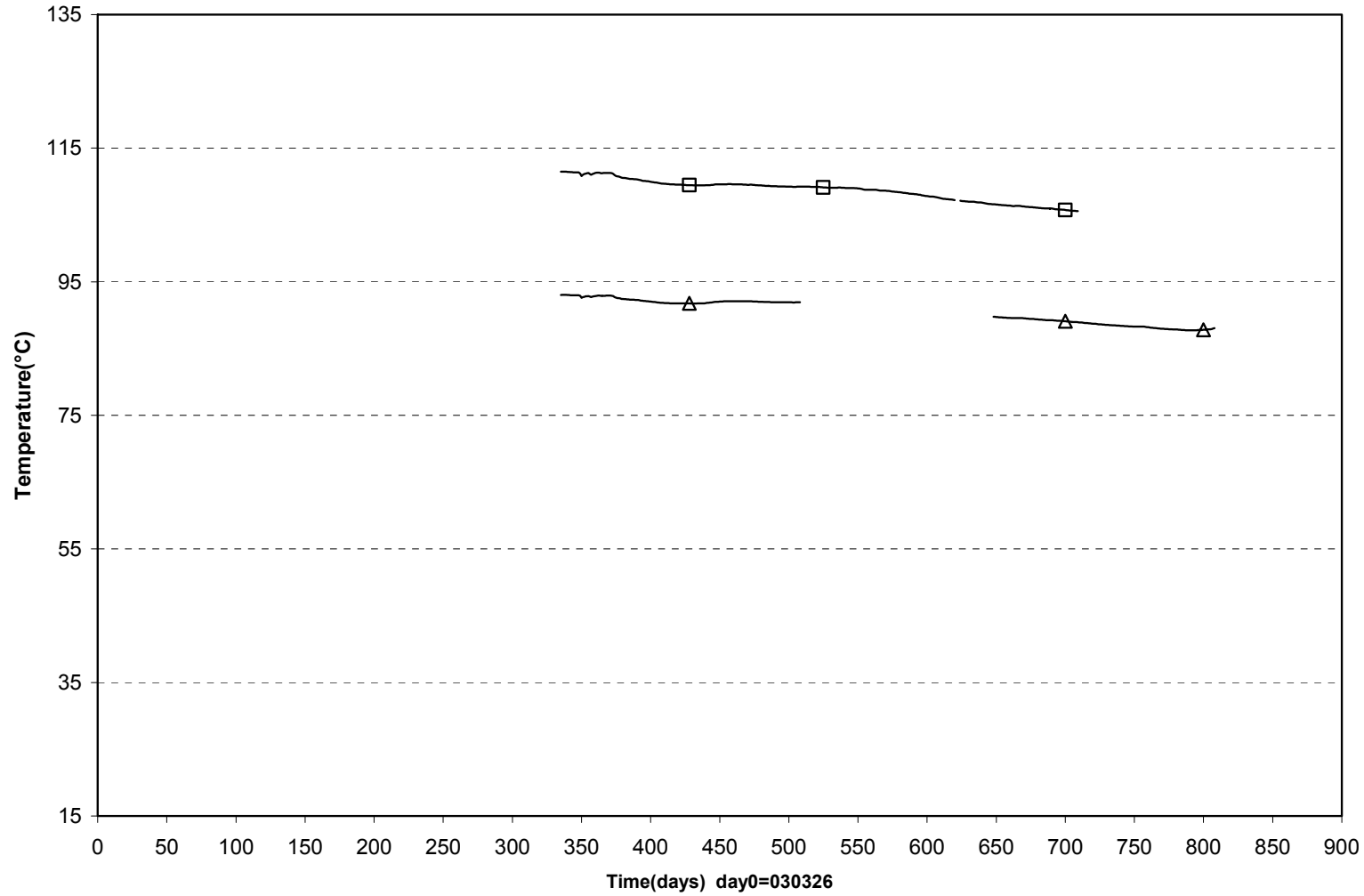
□ TB240(3950\90°\150) ■ TB241(3950\95°\360) ◇ TB242(3950\85°\400) ◆ TB243(3950\95°\440) △ TB244(3950\85°\480) ▲ TB245(3950\95°\520) × TB246(3950\85°\560)
 ✖ TB247(3950\95°\600) — TB248(3950\85°\640) ○ TB249(3950\95°\680) ● TB250(3950\85°\720) ◐ TB251(3950\95°\760) ● TB252(3950\85°\800) + TB253(3950\95°\825)

TBT\ Ring 10 (030326-050701)
 Temperature - Pentronic

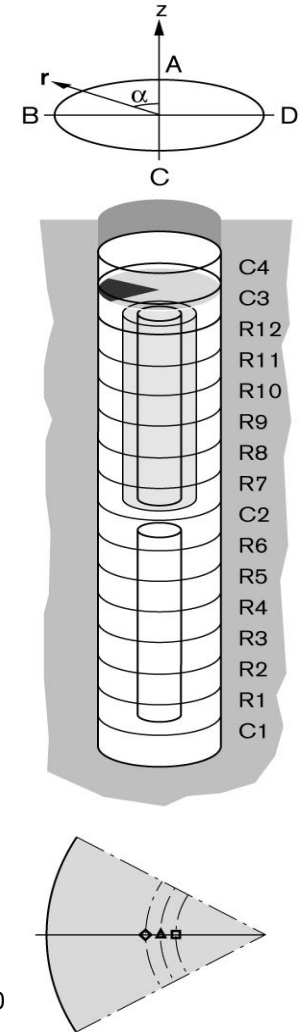


| | | | | | |
|-------------------------|-------------------------|-------------------------|-------------------------|-------------------------|-------------------------|
| □ TB254(5950\90°\360) | ■ TB255(5950\90°\420) | ◇ TB256(5950\90°\480) | □ TB257(5950\97.5°\540) | ■ TB258(5950\92.5°\555) | ◇ TB259(5950\87.5°\570) |
| ◆ TB260(5950\82.5°\585) | △ TB261(5950\97.5°\600) | ▲ TB262(5950\92.5°\615) | ○ TB263(5950\87.5°\630) | ● TB264(5950\82.5°\645) | × TB265(5950\97.5°\660) |
| □ TB266(5950\92.5°\675) | ■ TB267(5950\87.5°\690) | ◇ TB268(5950\82.5°\705) | ◆ TB269(5950\97.5°\720) | △ TB270(5950\92.5°\735) | ▲ TB271(5950\87.5°\750) |
| ○ TB272(5950\82.5°\765) | ● TB273(5950\97.5°\780) | × TB274(5950\92.5°\795) | ✱ TB275(5950\87.5°\810) | | |

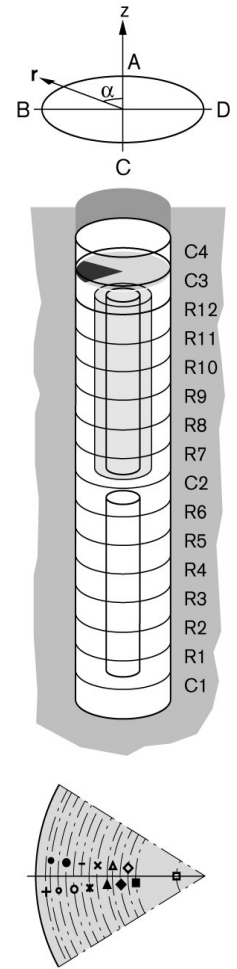
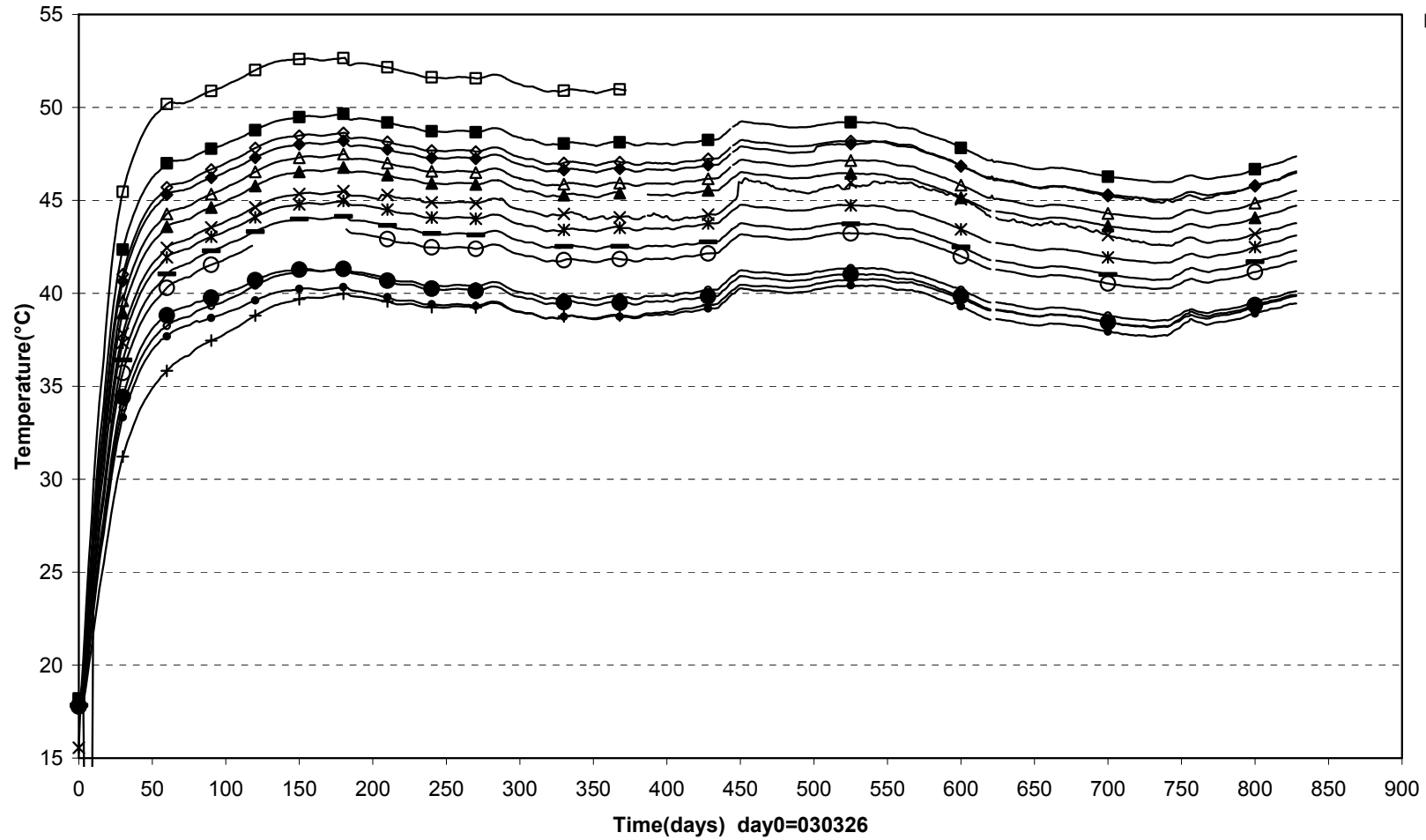
TBT\ Ring 12 (030326-050701)
 Temperature - Pentronic



□ TB290(6.881\90°\0.360) △ TB291(6.881\90°\0.420) ◇ TB292(6.881\90°\0.480)

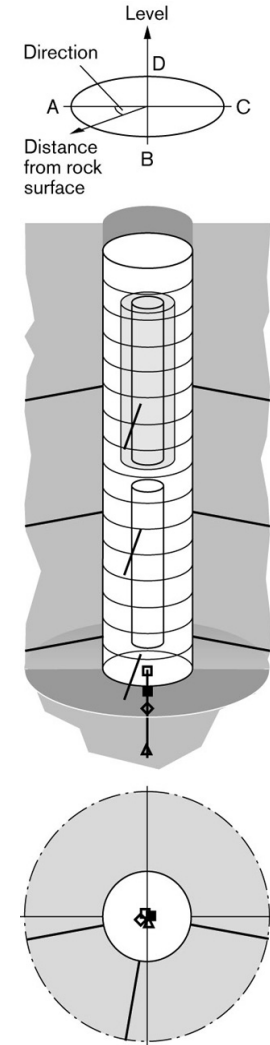
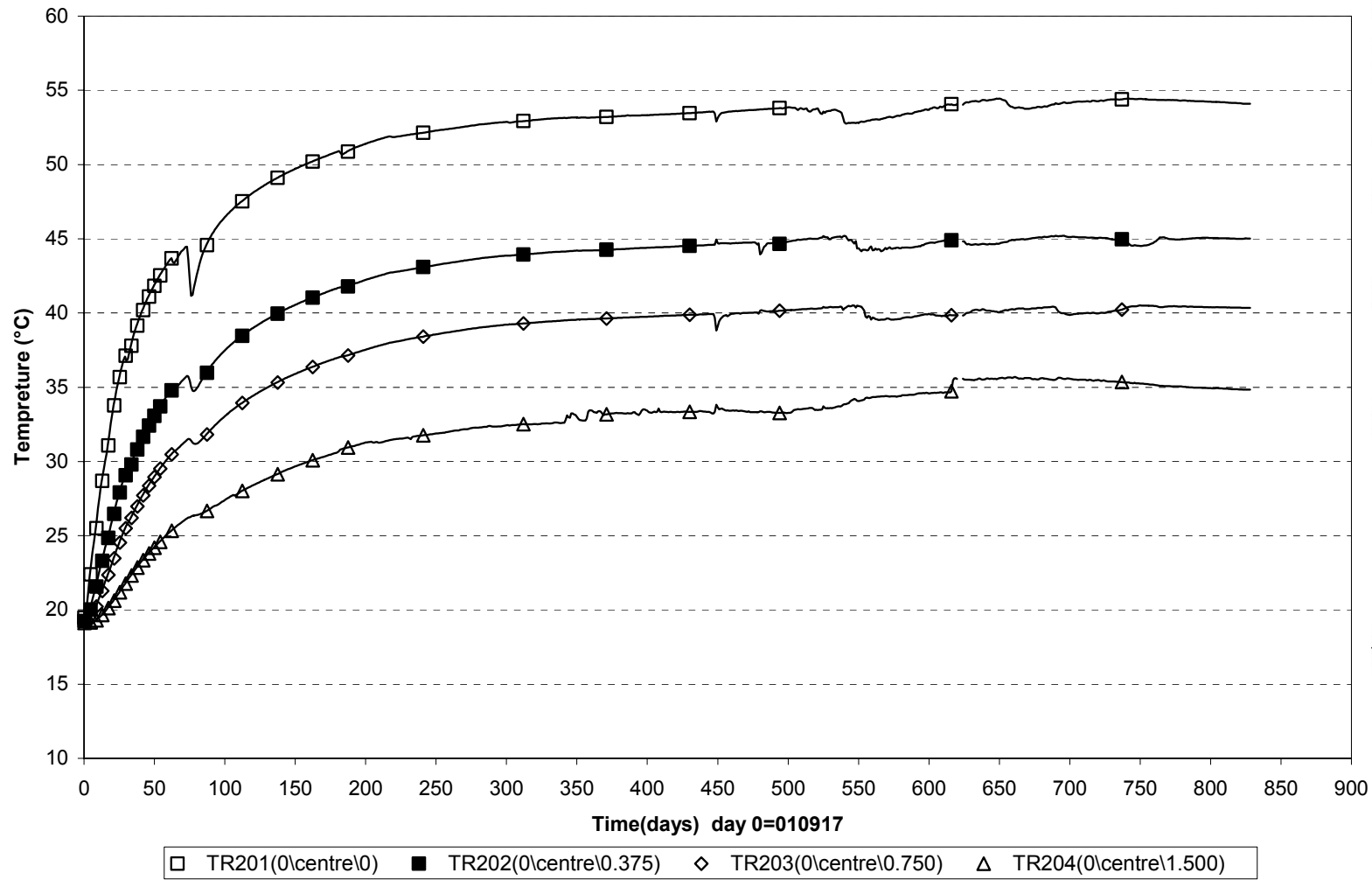


TBT\Cyl.3 (030326-050701)
 Temperature - Pentronic

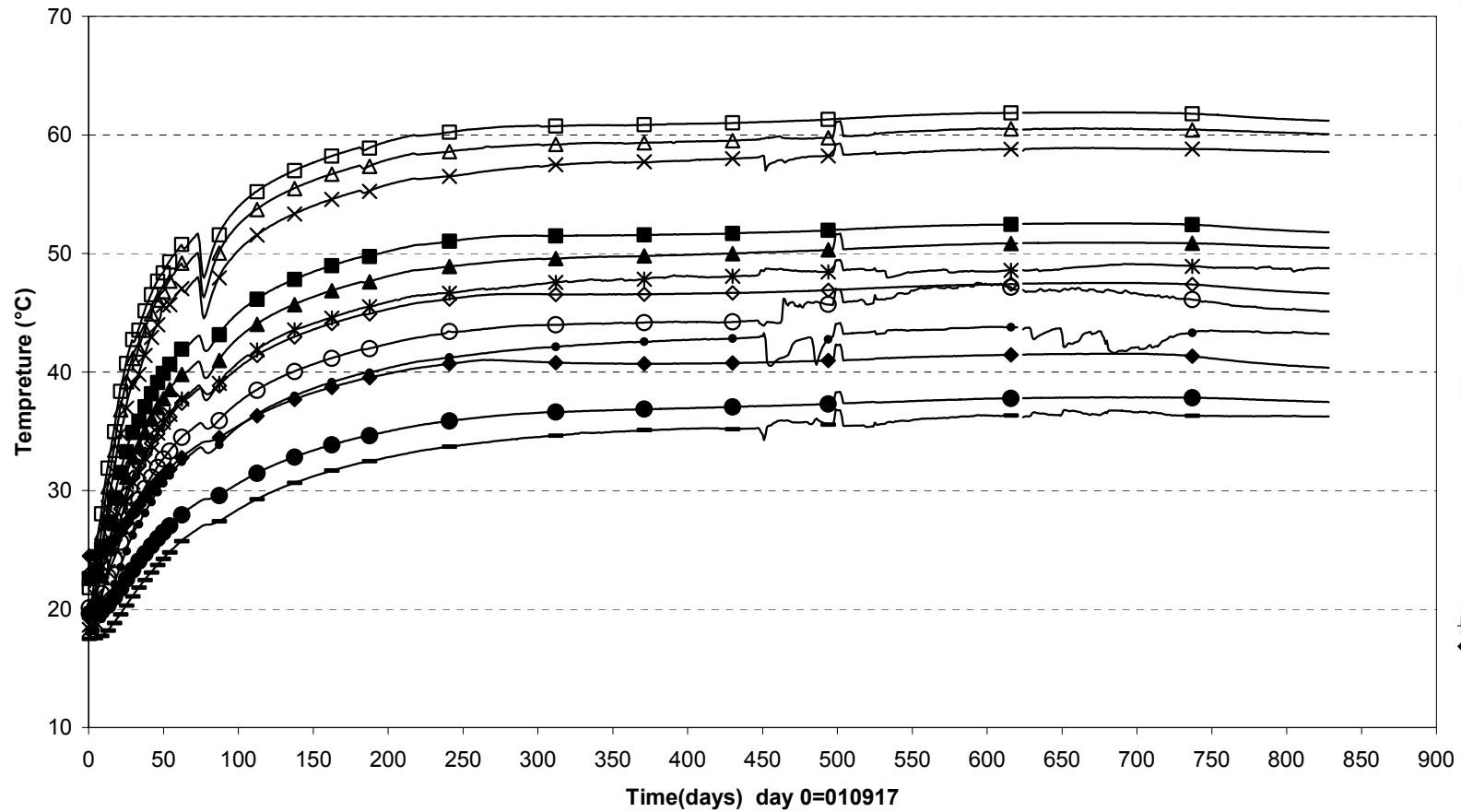


□ TB276(7450\90°\150) ■ TB277(7450\95°\360) ◇ TB278(7450\85°\400) ◆ TB279(7450\95°\440) △ TB280(7450\85°\480) ▲ TB281(7450\95°\520) × TB282(7450\85°\560)
 ✖ TB283(7450\95°\600) — TB284(7450\85°\640) ○ TB285(7450\95°\680) ● TB286(7450\85°\720) ◊ TB287(7450\95°\760) • TB288(7450\85°\800) + TB289(7450\95°\825)

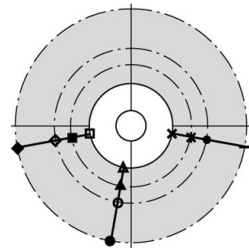
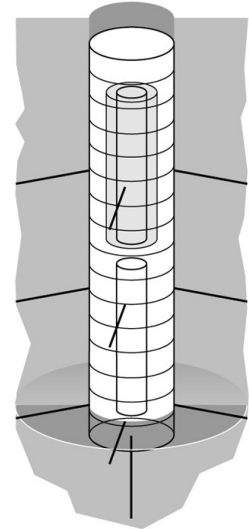
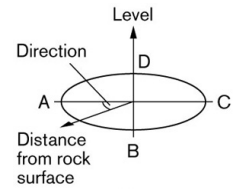
TBT\ Temperature in the rock-below the dep.hole (030326-050701)
 Temperature - Pentronic



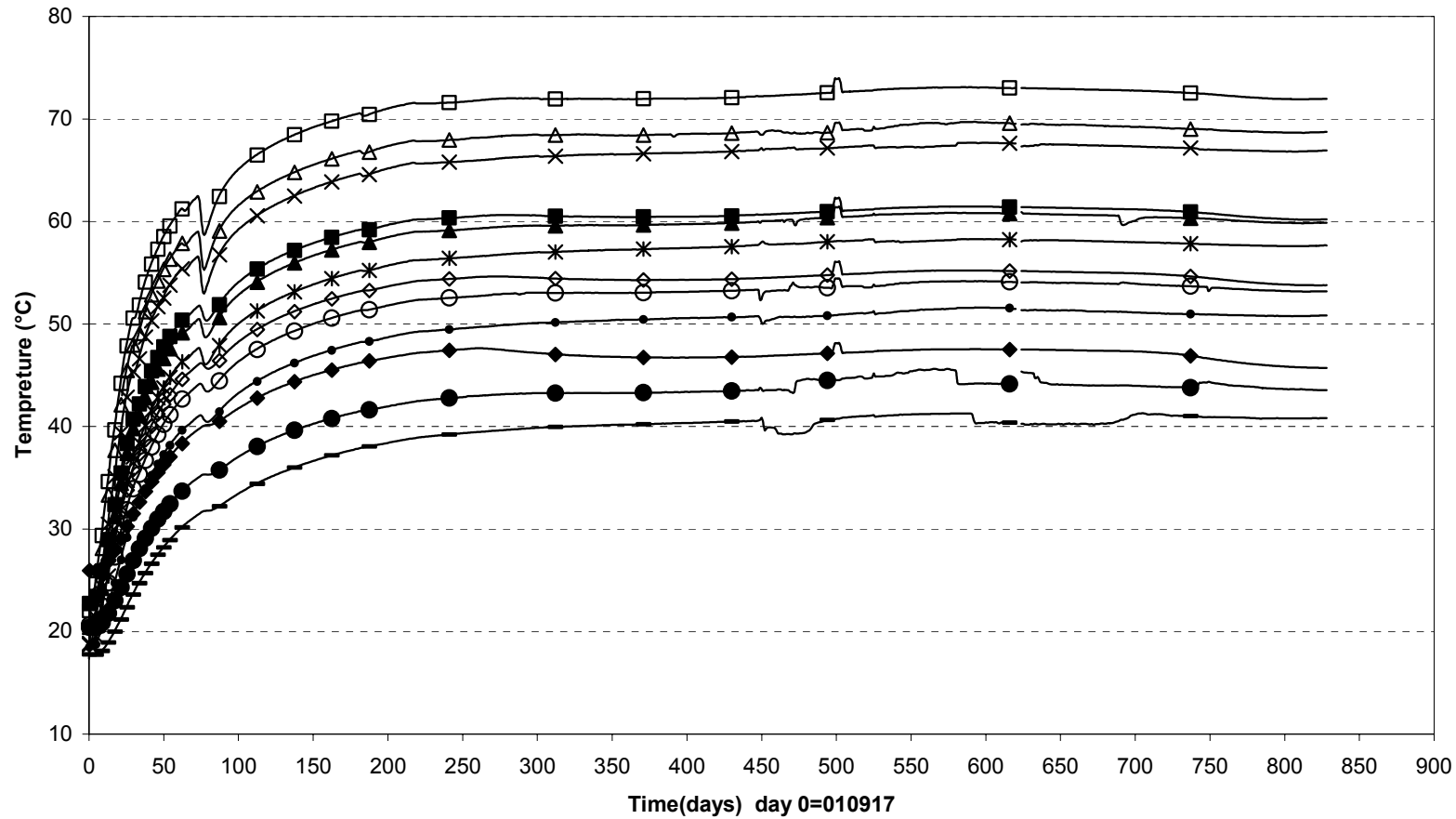
TBT\ Temperature in the rock-level 0,61 m (030326-050701)
 Temperature - Pentronic



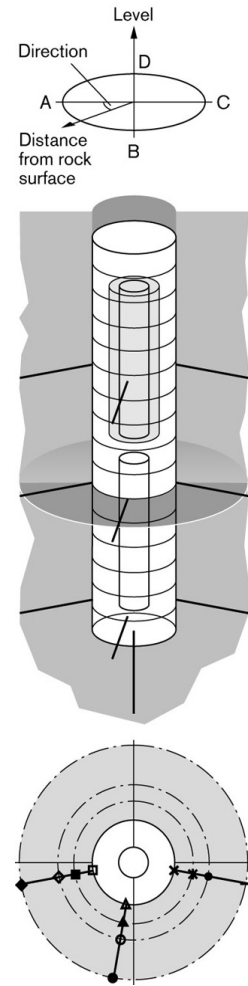
| | | | |
|--------------------------|--------------------------|--------------------------|--------------------------|
| □ TR205(0.61\10°\0.000) | ■ TR206(0.61\10°\0.375) | ◇ TR207(0.61\10°\0.750) | ◆ TR208(0.61\10°\1.500) |
| △ TR209(0.61\80°\0.000) | ▲ TR210(0.61\80°\0.375) | ○ TR211(0.61\80°\0.750) | ● TR212(0.61\80°\1.500) |
| × TR213(0.61\170°\0.000) | ✱ TR214(0.61\170°\0.375) | • TR215(0.61\170°\0.750) | - TR216(0.61\170°\1.500) |



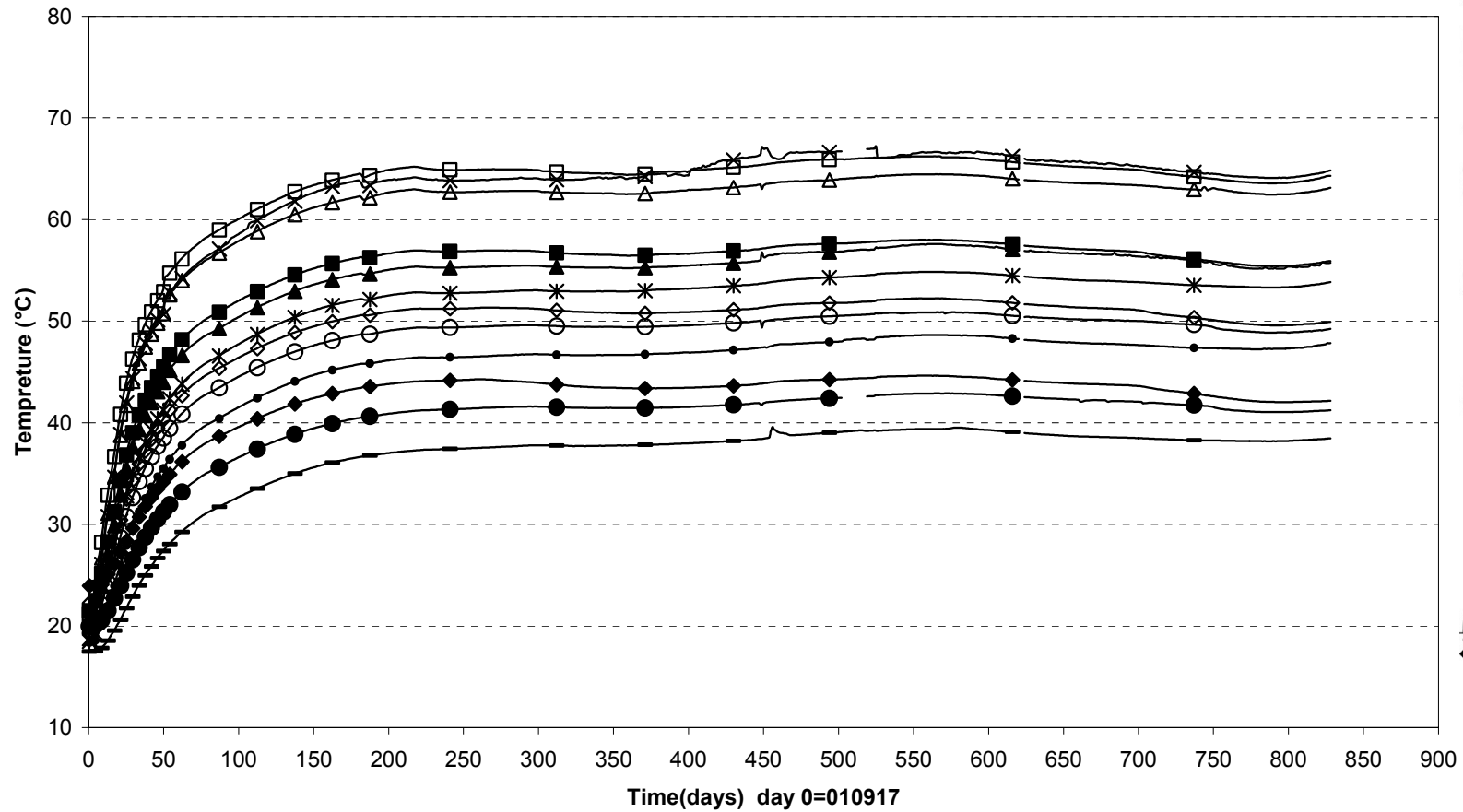
TBT\ Temperature in the rock-level 3,01 m (030326-050701)
 Temperature - Pentronic



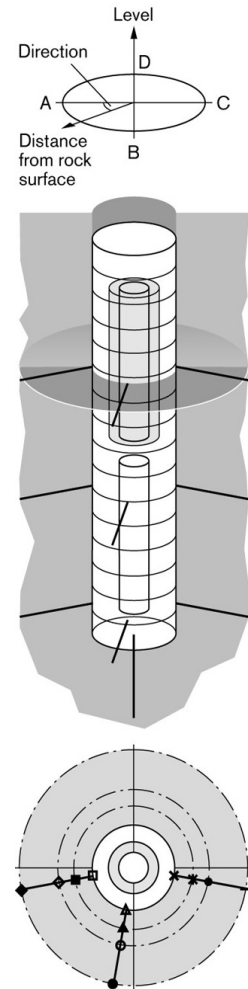
| | | | |
|--------------------------|--------------------------|--------------------------|--------------------------|
| □ TR217(3.01\10°\0.000) | ■ TR218(3.01\10°\0.375) | ◇ TR219(3.01\10°\0.750) | ◆ TR220(3.01\10°\1.500) |
| △ TR221(3.01\80°\0.000) | ▲ TR222(3.01\80°\0.375) | ○ TR223(3.01\80°\0.750) | ● TR224(3.01\80°\1.500) |
| × TR225(3.01\170°\0.000) | * TR226(3.01\170°\0.375) | • TR227(3.01\170°\0.750) | - TR228(3.01\170°\1.500) |



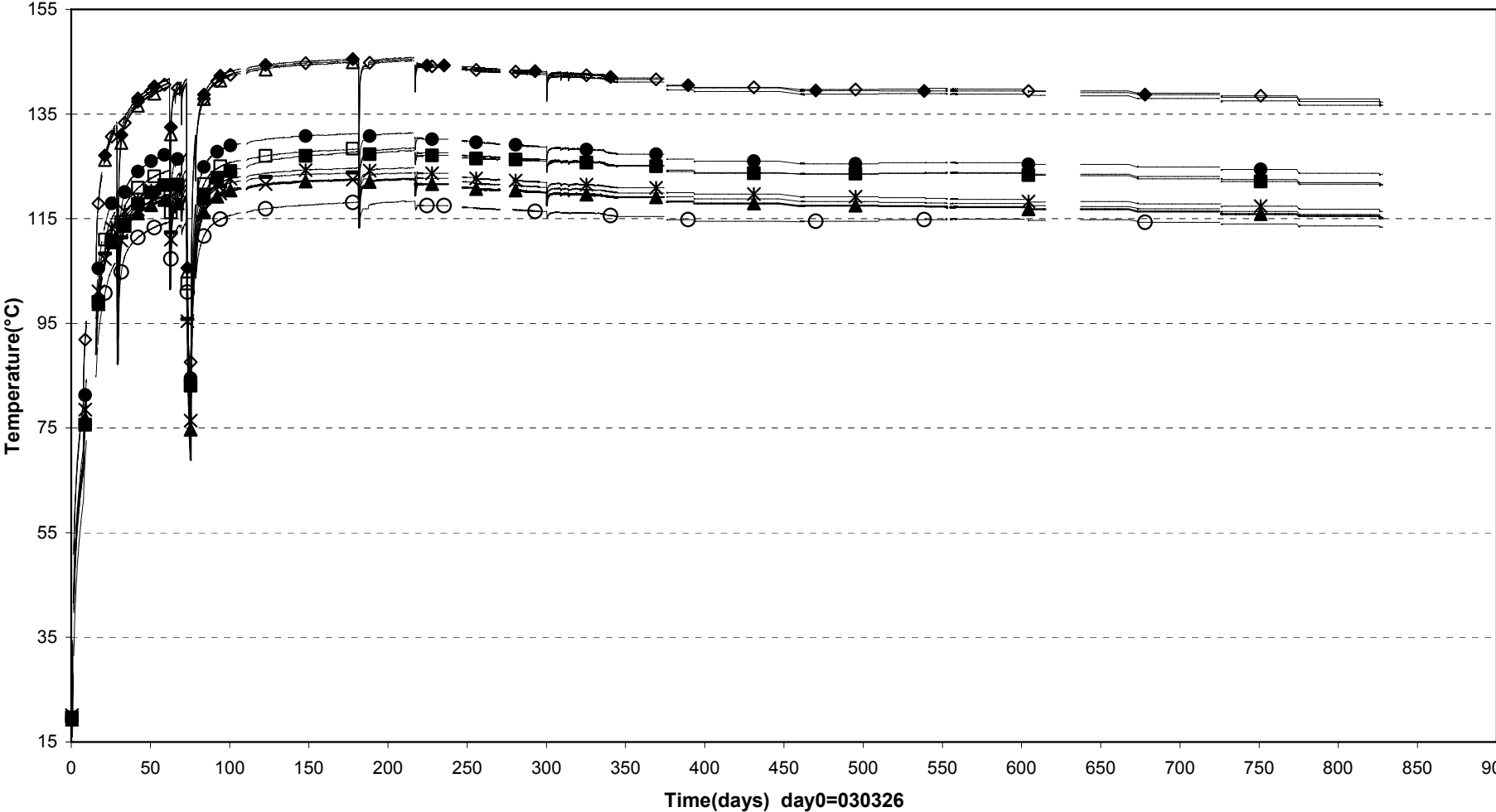
TBT\ Temperature in the rock-level 5,41 m (030326-050701)
 Temperature - Pentronic



| | | | |
|--------------------------|--------------------------|--------------------------|--------------------------|
| □ TR229(5.41\10°\0.000) | ■ TR230(5.41\10°\0.375) | ◇ TR231(5.41\10°\0.750) | ◆ TR232(5.41\10°\1.500) |
| △ TR233(5.41\80°\0.000) | ▲ TR234(5.41\80°\0.375) | ○ TR235(5.41\80°\0.750) | ● TR236(5.41\80°\1.500) |
| × TR237(5.41\170°\0.000) | ✱ TR238(5.41\170°\0.375) | • TR239(5.41\170°\0.750) | — TR240(5.41\170°\1.500) |

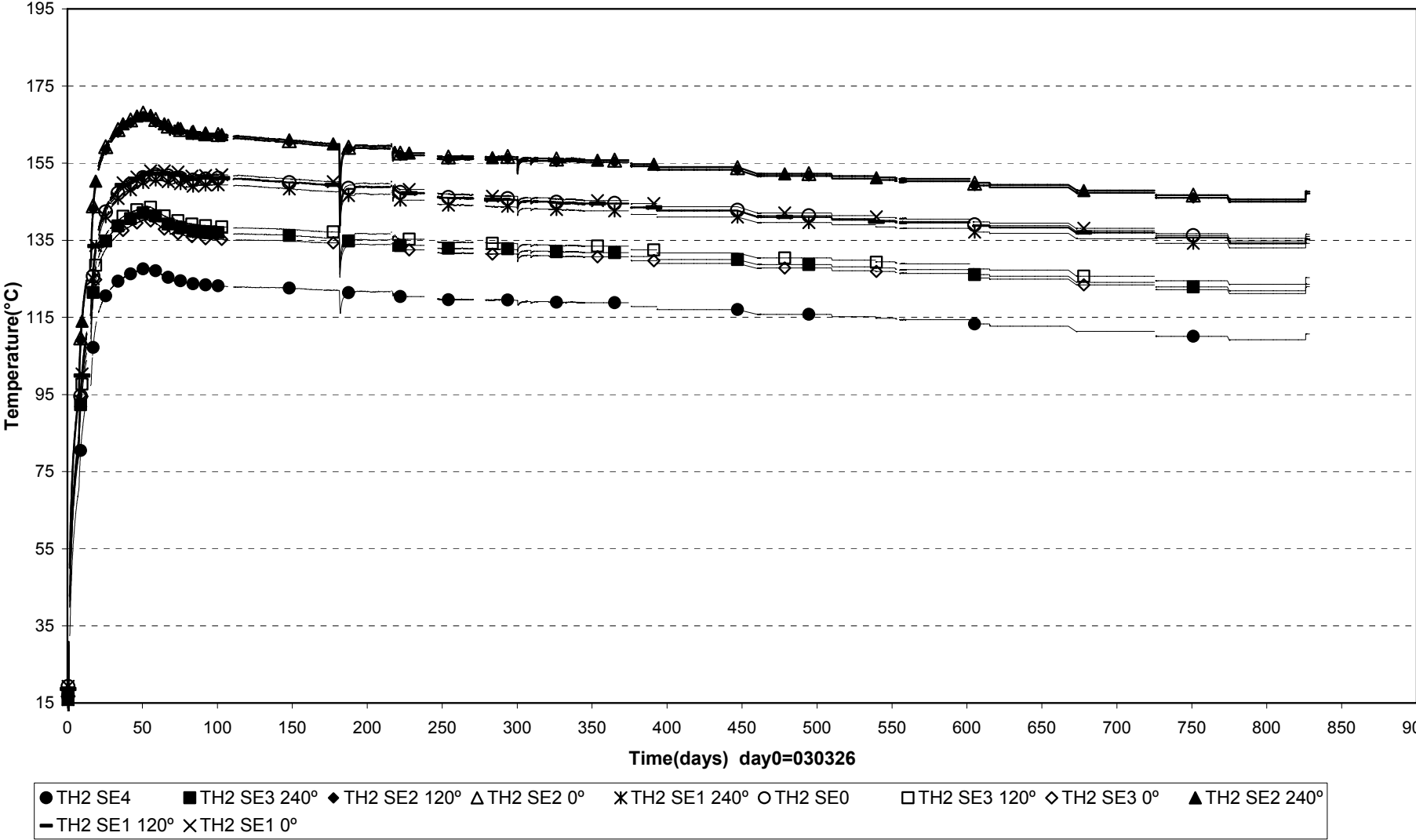


External temperatures Heater 1 (030326-050701)

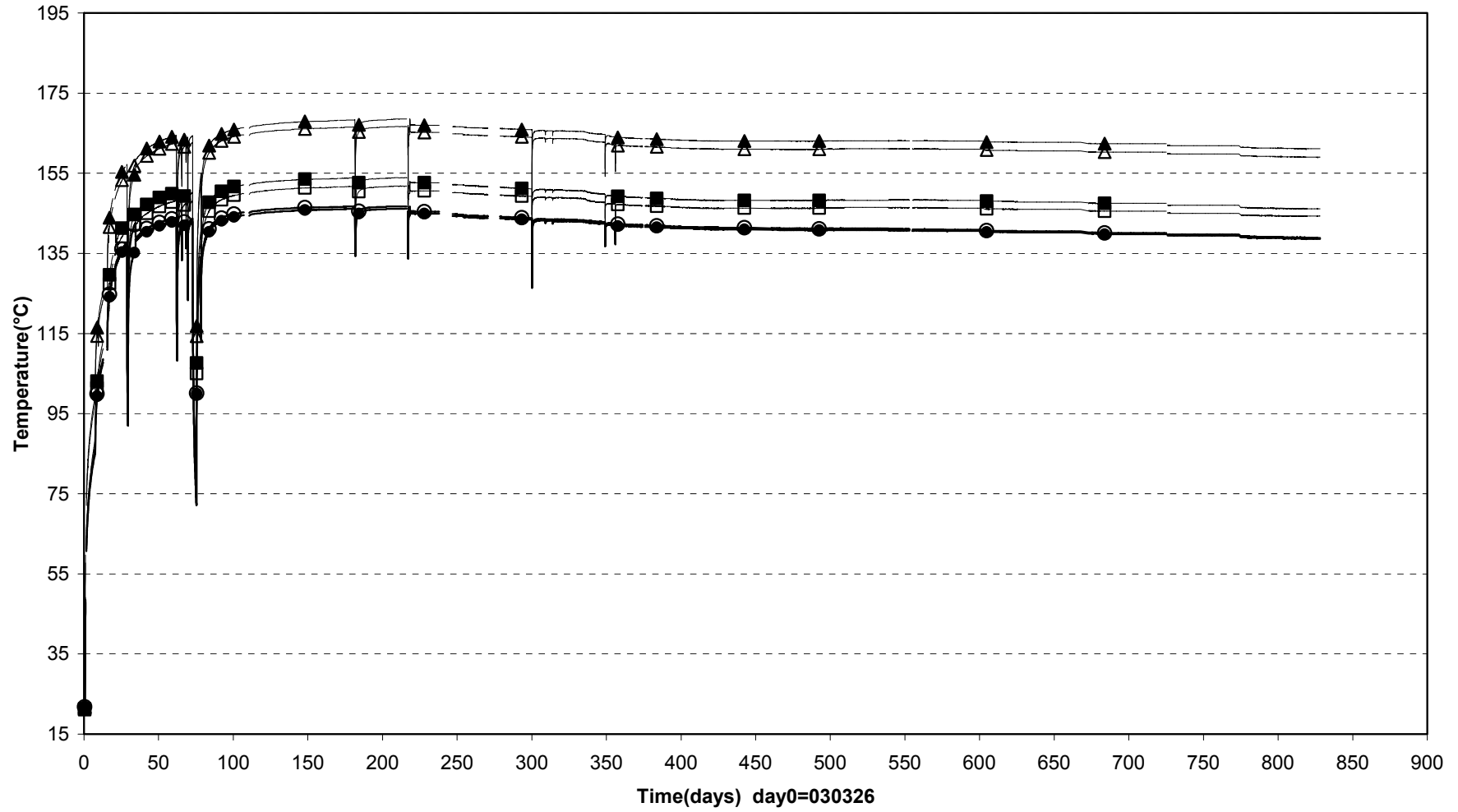


○ TH1 SE4 ● TH1 SE3 120° □ TH1 SE3 240° ■ TH1 SE3 0° ◆ TH1 SE2 120° ◇ TH1 SE2 240° △ TH1 SE2 0° ▲ TH1 SE1 120° — TH1 SE1 240°
 ✖ TH1 SE1 0° ✕ TH1 SE0

External temperatures Heater 2 (030326-050701)

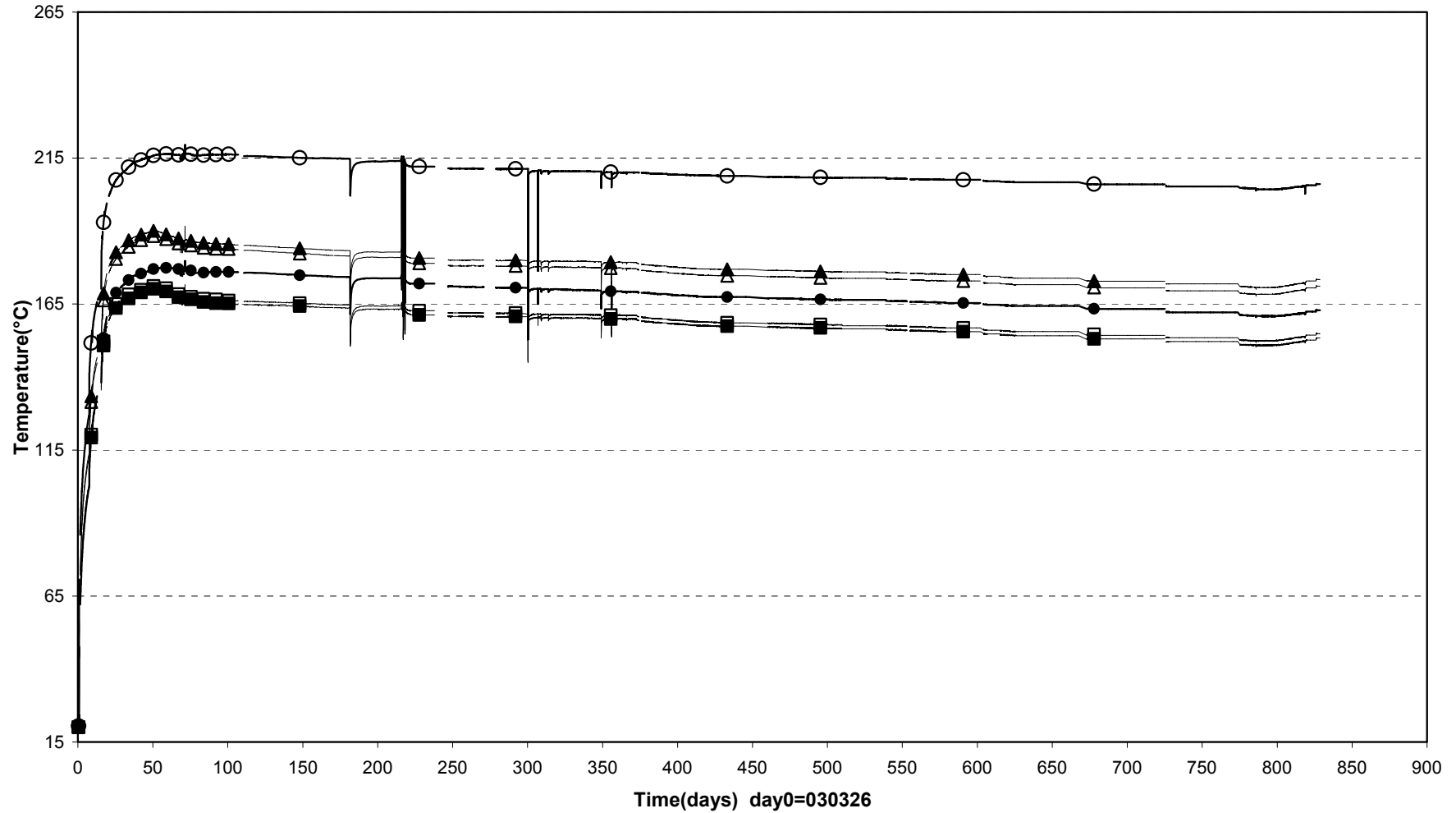


Internal temperatures Heater 1 (030326-050701)



□ TH1 SI1 0° ■ TH1 SI1 180° △ TH1 SI2 0° ▲ TH1 SI2 180° ○ TH1 SI3 0° ● TH1 SI3 180°

Internal temperatures Heater 2 (030326-050701)



□ TH2 SI1 0° ■ TH2 SI1 180° △ TH2 SI2 0° ▲ TH2 SI2 180° ○ TH2 SI3 0° ● TH2 SI3 180°